THE UNIVERSITY OF MANITOBA

Symmetrical and Asymmetrical Heat Transfer in Single-Phase Turbulent Flow in Rectangular Channels and Parallel Plates

by

Carl Chiu-Pang Chan

A Thesis

Submitted to the Faculty of Graduate Studies in Partial Fulfillment of the Requirements for the Degree of Master of Science

DEPARTMENT OF MECHANICAL ENGINEERING

Winnipeg, Manitoba

October, 1979

SYMMETRICAL AND ASYMMETRICAL HEAT TRANSFER
IN SINGLE-PHASE TURBULENT FLOW IN
RECTANGULAR CHANNELS AND
PARALLEL PLATES

BY

CARL CHIU-PANG CHAN

A dissertation submitted to the Faculty of Graduate Studies of the University of Manitoba in partial fulfillment of the requirements of the degree of

MASTER OF SCIENCE

ABSTRACT

The object of this work was to propose methods which are both simple and accurate for the prediction of symmetrical and asymmetrical heat transfer in single-phase turbulent fluid flow in rectangular channels and parallel plates. Existing heat-transfer correlations for circular tubes, symmetrically and asymmetrically heated rectangular channels and parallel plates were reviewed. New correlations, based on the Spalding-Jayatilleke P-function concept, were developed by the present author for symmetrically and asymmetrically heated parallel plates. The approach for the selection of the best methods for heat-transfer prediction was by comparison with all the available published experimental data. In the case of symmetrical heat transfer in rectangular channels and/or parallel plates, both Barrow's correlation and the present author's extension of the Spalding-Jayatilleke P-function method, with root mean square deviations of approximately 23% and 24% respectively, provided better results than the circular-tube correlations. Furthermore, for asymmetrical heat transfer in rectangular channels, the James-Martin-Martin correlation was found to be superior to all others with a root mean square deviation of approximately 13%. In the case of asymmetrical heat transfer in parallel plates, the present author's extension of the Spalding-Jayatilleke P-function method yielded better prediction than any existing correlation with a root mean square deviation of 17%.

ACKNOWLEDGEMENTS

The author is indebted to Dr. G. E. Sims for his supervision, valuable criticism, continuous encouragement and insurmountable patience. Thanks are also due to the University of Manitoba for the provision of a Postgraduate Fellowship.

TABLE OF CONTENTS

LIST OF FIGURES

LIST OF TABLES

NOMENCLATURE

Symbol	Meaning	Equation of first appearance
A	aspect ratio	(5.2)
b	a number	(6.6)
c	a constant	(3.22)
c_f	friction factor	(2.1)
c_p	specific heat at constant pressure	(3.1)
D	pipe diameter	(3.1)
D_e	hydraulic equivalent diameter	(2.4)
G	mass velocity	(3.1)
h	heat-transfer coefficient	(3.1)
k	(laminar) thermal conductivity	(3.1)
k_{tot}	total thermal conductivity	(3.12)
L	half of width of channel normal to heating surface	(4.4)
m	a number	(6.4)
N	number of data	(8.1)
n	a number	(6.1)
Nu	Nusselt number	(3.3)
P	quantity defined in equations (3.29), (4.16) and (5.10)	
PD_{rms}	percentage root mean square deviation	(8.1)
Pr	(laminar) Prandtl number	(3.3)
Pr_{tot}	total Prandtl number	(3.13)
Pr_{turb}	turbulent Prandtl number	(3.27)

$\dot{q}''$	heat flux	(3.11)
Re	Reynolds number	(2.2)
Re^*	laminar equivalent Reynolds number	(2.6)
s	channel spacing	(2.6)
St	Stanton number	(3.6)
T	absolute temperature	(6.4)
u	local time-mean velocity	(3.8)
$\bar{u}$	bulk velocity	(2.1)
u^+	local time-mean velocity, made dimensionless	(3.7)
$\bar{u}^+$	bulk velocity, made dimensionless	(3.21)
u_R^+	time-mean velocity at axis of pipe, made dimensionless	(3.23)
w	channel width	(2.6)
y	distance from and normal to wall	(3.9)
y^+	distance y, made dimensionless	(3.7)
Γ_{tot}	total thermal exchange coefficient	(3.11)
γ	a number	(4.1)
ε_{tot}	ratio of total viscosity to (laminar) dynamic viscosity	(3.16)
κ	a constant	(3.22)
μ	(laminar) dynamic viscosity	(3.1)
μ_R	viscosity ratio	(5.2)
μ_{tot}	total viscosity	(3.10)
ρ	density of fluid	(2.1)
τ_w	shear stress at wall	(2.1)
ϕ	specific enthalpy	(3.11)
$\bar{\phi}$	bulk value of ϕ over cross-section of flow	(3.25)

ϕ^+	specific enthalpy, made dimensionless	(3.18)
$\bar{\phi}^+$	bulk value of ϕ, made dimensionless	(3.26)
ϕ^*	geometry function	(2.7)

Subscripts

b	bulk condition
cp	constant-property condition
exp	experimental value
L	centre-line condition of rectangular channels or parallel plates
pred	predicted value
w	wall condition

CHAPTER 1

INTRODUCTION

The heat-transfer and flow friction characteristics for single-phase turbulent fluid flow in circular tubes have been the subject of a great deal of theoretical analysis and experimentation in the last seventy years. The circular passage has been analysed extensively because of its importance in technical application and because its simplicity makes it amenable to analysis. In recent years, rectangular channels and parallel plates have been used extensively in engineering systems, e.g. nuclear power reactors, solar energy collectors, compact heat exchangers, ventilating and air conditioning systems, etc. These applications may be under symmetrical or asymmetrical heating conditions. However, they have been investigated to a much lesser extent than the circular tubes.

The object of this present work is to obtain simple and directly-usable correlations for the prediction of symmetrical and asymmetrical heat transfer of single-phase turbulent flow in rectangular channels and parallel plates. Existing heat-transfer correlations for circular tubes, symmetrically and asymmetrically heated rectangular channels and parallel plates were reviewed. New correlations, based on the Spalding-Jayatilleke[22,43]*

---

* Superscript numbers refer to literature references listed in the thesis section entitled "References".

P-function concept, were developed by the present author for the symmetrically and asymmetrically heated parallel plates. The advantages of the Spalding-Jayatilleke method are that:

1. it is a delicate blend of theory and empiricism;
2. there is some distinct physical significance to the various terms appearing in the equation(s);
3. it is simple to use.

The approach for the selection of the best correlations for heat-transfer prediction was by comparison with all the available published experimental data.

The body of the work is divided into four major areas. In Chapter 2, the friction factor for turbulent flow in a rectangular geometry and parallel plates is discussed. In Chapter 3, 4 and 5, the heat-transfer correlations are outlined. The effect of fluid property variations on heat transfer is investigated in Chapter 6. Chapter 7, 8 and 9 consist of the test results, conclusions and recommendations.

CHAPTER 2

FRICTION FACTOR

2.1 General

In the solution of practically all heat-transfer convection problems, the corresponding fluid-dynamic problem must first be solved, if it is not indeed completely coupled to the heat-transfer problem. Although this work is not on viscous fluid dynamics, the friction factor in fully-developed turbulent non-circular duct flow is investigated in detail. The effect of the friction factor on heat transfer is demonstrated in the later chapters of this work.

2.2 Circular Tubes

2.2.1 Definition

Consider the steady flow of an imcompressible fluid in a long circular tube. Let the bulk velocity be $\bar{u}$. The friction factor, c_f, is defined by

$$c_f \equiv \frac{\tau_w}{\frac{1}{2}\rho\bar{u}^2} \tag{2.1}$$

where τ_w is the shear stress at the tube wall and ρ is the density of the fluid.

2.2.2 Developed Turbulent Flow

For turbulent flow in smooth tubes, Blasius's empirical formula[31] gives

$$c_f = 0.079\ Re^{-\frac{1}{4}} \qquad (2.2)$$

where Re is the Reynolds number. It agrees closely with experimental results for Reynolds numbers between 3000 and 10^5. It is both explicit and simple to apply. With some theoretical foundation, the Karman-Nikuradse[24] (also known as Karman-Prandtl and Prandtl-Nikuradse) formula gives

$$\frac{1}{\sqrt{c_f}} = 4.0 \log_{10}(Re\sqrt{c_f}) - 0.4 \qquad (2.3)$$

Equation (2.3) is inconvenient to use because one cannot solve it directly for c_f. The two formulas (2.2) and (2.3) are plotted in Figure 2.1. They agree very well with one and other for Reynolds numbers between 4000 and 10^5.

2.3. Rectangular Channels and Parallel Plates

It is quite customary to apply the concept of hydraulic equivalent diameter in the calculation of friction factor for developed turbulent flow in channels of

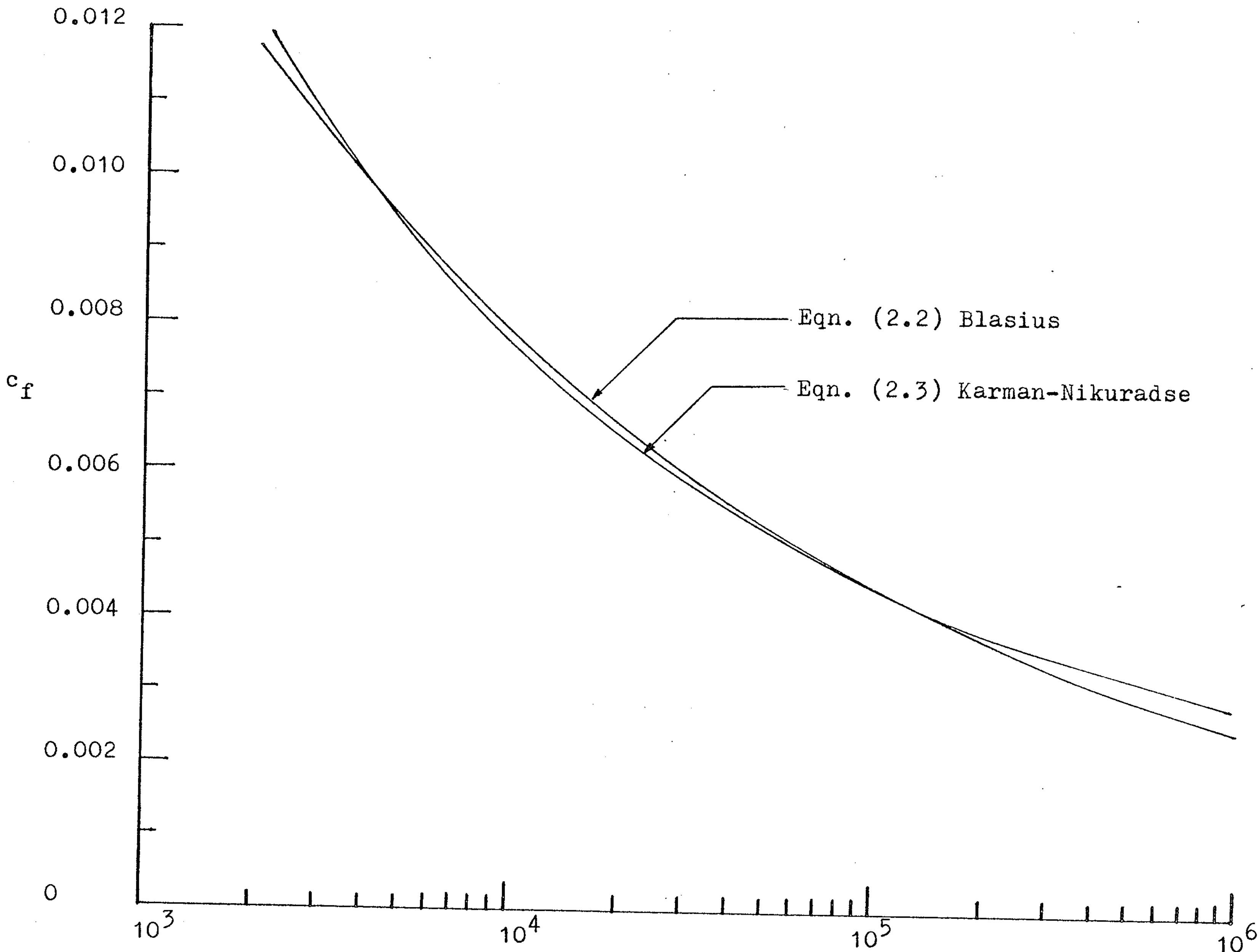

Fig. 2.1 Friction Factor

rectangular or other non-circular cross-section[33]. The hydraulic equivalent diameter, D_e, is defined as

$$D_e \equiv 4 \times \frac{\text{Flow Area}}{\text{Perimeter}} \qquad (2.4)$$

However, there have also been theoretical analyses[12] and experiments[16,29] which indicate significant errors may result . Because of these contradictory reports, a review of the literature was done by the present author, as summarized in Table 2.1. Some of the more recent and important papers are discussed in the rest of this chapter.

In 1962, Hartnett et al.[17] made a detailed survey of the literature. In addition, friction factors for ducts of aspect ratio 1:1, 5:1 and 10:1 were predicted by the method of Deissler[10] and Deissler and Taylor[11], and experiments were also performed on these ducts. The calculated and measured results were found to be in agreement for ducts having large aspect ratios. As for aspect ratios less than 5:1, the predicted values of friction factor were lower than the experimental data, with a maximum difference of only 12% evident for the square duct. A plot was made by Hartnett et al. to compare the Blasius correlation with all available experimental data. Those data included

Table 2.1 Investigations on Friction Factor

1. Rectangular Channels

Investigator(s)	Year	Ref.	Test Fluid	Dimensions inches	D_e inches	Re	Channel Length / D_e
Schiller	1923	(41)	Water	0.709x 0.709	0.709	8.6×10^2 to 3.8×10^4	56
				1.098x 0.312	0.486	6.4×10^2 to 5.8×10^4	162
Cornish	1928	(7)	Water	0.464x 0.159	0.237	2.7×10^2 to 6.37×10^4	200
Lea & Tadros	1931	(28)	Water	0.257x 0.257	0.257	3.8×10^2 to 1.6×10^4	-
				0.371x 0.158	0.222	3.5×10^2 to 1.3×10^4	
Allen & Grundberg	1937	(1)	Water	1.004x 0.256	0.410	5.52×10^2 to 3.116×10^3	440
Washington & Marks	1937	(46)	Air	0.563x 5.0	1.010	3.57×10^3 to 3.88×10^4	48
Nikuradse	1939	(35)	Water	1.102x 0.315	0.489	8.8×10^2 to 10^5	-

Table 2.1 (cont'd)

Investigator(s)	Year	Ref.	Test Fluid	Dimensions inches	D_e inches	Re	Channel Length / D_e
Huebscher	1947	(20)	Air	7.88x 7.88	7.88	$5x10^4$ to $5x10^5$	84
				4.46x 36	8.0	$1.8x10^4$ to $4.9x10^5$	84
Eckert & Irvine	1957	(15)	Air	1.5x0.5	0.75	$1.4x10^2$ to $1.4x10^4$	184
Hartnett et al.	1962	(17)	Air	0.5635x 0.5635	0.5635	10^3 to $1.2x10^5$	256
				0.3115x 1.551	0.518	"	278
				0.3115x 3.112	0.566	"	254
Leu-theusser	1963	(29)	Air	3.0x3.0	3.0	10^4 to 10^5	288
				3.0x9.0	4.5	"	192
Maurer & LeTourneau	1964	(32)	Water	0.087x 1.0	1.6	$4x10^3$ to $5x10^5$	169
Brundrett & Burroughs	1967	(5)	Air	3.767x 3.767	3.767	$3x10^4$ to $8x10^4$	96
Jones	1975	(23)	Water	26:1	-	$7x10^3$ to 10^5	260
				31:1	-		500
				12.8:1	-		-

Table 2.1 (cont'd)

2. Parallel Plates

Inves-tigator(s)	Year	Ref.	Test Fluid	Dimen-sions inches	D_e inches	Re	Channel Length / D_e
Davies & White	1928	(8)	Water	37:1 to 169:1	0.522 to 0.0117	1.25×10^2 - 9.2×10^3	38 to 170
Washington & Marks	1937	(46)	Air	0.25x5.0	0.476	1.04×10^3 - 2.8×10^4	101
				0.125x 5.0	0.244	4.12×10^2 - 1.7×10^4	197
Whan & Rothfus	1959	(47)	Water	0.7x 14.0	1.333	8×10^2 - 4×10^4	180
Barrow	1962	(3)	Air	9.3x 0.32	0.62	10^4 - 2.5×10^4	156
Patel & Head	1969	(37)	Air	0.25x 12.0	0.49	2×10^2 - 8×10^3	147

Year: 1923 - 1962

Aspect Ratio: 1:1 - 169:1

Reynolds Number: $1.25 \times 10^2 - 5 \times 10^5$

It was concluded by Hartnett et al. that, with the hydraulic equivalent diameter, the Blasius circular tube correlation accurately predicts the friction factor for flow through rectangular channels at any aspect ratio for Reynolds numbers between 6×10^3 and 5×10^5. Maurer and LeTourneau[32] did experiments on narrow rectangular channels at Reynolds numbers from 4×10^3 to 5×10^5. Their results were in agreement with the works of Hartnett et al., i.e the concept of hydraulic equivalent diameter can be applied. Barrow[3] suggested the using of hydraulic equivalent diameter with the Blasius correlation for parallel plates.

However, the presence of secondary currents in turbulent non-circular conduit flow[4,19] made it doubtful that a single unique resistance law, such as the Blasius equation, could describe friction phenomena in rectangular channels by simply using the hydraulic equivalent diameter as the characteristic length parameter. In Leutheusser's work[29], it was found that, by using hydraulic equivalent diameter, the function relating friction factor with Reynolds number was not unique. He considered the conventional use of hydraulic equivalent diameter not only implied absence of shape effects on the resistance function, but also presumed the existence of wall and Reynolds similarity in the general case of channel flow. His experimental results showed that there was a trend toward a more rapid decrease of friction factor with increasing Reynolds number as compared to the Karman-Nikuradse equation. For Reynolds numbers greater than approximately 5×10^4, all the data lay consistently below the Karman-Nikuradse line by about 20%. Brundrett and Burroughs[5] also found that, with the explanation of stagnation in the duct corners, the friction factor was slightly lower for square ducts as compared with circular tubes for Reynolds numbers between 3×10^4 and 8×10^4. Although these authors have disproved the use of hydraulic equivalent diameter with circular tube correlation, they did not suggest new equations. As for turbulent flow between parallel plates, Patel and Head[37] pointed out the inaccuracy in measurements of the early researchers and proposed a new correlation

$$c_f = 0.0376 \, Re^{1/6} \qquad (2.5)$$

for Re greater than 2.8×10^3 and hydraulic equivalent diameter as the length parameter. However, the Reynolds numbers of their experiments were never greater than 10^4.

Jones[23] obtained friction factor data for channels having aspect ratios between unity and 39:1 in the literature and, in conjunction with his new experimental data, examined for deviations from the smooth circular tube line. It was found that at constant Reynolds number (based on hydraulic equivalent diameter) the friction factor increases monotonically with increasing aspect ratio. It was thus concluded by Jones that the hydraulic equivalent diameter is not the proper length dimension to use in Reynolds number to insure similarity between the circular and rectangular channels. Instead, it was determined that if a modified Reynolds number, Re*, was obtained so that geometric similarity was provided in laminar flow by the relation $c_f = 16/Re^*$ for all geometries, that this Reynolds number also provided good similarity in fully developed turbulent flow within an approximately 5% scatter band about the smooth tube line. By using this "laminar equivalent Reynolds number", Re*, Jones stated that circular tube methods may be readily applied to rectangular ducts thereby eliminating large errors in estimation of friction factor.

Mathematically,

$$Re^* = \phi^*(\frac{w}{s})\ Re \qquad (2.6)$$

where w is the channel width, s is the channel spacing, Re is as before and the geometry function $\phi^*(\frac{w}{s})$ is given by

$$\phi^*\left(\frac{w}{s}\right) = \frac{2}{3}\left(1 + \frac{s}{w}\right)^2 \left\{1 - \frac{192}{\pi^5}\frac{s}{w}\right.$$

$$\left.\sum_{n=0}^{\infty} \frac{1}{(2n+1)^5}\tanh\frac{(2n+1)\pi w}{2s}\right\} \qquad (2.7)$$

The function $\phi^*\left(\frac{w}{s}\right)$ is shown graphically in Figure 2.2. An approximate relationship which will give $\phi^*\left(\frac{w}{s}\right)$ within about 2% is

$$\phi^*\left(\frac{w}{s}\right) \approx \frac{2}{3} + \frac{11}{24}\frac{s}{w}\left(2 - \frac{s}{w}\right) \qquad (2.8)$$

In this present work, the hydraulic equivalent diameter concept was adopted because it is widely used and easy to apply. Furthermore, correction of friction factor for rectangular channels and parallel plates as proposed by the Jones method[23] was also considered.

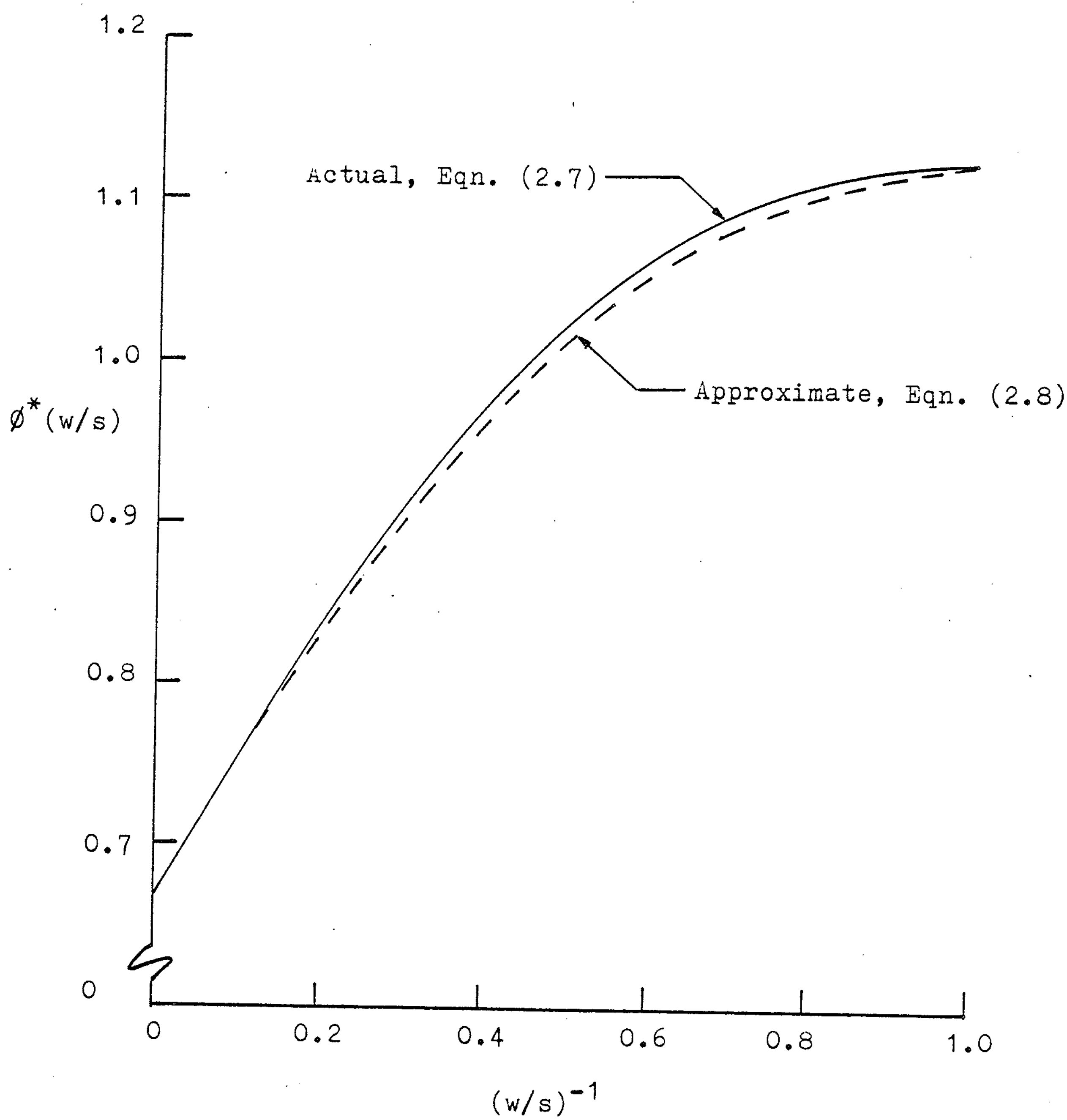

Fig. 2.2 Geometry Function for Calculation of Laminar Equivalent Reynolds Number

CHAPTER 3

CIRCULAR TUBE HEAT-TRANSFER THEORY

3.1 General

There is a voluminous literature on the subject of heating or cooling of fluids inside circular tubes, and many design equations of varying degrees of generality are available. In the calculation of heattransfer in turbulent non-circular duct flow, the practice until recently has been to use circular-tube correlations on the assumption that they can be applied by using the concept of hydraulic equivalent diameter. This practice has been adopted for both symmetrical and asymmetrical heat-transfer conditions. In this chapter, circular-tube heat-transfer correlations are investigated.

3.2 Correlations Obtained from Dimensional Analysis

For turbulent flow in tubes, dimensional analysis gives

$$\frac{hD}{k} \doteq f\left(\frac{DG}{\mu}, \frac{c_p \mu}{k}\right) \tag{3.1}$$

where the function is to be determined experimentally. For moderate temperature differences between fluid and tube surface, the Dittus-Boelter[13] and Sieder-Tate[42] equations are commonly used. The Dittus-Boelter equation evaluates all physical properties at the bulk temperature of the fluid

$$\frac{hD}{k_b} = 0.024 \left(\frac{DG}{\mu_b}\right)^{0.8} \left(\frac{c_p\mu}{k}\right)_b^{0.4} \tag{3.2}$$

or

$$Nu = 0.024Re^{0.8}Pr^{0.4} \tag{3.3}$$

The Sieder-Tate equation evaluates all physical properties at the bulk temperature, except μ_w in a viscosity-ratio term

$$\frac{hD}{k_b} = 0.027 \left(\frac{DG}{\mu_b}\right)^{0.8} \left(\frac{c_p\mu}{k}\right)_b^{0.33} \left(\frac{\mu_b}{\mu_w}\right)^{0.14} \tag{3.4}$$

or

$$Nu = 0.027Re^{0.8}Pr^{0.33}\left(\frac{\mu_b}{\mu_w}\right)^{0.14} \tag{3.5}$$

3.3 The Petukhov and Popov Equation

Petukhov and Popov[39] used the integral formulation developed by Lyon[27] and numerically solved for the Stanton number using velocity distribution and eddy diffusivity equations proposed by Reichardt[40]. They then developed a Stanton number equation which reasonably approximated the values yielded by their numerical solution. Their recommended equation is

$$St = \frac{\frac{c_f}{2}}{1.07 + 12.7\sqrt{\frac{c_f}{2}}(Pr^{2/3} - 1)} \tag{3.6}$$

where the friction factor, c_f, may be calculated from the Karman-Nikuradse equation

$$\frac{1}{\sqrt{c_f}} = 4.0 \log_{10} (Re\sqrt{c_f} - 0.4) \tag{2.3}$$

and St is the Stanton number defined as h/Gc_p.

3.4 The Spalding-Jayatilleke P-Function

Spalding and Jayatilleke[22,43] referred to the extra resistance to heat transfer in the viscous sublayer (see Figure 3.1) of a turbulent flow as $Pr_{turb}P$. A relationship was developed between P and essentially the laminar Prandtl number of the fluid. Then, from the P-function, the Stanton number of the fluid can be calculated. It is beneficial to review their work in detail here because in the next two chapters, the present author extends the P-function to symmetrical and asymmetrical heating conditions in parallel plates.

Based on the observation that pipe velocity profiles resemble that of a Couette flow remarkably, Spalding and Jayatilleke[22,43] applied the Couette flow analysis to pipe flows.

From dimensional analysis, the velocity profile is

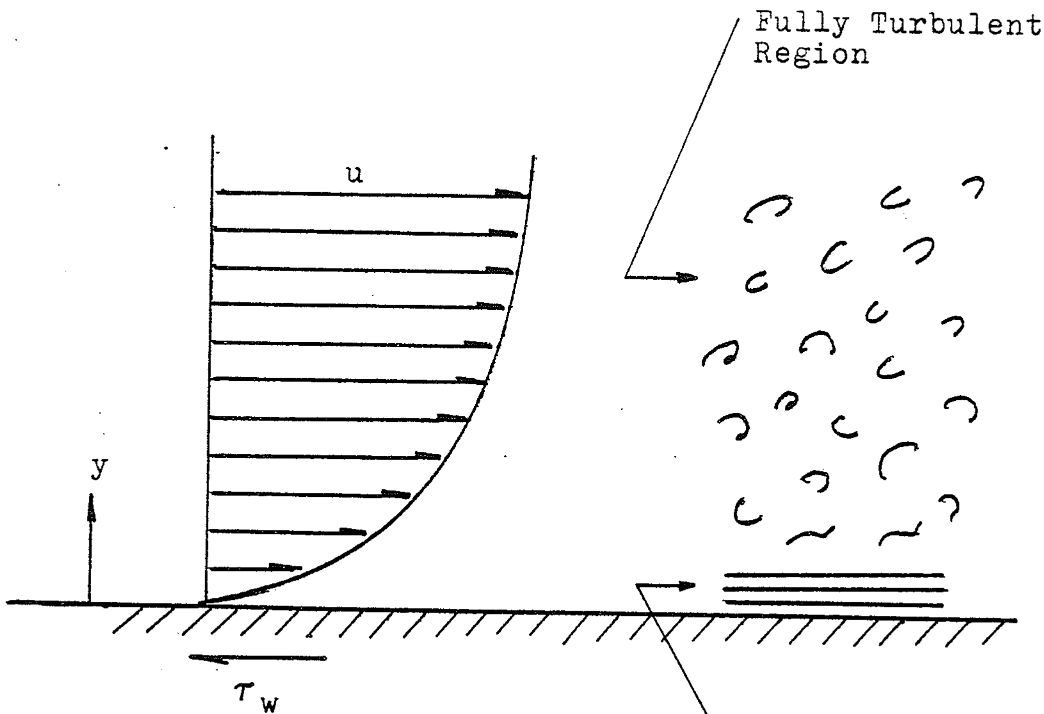

Fig. 3.1 Velocity Profile

expressible by a unique relationship of the form

$$u^+ = u^+(y^+) \tag{3.7}$$

where
$$u^+ \equiv \frac{u}{\sqrt{\frac{\tau_w}{\rho}}} \tag{3.8}$$

and
$$y^+ \equiv \frac{y\sqrt{\tau_w \rho}}{\mu} \tag{3.9}$$

A total viscosity, μ_{tot}, is defined by

$$\mu_{tot} \equiv \frac{\tau}{\frac{du}{dy}} \tag{3.10}$$

and a total thermal exchange coefficient, Γ_{tot}, of specific enthalpy, ϕ, by

$$\Gamma_{tot} \equiv \frac{\dot{q}''_w}{\frac{d\phi}{dy}} \tag{3.11}$$

where $\dot{q}''_w$ is the heat flux from wall into the fluid stream. So,

$$\Gamma_{tot} = \frac{k_{tot}}{c_p} \tag{3.12}$$

where k_{tot} is the total thermal conductivity and c_p the specific heat at constant pressure of the fluid.

The total Prandtl number, Pr_{tot}, is defined by

$$Pr_{tot} \equiv \frac{\mu_{tot}}{\Gamma_{tot}} \tag{3.13}$$

or $$Pr_{tot} = \frac{\mu_{tot} c_p}{k_{tot}} \tag{3.14}$$

Dimensional analysis leads to the result

$$Pr_{tot} = Pr_{tot}(y^+, Pr) \tag{3.15}$$

where Pr is the laminar Prandtl number of the fluid. The dimensionless total viscosity, $\frac{\mu_{tot}}{\mu}$, is however a function of y^+ alone i.e.

$$\frac{\mu_{tot}}{\mu} = \varepsilon_{tot}(y^+) \tag{3.16}$$

By virtue of the constancy of shear stress and heat flux in Couette flow, it may be shown that

$$\frac{\mu_{tot}}{\mu} = \varepsilon_{tot} = \frac{dy^+}{du^+} \tag{3.17}$$

and $$\frac{\varepsilon_{tot}}{Pr_{tot}} = \frac{dy^+}{d\phi^+} \tag{3.18}$$

where $$\phi^+ \equiv \frac{(\phi - \phi_w)\sqrt{\tau_w \rho}}{\dot{q}''_w} \tag{3.19}$$

By elimination of ε_{tot} from equations (3.17) and (3.18), there is obtained the important result

$$\phi^+ = \int_0^{u^+} Pr_{tot} du^+ \tag{3.20}$$

In principle, $\emptyset^+$ can be evaluated, since Pr_{tot} can be related to u^+ by means of equations (3.7) and (3.15).

The friction factor, c_f, as defined in section 2.2.1 is

$$c_f = \frac{\tau_w}{\frac{1}{2} \rho \bar{u}^2} \qquad (2.1)$$

or

$$\frac{c_f}{2} = \left(\frac{1}{\bar{u}^+}\right)^2 \qquad (3.21)$$

Since the $u^+(y^+)$ relationship is normally taken as having the form[25]

$$u^+ = \frac{1}{\kappa} \ln y^+ + c \qquad (3.22)$$

over the great part of the pipe area, it can be shown that, for circular pipe,

$$\bar{u}^+ = u_R^+ - \frac{3}{2\kappa} \qquad (3.23)^*$$

where u_R^+ is the dimensionless centre-line velocity and κ is a constant, usually taken as equal to 0.4.

Then it follows from equations (3.21) and (3.23) that

$$\frac{1}{\sqrt{\frac{c_f}{2}}} = u_R^+ - \frac{3}{2\kappa} \qquad (3.24)$$

The Stanton number is defined by

$$St \equiv \frac{\dot{q}''_w}{(\emptyset_w - \bar{\emptyset})\, \rho \bar{u}} \qquad (3.25)$$

* Appendix A Section A.1 shows the derivation of equation (3.23)

which can be reduced to

$$St \equiv \frac{1}{\bar{\phi}^+ \bar{u}^+} \tag{3.26}$$

where $\bar{\phi}$ is the mixed mean value of ϕ over the pipe cross-section and $\bar{\phi}^+$ the corresponding non-dimensional value. It is possible to derive a relation between $\bar{\phi}^+$ and ϕ_R^+ on the basis of the $\phi^+ \sim y^+$ relation being logarithmic over most of the stream as a consequence of Pr_{tot} having a constant value Pr_{turb} within the turbulent core*, this being

$$\bar{\phi}^+ = \phi_R^+ - Pr_{turb}\left(\frac{3}{2\kappa} - \frac{5}{4\kappa^2 \bar{u}^+}\right) \tag{3.27**}$$

From equations (3.20), (3.21), (3.23), (3.26) and (3.27), there is a relationship between the friction factor and the Stanton number,

$$\frac{\sqrt{\frac{c_f}{2}}}{St} = \int_0^{u_R^+} (Pr_{tot} - Pr_{turb})du^+ + \frac{Pr_{turb}}{\sqrt{\frac{c_f}{2}}}\left(1 + \frac{5}{4\kappa^2} \cdot \frac{c_f}{2}\right)$$

(3.28)#

---

* Appendix A, Section A.2 demonstrates that Pr_{turb} = constant in the turbulent core.

** Appendix A, Section A.3 shows the derivation of equation (3.27)

\# Appendix A, Section A.4 shows the derivation of equation (3.28)

The term on the left-hand side, being proportional to the inverse of the Stanton number, represents the total resistance to transfer of ϕ. The right-hand side is the sum of two resistances in series. The latter term is what would remain if Pr_{tot} was made equal to Pr_{turb} over the whole cross-section of the circular pipe. The first term of the right-hand side then represents the extra thermal resistance which arises solely due to any differences between Pr_{tot} and Pr_{turb}. P is defined as

$$P \equiv \int_0^{u_R^+} \left(\frac{Pr_{tot}}{Pr_{turb}} - 1\right) du^+ \qquad (3.29)$$

It is known from experiment that Pr_{tot} differs significantly from Pr_{turb} only in the region very close to the wall ($0 \leq u^+ \leq 20$), i.e. in the "viscous sublayer". Pr_{turb} P therefore represents the extra thermal resistance offered by the viscous sublayer on account of the total Prandtl number in it being different from that in turbulent core.

Equation (3.28) can now be written as

$$\frac{\sqrt{\frac{c_f}{2}}}{St} = Pr_{turb}\, P + \frac{Pr_{turb}}{\sqrt{\frac{c_f}{2}}}\left(1 + \frac{5}{4\kappa^2}\,\frac{c_f}{2}\right) \qquad (3.30)$$

Spalding and Jayatilleke[22, 43] recommend

$$P = 9.24 \left\{ \left(\frac{Pr}{Pr_{turb}}\right)^{3/4} - 1 \right\} \tag{3.31}$$

$$Pr_{turb} = 0.9$$

$$\kappa = 0.4$$

and c_f can be calculated by the use of Karman-Nikuradse equation. Equation (3.31) is a simplified formula for

$$P = 9.24 \left\{ \left(\frac{Pr}{Pr_{turb}}\right)^{3/4} - 1 \right\} \times \left\{ 1 + 0.28 \exp\left(-0.007\frac{Pr}{Pr_{turb}}\right) \right\} \tag{3.32}$$

By substituting P, Pr_{turb}, κ , c_f into equation (3.30), the value of Stanton number can be obtained.

CHAPTER 4

PARALLEL - PLATE THEORY WITH SYMMETRICAL HEATING

4.1 General

Correlations which are equivalent to those such as Dittus-Boelter[13] or Sieder-Tate[42] for turbulent flow in rectangular channels and parallel plates are practically unavailable. The present author could find only Barrow's work[2] in the literature. Because of the scarcity of existing equations, a new correlation for parallel-plate symmetrical heating is developed by the present author in this chapter. This new correlation is basically an extension of the Spalding-Jayatilleke[22,43] P-function (see Section 3.4 and Appendix A) to cover the parallel-plate geometry. The parallel-plate configuration is selected because this avoids the complication of secondary flows and makes the assumption of one-dimensional flow analysis applicable.

4.2 Barrow Equation

Barrow[2] determined the heat-transfer coefficient by Mizushina's[34] extension of Reynolds analogy between the transfer of heat and the transfer of momentum. The velocity distribution was divided in two regions: for viscous sublayer,

$$u^+ = y^+$$

and for turbulent core

$$u^+ = 6.2 \log y^+ + 3.6$$

No account was taken of the buffer or transition zone. His semi-theoretical analysis results in the following equation for turbulent flow between parallel plates.

$$Nu = \frac{0.1986\ Re^{7/8} Pr}{5.03(2+\gamma)Re^{1/8} + 9.74\left\{Pr - (2+\gamma)\right\}} \qquad (4.1)$$

The Reynolds number is based on the hydraulic equivalent diameter of the parallel plates. Barrow stated that equation (4.1) is applicable to both symmetrical or asymmetrical heating conditions depending on the value of γ, where γ equals the heat transfer at one surface divided by the heat transfer at the other surface. For symmetrical heating, γ is equal to -1. As a result, equation (4.1) can be re-written as

$$Nu = \frac{0.1986\ Re^{7/8} Pr}{5.03\ Re^{1/8} + 9.74(Pr - 1)} \qquad (4.2)$$

4.3 Extension of Spalding-Jayatilleke P-Function

4.3.1 The Friction Factor

Following Spalding and Jayatilleke's work (see Section 3.4 and Appendix A), $\bar{u}$ is defined through

$$(\text{Area})\rho\bar{u} = \rho\int_{\text{Area}} u\,d(\text{Area}) \qquad (4.3)$$

For parallel plates, area per unit width = 2L (see Figure 4.1) Then equation (4.3) becomes

$$2L\rho\bar{u} = 2\rho\int_0^L u\,.dy \qquad (4.4)$$

Using the equivalent dimensionless parameters, equation (4.4) can be re-written as

$$\bar{u}^+ = \frac{1}{y_L^+}\int_0^{y_L^+} u^+\,dy^+ \qquad (4.5)$$

Substitution of the logarithmic expression for u^+, i.e. equation (3.22), into equation (4.5) and integration yields the relationship between bulk velocity $\bar{u}^+$ and centre-line velocity u_L^+ as

$$\bar{u}^+ = u_L^+ - \frac{1}{\kappa} \qquad (4.6)$$

Again defining c_f as in equation (2.1) and u^+ in the usual way, it then follows from equations (3.21) and (4.6) that

$$\frac{1}{\sqrt{\frac{c_f}{2}}} = u_L^+ - \frac{1}{\kappa} \qquad (4.7)$$

4.3.2 <u>The Stanton Number</u>

For the case of heat transfer, parallel to

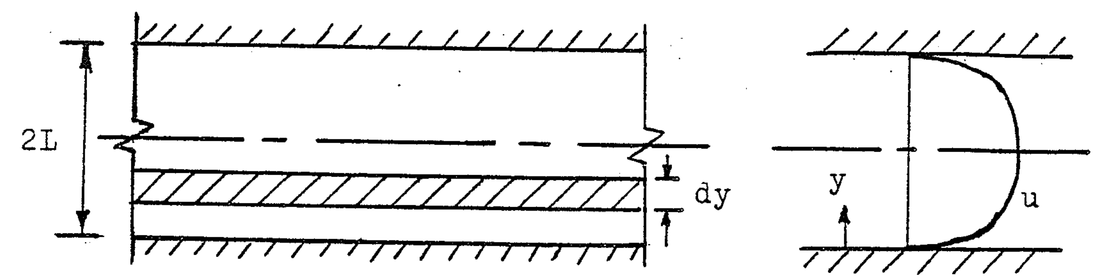

Fig. 4.1 Parallel Plates

equation (4.3), it can be stated that

$$(\text{Area})\rho\bar{u}\,\bar{\phi} = \rho\int_{\text{Area}} u\phi\, d(\text{Area}) \tag{4.8}$$

or,

$$\bar{u}^+\,\bar{\phi}^+ = \frac{1}{y_L^+}\int_0^{y_L^+} u^+\,\phi^+\,dy^+ \tag{4.9}$$

Now,

$$u^+ = \frac{1}{\kappa}\ln y^+ + c \tag{3.22}$$

over most of the flow area. The profile of ϕ (and temperature) is shown in Figure 4.2.

Again,

$$\phi^+ = \int_0^{u^+} Pr_{tot}\,du^+ \tag{3.20}$$

For obtaining $\bar{\phi}^+$, one uses

$$\phi^+ = Pr_{turb}\,u^+ \tag{4.10}$$

since over most of the cross-section (the turbulent core) Pr_{tot} has the constant value Pr_{turb}.

Substitution of equations (3.22) and (4.10) into (4.9) and integration yields

$$\bar{u}^+\,\bar{\phi}^+ = Pr_{turb}\left\{\frac{1}{\kappa^2}\ln^2 y_L^+ - \frac{2}{\kappa}\left(\frac{1}{\kappa} - c\right)\ln y_L^+ + \left(\frac{2}{\kappa^2} - \frac{2c}{\kappa} + c^2\right)\right\}$$

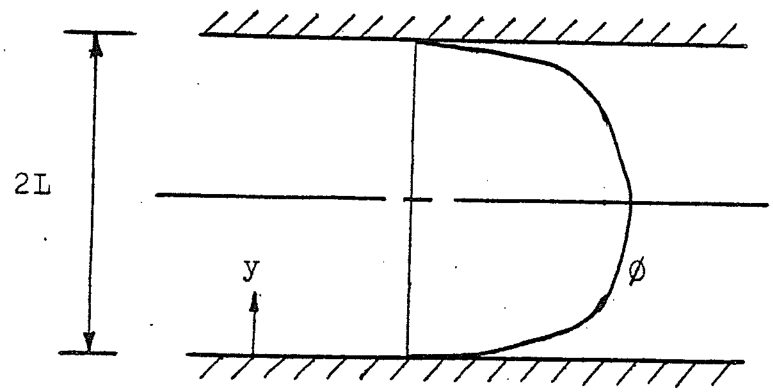

Fig. 4.2 Profile of ø (and Temperature)

With $u_L^+ = \frac{1}{\kappa}\ln L^+ + c$, equation (4.6) and $\emptyset_L^+ = Pr_{turb}\, u_L^+$, the above expression becomes

$$\bar{\emptyset}^+ = \emptyset_L^+ - Pr_{turb}\left(\frac{1}{\kappa} - \frac{1}{\kappa^2 \bar{u}^+}\right) \tag{4.11}$$

From equations (4.11) and (3.20) written at L, the following equation is obtained:

$$\bar{\emptyset}^+ = \int_0^{u_L^+} (Pr_{tot} - Pr_{turb})\,du^+ - Pr_{turb}\left(\frac{1}{\kappa} - \frac{1}{\kappa^2 \bar{u}^+}\right) + \int_0^{u_L^+} Pr_{turb}\,du^+ \tag{4.12}$$

Combining equations (3.21) and (3.26)

$$\bar{\emptyset}^+ = \frac{\sqrt{\frac{c_f}{2}}}{St} \tag{4.13}$$

is obtained. The last term of equation (4.12), with equations (4.6) and (3.21), becomes

$$\int_0^{u_L^+} Pr_{turb}\,du^+ = Pr_{turb}\left(\frac{1}{\sqrt{\frac{c_f}{2}}} + \frac{1}{\kappa}\right) \tag{4.14}$$

Substitution of equations (4.13) and (4.14) into (4.12) yields

$$\frac{\sqrt{\frac{c_f}{2}}}{St} = \int_0^{u_L^+} (Pr_{tot} - Pr_{turb})\,du^+ + \frac{Pr_{turb}}{\sqrt{\frac{c_f}{2}}}\left(1 + \frac{1}{\kappa^2}\cdot\frac{c_f}{2}\right) \tag{4.15}$$

Using Spalding-Jayatilleke's concept of "extra thermal resistance" of the viscous sublayer (first term on the right-hand side of equation (4.15)) and the definition,

$$P \equiv \int_0^{u_L^+} \left(\frac{Pr_{tot}}{Pr_{turb}} - 1\right) du^+ \qquad (4.16)$$

one can re-state equation (4.15) as

$$\frac{\sqrt{\frac{c_f}{2}}}{St} = Pr_{turb}\, P + \frac{Pr_{turb}}{\sqrt{\frac{c_f}{2}}} \left(1 + \frac{1}{\kappa^2} \cdot \frac{c_f}{2}\right) \qquad (4.17)$$

With the proper values of P, Pr_{turb}, κ and c_f, the Stanton number for symmetrical heating in parallel plates can be calculated by means of equation (4.17).

CHAPTER 5

PREDICTIVE METHOD WITH ASYMMETRICAL HEATING

5.1 General

As in the case of symmetrical heating, there are very few correlations for asymmetrical heating in rectangular channels and parallel plates. Barrow's work[2,3] involves an analytical solution with an experimental comparison. James et al.[21] proposed an experimentally-determined correlation. Here again, the present author develops a further extension of the Spalding-Jayatilleke P-function (see Section 3.4, 4.3 and Appendix A) to cover asymmetrical heating in parallel-plates.

5.2 Barrow Equation

As mentioned in Section 4.2, equation (4.1) is applicable to both symmetrical and asymmetrical heating conditions for turbulent flow between parallel plates. Equation (4.1) is repeated here:

$$Nu = \frac{0.1986\ Re^{7/8}\ Pr}{5.03\ (2+\gamma)\ Re^{1/8} + 9.74 \left\{ Pr - (2+\gamma) \right\}} \tag{4.1}$$

In the case of asymmetrical heating where one surface is heated while the opposite one is insulated, the value of γ is equal to zero. Thus, equation (4.1) becomes

$$Nu = \frac{0.1986\ Re^{7/8}\ Pr}{10.06\ Re^{1/8} + 9.74\ (Pr - 2)} \tag{5.1}$$

5.3 James-Martin-Martin Equation

James et al.[21] carried out experiments on heat transfer from one side of a rectangular-section duct to an internally flowing fluid. A correlation for the data was developed in terms of the Nusselt, Reynolds and Prandtl numbers and the viscosity and aspect ratio of the duct, based purely on experimental results. The correlation is

$$Nu = \frac{0.104\ Re^{0.0016Pr + 0.75}\ Pr^{0.4}\ \mu_R^{213\ Re^{-0.9}}}{e^{0.0134Pr}(2.05 + 1.62\ e^{-A})} \tag{5.2}$$

The aspect ratio, A, is defined by

$$A \equiv \frac{\text{Width of channel normal to heating surface}}{\text{Breadth of heating surface}} \tag{5.3}$$

The viscosity ratio $\mu_R = \frac{\mu_b}{\mu_w}$ where μ_b is the viscosity evaluated at the bulk temperature and μ_w is the viscosity evaluated at the temperature of the heat-transfer surface. The Reynolds number is based on the hydraulic equivalent diameter. The recommended range of validity of equation (5.2) is over the following ranges of Prandtl and Reynolds numbers and viscosity and aspect ratios:

	With reasonable certainty	With moderate confidence
Re:	$3 \times 10^3 - 1 \times 10^5$	$3 \times 10^3 - 2 \times 10^5$
Pr:	6.5 - 100	0.7 - 100
A :	0.5 - 4.0	Any value
μ_R:	1.5 - 9	1 - 10

5.4 Extension of Spalding-Jayatilleke P-Function

5.4.1 Velocity and Temperature Distributions

In the case of asymmetrical heating, the velocity and temperature profiles are dissimilar as illustrated in Fig. 5.1. The wall distance where the local temperature equals the bulk temperature of fluid is different from the wall distance where the local velocity equals the average velocity. In order to have a relatively simple analytical solution without sacrificing much accuracy, the present author assumes two approximated ϕ (and temperature) profiles.

In Figure 5.2(A), the ϕ profile is

$$\phi^+ = \phi_L^+ \text{ for } 0 \leq y \leq 2L \tag{5.4}$$

Figure 5.2(B) shows a profile which consists of two portions:

$$\phi^+ = \int_0^{u^+} Pr_{tot}\, du^+ \text{ for } 0 < y \leq L \tag{5.5}$$

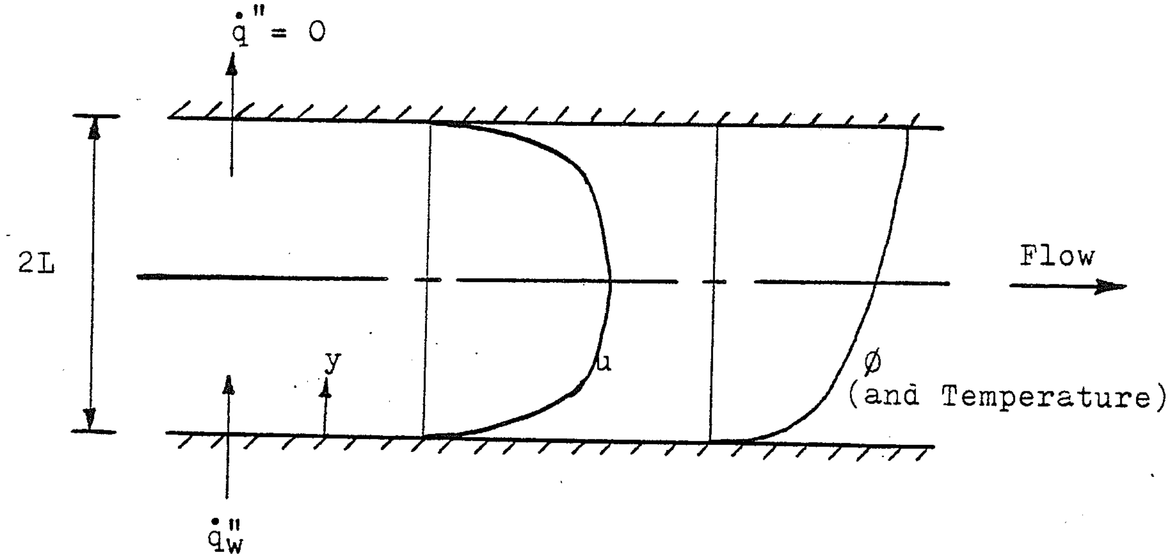

Fig. 5.1 Asymmetric Heating

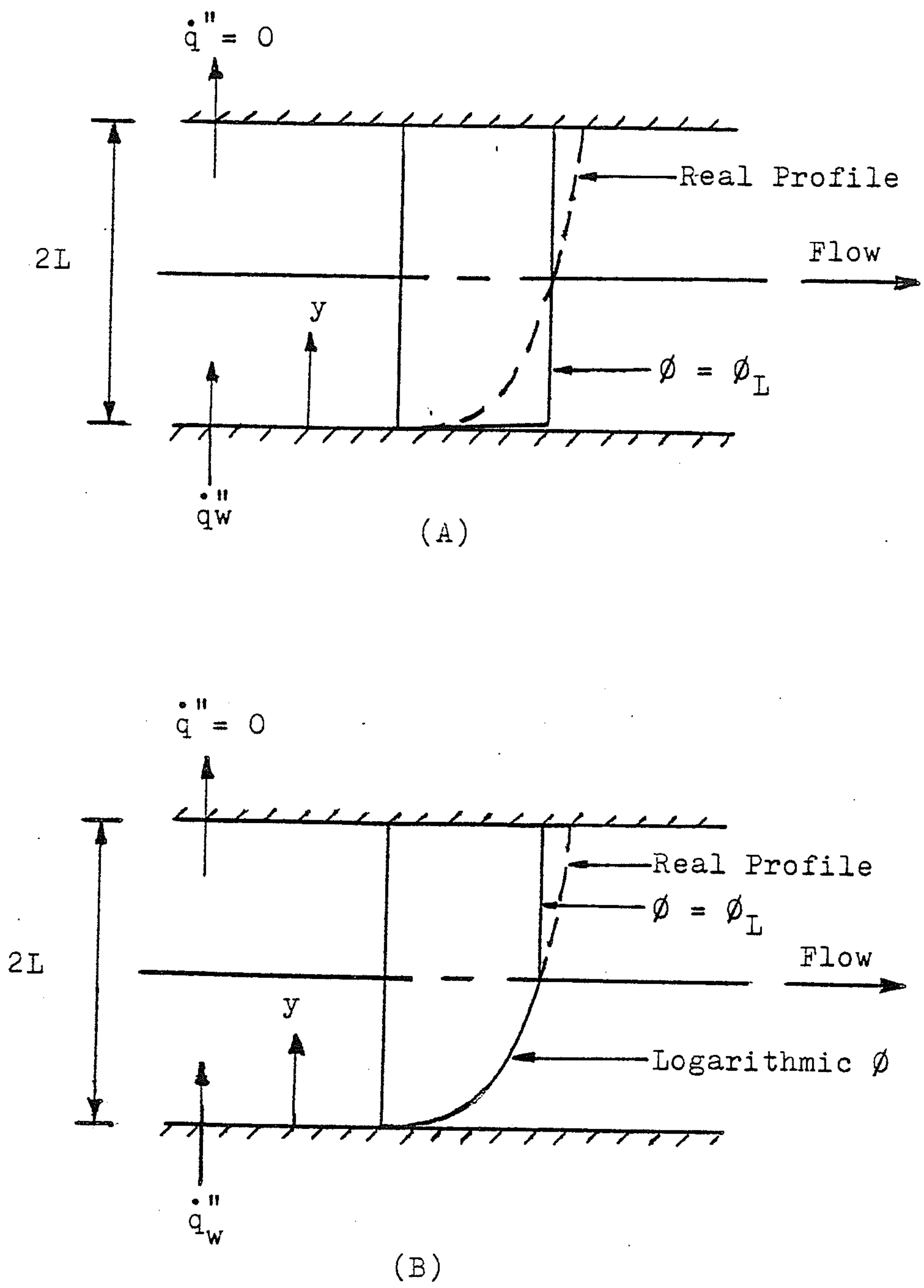

Fig. 5.2 Profiles of $\emptyset$ (and Temperature)

and $\qquad \phi^+ = \phi_L^+ \qquad$ for $L \leqslant y \leqslant 2L$ $\qquad$ (5.6)

For identification purpose, Figure 5.2(A) is referred to as the uniform temperature profile while Figure 5.2(B) as the two-portion temperature profile.

5.4.2 <u>The Uniform Temperature Profile</u>

From equation (5.4), it is obvious that

$$\bar{\phi}^+ = \phi_L^+ \tag{5.7}$$

The expression for ϕ_L^+, based on equation (3.20), is

$$\phi_L^+ = \int_0^{u_L^+} Pr_{tot}\, du^+$$

Thus,

$$\bar{\phi}^+ = \int_0^{u_L^+} (Pr_{tot} - Pr_{turb})\, du^+ + \int_0^{u_L^+} Pr_{turb}\, du^+ \tag{5.8}$$

Equations (4.13) and (4.14) in Section 4.3.2 are also valid here. As a result, equation (5.8) becomes

$$\frac{\sqrt{\frac{c_f}{2}}}{St} = \int_0^{u_L^+} (Pr_{tot} - Pr_{turb})\, du^+ + \frac{Pr_{turb}}{\sqrt{\frac{c_f}{2}}} \left(1 + \frac{1}{\kappa}\sqrt{\frac{c_f}{2}}\right) \tag{5.9}$$

Again, using Spalding-Jayatilleke's concept of "extra thermal resistance" of the viscous sublayer, with the definition,

$$P \equiv \int_0^{u_L^+} \left(\frac{Pr_{tot}}{Pr_{turb}} - 1\right) du^+ \tag{5.10}$$

one can re-state equation (5.10) as

$$\frac{\sqrt{\frac{c_f}{2}}}{St} = Pr_{turb}\, P + \frac{Pr_{turb}}{\sqrt{\frac{c_f}{2}}}\left(1 + \frac{1}{\kappa}\sqrt{\frac{c_f}{2}}\right) \tag{5.11}$$

5.4.3 <u>The Two-Portion Temperature Profile</u>

Parallel to equation (4.9), it can be stated that

$$\overline{u^+\phi^+} = \frac{1}{y_{2L}^+}\int_0^{y_{2L}^+} u^+\phi^+\, dy^+$$

$$= \frac{1}{y_{2L}^+}\int_0^{y_L^+} u^+\phi^+\, dy^+ + \frac{1}{y_{2L}^+}\int_{y_L^+}^{y_{2L}^+} u^+\phi^+\, dy^+ \tag{5.12}$$

As shown in Figure 5.2(B), ϕ^+ is logarithmic for $0 < y^+ \leq y_L^+$. Therefore, with equations (3.22) and (4.10), the first term on the right-hand side of equation (5.12) becomes

$$\frac{1}{y_{2L}^+}\int_0^{y_L^+} u^+\phi^+ dy^+ = \frac{Pr_{turb}}{2y_L^+}\int_0^{y_L^+}\left(\frac{1}{\kappa}\ln y^+ + c\right)^2 dy^+$$

$$= \frac{Pr_{turb}}{2}\left\{\frac{1}{\kappa^2}\ln^2 y_L^+ - \frac{2}{\kappa}\left(\frac{1}{\kappa} - c\right)\ln y_L^+ + \left(\frac{2}{\kappa^2} - \frac{2c}{\kappa} + c^2\right)\right\} \qquad (5.13)$$

With $\phi^+ = \phi_L^+$ for $y_L^+ \leq y^+ \leq y_{2L}^+$, the second term on the right-hand side of equation (5.12) becomes

$$\frac{1}{y_{2L}^+}\int_{y_L^+}^{y_{2L}^+} u^+\phi^+ dy^+ = \frac{\phi_L^+}{2y_L^+}\int_0^{y_L^+}\left(\frac{1}{\kappa}\ln y^+ + c\right)dy^+$$

$$= \frac{\bar{u}^+\phi_L^+}{2} \qquad (5.14)$$

where $\bar{u}^+$ is given by equation (4.6).

Substituting equations (5.13) and (5.14) into equation (5.12) and simplifying gives

$$\bar{\phi}^+ = \phi_L^+ - Pr_{turb}\left(\frac{1}{2\kappa} - \frac{1}{2\kappa^2\bar{u}^+}\right) \qquad (5.15)$$

As in the case of the uniform temperature profile,

$$\phi_L^+ = \int_0^{u_L^+} Pr_{tot}\, du^+$$

Then

$$\bar{\phi}^+ = \int_0^{u_L^+}(P_{tot} - Pr_{turb})du^+ - Pr_{turb}\left(\frac{1}{2\kappa} - \frac{1}{2\kappa^2\bar{u}^+}\right) + \int_0^{u_L^+} Pr_{turb}\, du^+ \qquad (5.16)$$

Or
$$\frac{\sqrt{\frac{c_f}{2}}}{St} = Pr_{turb}\, P + \frac{Pr_{turb}}{\sqrt{\frac{c_f}{2}}}\left(1 + \frac{1}{2\kappa}\sqrt{\frac{c_f}{2}} + \frac{1}{2\kappa^2} \cdot \frac{c_f}{2}\right) \tag{5.17}$$

With the proper values of P, Pr_{turb}, κ and c_f, the Stanton number for asymmetrical heating in parallel plates can be calculated.

5.4.4 The Real Temperature Profile

The real temperature profile would fall between the uniform temperature profile and the two-portion temperature profile. The uniform temperature profile, with

$$\bar{\phi}^+ = \phi_L^+ \tag{5.7}$$

yields the maximum value of $\bar{\phi}^+$. The two-portion temperature profile, with

$$\bar{\phi}^+ = \phi_L^+ - Pr_{turb}\left(\frac{1}{2\kappa} - \frac{1}{2\kappa^2 \bar{u}^+}\right) \tag{5.15}$$

would give the minimum value of $\bar{\phi}^+$.

5.5 Summary of Spalding-Jayatilleke P-Function Method and its Extensions

In Sections 3.4, 4.3 and 5.4, the Spalding-Jayatilleke P-function concept for circular tubes and parallel plates under symmetrical and asymmetrical heat-transfer conditions are discussed in details. The following is a summary of the applicable equations:

1. For circular tubes with axially symmetrical heating

$$\frac{\sqrt{\frac{c_f}{2}}}{St} = Pr_{turb}\, P + \frac{Pr_{turb}}{\sqrt{\frac{c_f}{2}}}\left(1 + \frac{5}{4\kappa^2}\,\frac{c_f}{2}\right) \qquad (3.30)$$

2. For parallel plates with symmetrical heating

$$\frac{\sqrt{\frac{c_f}{2}}}{St} = Pr_{turb}\, P + \frac{Pr_{turb}}{\sqrt{\frac{c_f}{2}}}\left(1 + \frac{1}{\kappa^2}\,\frac{c_f}{2}\right) \qquad (4.17)$$

3. For parallel plates with asymmetrical heating

A. with the uniform temperature profile

$$\frac{\sqrt{\frac{c_f}{2}}}{St} = Pr_{turb}\, P + \frac{Pr_{turb}}{\sqrt{\frac{c_f}{2}}}\left(1 + \frac{1}{\kappa}\sqrt{\frac{c_f}{2}}\right) \qquad (5.11)$$

B. with the two-portion temperature profile

$$\frac{\sqrt{\frac{c_f}{2}}}{St} = Pr_{turb}\, P + \frac{Pr_{turb}}{\sqrt{\frac{c_f}{2}}}\left(1 + \frac{1}{2\kappa}\sqrt{\frac{c_f}{2}} + \frac{1}{2\kappa^2}\,\frac{c_f}{2}\right)$$

(5.17)

CHAPTER 6

EFFECT OF THE VARIATION OF FLUID PROPERTIES ON HEAT TRANSFER

Fluid physical properties depend on temperature. As a result, heat-transfer correlations obtained with the assumption of constant physical properties can only be used in practice either at small temperature differences in a flow or with physical properties changing slightly in the temperature range considered. For such cases the effect of changing physical properties can be approximately accounted for by choosing the properties at the bulk fluid temperature. However, in heat-transfer systems with large temperature drops and high heat fluxes, it is impractical to consider physical properties constant because sizable errors may result. Under such conditions the analysis of heat transfer should include the dependence of physical properties on temperature. In Chapters 3, 4 and 5, the heat-transfer correlations of circular tubes, rectangular channels and parallel plates are discussed. All these correlations, with the exceptions of Sieder-Tate (see Section 3.2) and James-Martin-Martin (see Section 5.3) equations, are based on constant physical fluid properties. In order to apply these correlations properly, the as-measured experimental heat-transfer data should be corrected to constant-property values. Here, some simple and widely-used methods of constant-property correction are examined.

For liquids far from their critical point, only dynamic viscosity varies greatly with temperature; all the other physical properties depend on temperature rather weakly. Therefore, while investigating non-isothermal liquid flow, a model with variable viscosity may be used as a good approximation, other physical properties being assumed constant. It is found that an equation of the following type often provides an excellent approximation:

$$\frac{Nu}{Nu_{cp}} = \frac{St}{St_{cp}} = \left(\frac{\mu_b}{\mu_w}\right)^n \qquad (6.1)$$

where the subscript cp refers to the appropriate constant-property solution or small-temperature-difference experimental result. The viscosity μ_b is evaluated at the bulk temperature, while μ_w is evaluated at the wall temperature. The exponent n is a function of geometry and the type of flow.

Sieder and Tate [42] suggested n = 0.14 for heating, i.e

$$\frac{Nu}{Nu_{cp}} = \left(\frac{\mu_b}{\mu_w}\right)^{0.14} \qquad (6.2)$$

Deissler[9], in a theoretical work, made the recommendations summarized in Table 6.1. Petukhov[38] suggested the use of equation (6.1) with n = 0.11 for the case of heating, being recommended over a range of 0.008 to 40 for μ_w/μ_b, 10^4 to 1.25×10^5 for Re, and 2 to 140 for Pr. James et al.[21] discovered experimentally that, in the case of asymmetrical heating in rectangular channels, the influence of viscosity

Table 6.1

Deissler's[9] Viscosity-Ratio Exponents

Pr	$\frac{\mu_b}{\mu_w} < 1$ (Cooling)	$\frac{\mu_b}{\mu_w} > 1$ (Heating)
1	0.19	0.20
3	0.21	0.27
10	0.22	0.36
30	0.21	0.39
100	0.20	0.42
1000	0.20	0.46

ratio decreases as the Reynolds number increases, becoming negligible when Re exceeds a value of about 5×10^4. This trend is explained from the increasing concentration of the resistance to the heat transfer in the turbulent core as the Reynolds number rises[21]. The recommended equation is

$$\frac{Nu}{Nu_{cp}} = \left(\frac{\mu_b}{\mu_w}\right)^{213Re^{-0.9}} \tag{6.3}$$

For gases, the viscosity, thermal conductivity, and density are functions of absolute temperature, T. Fortunately the absolute temperature dependence tends to be similar for different gases, although the similarity does break down at the temperature extremes. Thus it is found that the temperature-dependent-property effects can usually be adequately correlated by the equation

$$\frac{Nu}{Nu_{cp}} = \frac{St}{St_{cp}} = \left(\frac{T_b}{T_w}\right)^m \tag{6.4}$$

Kays[26] on the basis of theoretical and experimental works, recommended the following for turbulent flow of a gas in a circular tube:

$$\begin{aligned} &\frac{T_b}{T_w} < 1 \qquad \text{(Heating)} \qquad m = 0.5 \\ &\frac{T_b}{T_w} > 1 \qquad \text{(Cooling)} \qquad m = 0 \end{aligned} \tag{6.5}$$

In his thorough discussion, Petukhov[38] proposed

$$m = b \log \frac{T_w}{T_b} + 0.36$$

$$\frac{T_b}{T_w} < 1 \qquad \text{(Heating)} \qquad b = 0.3 \qquad (6.6)$$

$$\frac{T_b}{T_w} > 1 \qquad \text{(Cooling)} \qquad b = 0$$

For heated air, Petukhov stated that $m = 0.5$ produces slightly better results.

It is important to recognise that all the above constant-property corrections, with the exception of that of James et al.[21], are for turbulent flow in circular tubes with symmetrical heat transfer. However, in the absence of other appropriate corrections, they are commonly applied to non-circular ducts with symmetrical or asymmetrical heat transfer. The correction by James et al. is intended for turbulent flow in rectangular channles under asymmetrical heat-transfer conditions.

CHAPTER 7

EXPERIMENTAL DATA

7.1 General

In Chapters 3, 4 and 5, a collection of heat-transfer equations have been reviewed and developed. The criteria for the selection of the most suitable ones for engineering applications are their agreement with experimental data and ease of application. Hence a part of the present task has been the collection of all available experimental results for symmetrical and asymmetrical heat transfer in rectangular channels and parallel plates, covering a large range of parameters such as Prandtl, Reynolds and Nusselt numbers.

7.2 Symmetrical Heat Transfer

Unfortunately, most of the experimental works on symmetrical heat transfer in rectangular ducts fall in the category of boiling burnout tests. However, there are a number of experimental investigations on single-phase heat-transfer characteristics of rectangular ducts of different aspect ratios with the particular aim of determining whether the heat transfer is greatly affected by the thermal boundary conditions. A literature survey revealed the works by Levy et al.[30] and Novotny et al.[36] and these are summarized in Table 7.1.

Table 7.1 Experimental Investigations on Symmetrical Heat Transfer

Investigator(s)	Year	Ref	Test Fluid	Test Section No.	Test Section Dimensions inches	D_e inches	Aspect Ratio A	Pr	Re
Levy, Fuller & Niemi	1959	(30)	Water	4	0.118 x 2.405	0.225	1:20.4*	1.33	7.1×10^3
			"	11	0.114 x 2.349	0.218	1:20.6*	to	to
			"	5	variable 0.14 x 2.40 nominal	0.31 nominal	variable* 1:17.1 nominal	7.30	2×10^5
Novotny, McComas, Sparrow & Eckert	1964	(36)	Air	-	0.98 x 0.98	0.98	1:1	0.7	10^4
			"	-	0.604 x 3.0	1.0	1:5*	"	to
			"	-	0.4 x 4.0	0.727	1:10*	"	1.4×10^5

* Approaching parallel plates conditions.

Levy et al.[30] presented heat-transfer coefficients for water flowing vertically in thin rectangular channels (0.1" x 2.5" approximately) 18 and 36 inches long and heated electrically around the entire periphery. The Prandtl numbers, Pr, were in the 1.33 to 7.30 range owing to the changing of the fluid properties of water caused by the large axial temperature difference. Each test run had a fixed fluid flow rate and hence a fixed nominal Reynolds number. However, variations in actual Reynolds number occurred along the duct because of axial changes in temperature. Two data, those with the lowest and highest actual Reynolds number, of each test run were selected for comparison purposes. Owing to the large temperature differences, Levy et al. had accounted for the variation in fluid properties by using the Sieder-Tate correction (see Chapter 6). Test Section No. 4 was made up of two L strips and had very sharp corners, while Test Section No. 11 was fabricated from a circular tube and had round edges. Section No. 5 had a variable cross-section with round corners and hydraulic equivalent diameter generally 50% larger than the last two sections. The experimental data are in Table B.1 of Appendix B.

Novotny et al.[36] presented fully developed heat-transfer results for turbulent flow of air in rectangular ducts with aspect ratios of 1:1, 1:5 and 1:10. The heating condition was such that the two longer top and bottom walls of the rectangle were uniformly heated, while the two shorter walls were unheated. Uniform heat generation in the top and bottom walls of the test section was achieved by passing an electric current longitudinally through the duct walls. To approach as closely as possible the condition of adiabatic side walls, the latter were made of a fabricated board which had a small thermal conductivity of 0.15 Btu/hr-ft-^{o}F. A summary of the experimental data is given in Table B.2 of Appendix B. The Reynolds number range of the runs was approximately 10^4 to 1.4×10^5. The lower end of the Reynolds number range lies above the limit at which free convection effects are noticeable, while the upper end of the range lies below the limit of significant compressibility effects.

7.3 Asymmetrical Heat Transfer

Table 7.2 is a summary of recent experimental works on asymmetrical heat transfer in rectangular channels and parallel plates under fully-developed turbulent conditions.

Barrow[3] carried out heat-transfer experiments with a 0.32" x 9.3" duct. The lower wall was heated electrically while the upper wall was insulated. The spacers or side walls of the channel were made of hardwood to reduce heat conduction from the lower to the upper wall to a minimum. The experimental heat-transfer coefficients were calculated based on (a) electrical power measurement and (b) thermocouple-probe readings. The reuslts are tabulated in Table

Table 7.2 Experimental Investigations on Asymmetrical Heat Transfer

Inves-tigator (s)	Year	Ref.	Test Fluid	Test Section Dimensions inches	D_e inches	Aspect Ratio A	Pr	Re
Barrow	1962	(3)	Air	0.32 x 9.3	0.62	0.0344*	0.7	10^4 to 4×10^4
Hines	1963	(18)	RP-1 Kerosene	0.5 x 0.319	0.39	1.57	18 to 22	2.7×10^4 to 1.9×10^5
Sparrow, Lloyd & Hixon	1966	(44)	Air	0.6 x 3.0	1.0	0.02*	0.7	1.8×10^4 to 1.42×10^5
James, Martin & Martin	1966	(21)	Water	0.125 x 0.25	0.167	0.5		
			and	0.25 x 0.25	0.25	1.0	6.5	4×10^3
			Glycerine	0.5 x 0.25	0.333	2.0	32.5	to
				0.625 x 0.25	0.357	2.5	100	10^5
			Mixture	0.75 x 0.25	0.275	3.0		
				1.00 x 0.25	0.400	4.0		

Table 7.2 (cont'd)

Investigator(s)	Year	Ref.	Test	Test Section Dimensions inches	D_e inches	Aspect Ratio A	Pr	Re
Bruzzi	1969	(6)	Arcton-113	0.127 x 0.25	0.168	0.54	6.9	5.6×10^3
				0.275 x 0.25	0.262	1.12	to	to
				0.752 x 0.25	0.375	3.01	8.1	4.7×10^4
Tan & Charters	1970	(45)	Air	1.87 x 5.5	2.8	0.34*	8.1	9.5×10^3 to 2.2×10^4

* Approaching parallel plates conditions.

B.3 of Appendix B.

Forced-convection heat transfer to RP-1 kerosene was investigated under asymmetric heating conditions by Hines[18]. The experimental technique was to electroplate a copper heating strip to one side of a 0.50" x 0.319" rectangular cross-sectioned stainless steel channel of 0.010" wall thickness. When electrical current was passed along the tube, approximately 95% of the resistance heating occurred in the copper strip and adjacent channel wall, producing an asymmetric heat input to the fluid. Data were gathered at liquid velocities to 120 ft/sec. and heat fluxes to 2.36 Btu/sq in-sec. Experimental results are presented in Table B.4 of Appendix B. Hines did not specify the exact Prandtl number of RP-1 Kerosene. The two extreme cases are considered here: Pr = 18 and Pr = 22.

Sparrow et al.[44] used the same rectangular duct (0.6" x 3") as that in experiments of Novotny et al.[36]. Again, air was used as the testing fluid. Unlike the latter, only one of the two long sides was heated. The results are shown in Table B.5 of Appendix B.

The apparatus of James et al.[21] consisted of a burner which generated a stream of hot combustion products. These gases passed over fins machined on one end of a copper block. Heat was transferred by conduction through the block to a liquid stream flowing in a channel of rectangular section constructed on part of the long face on the block remote from the fins. The test liquids were mixtures of distilled water and chemically pure glycerine. Measurements were made of the heat-transfer coefficient between the heated surface and the liquid for the following conditions:

Re	3×10^3 to 10×10^4
Pr	6.5, 32.5, 100
A	0.5, 1, 2, 2.5, 3, 4
Δt_b	40^oF to 150^oF

where the bulk temperature difference $\Delta t_b = t_w - t_b$ and t_w and t_b are the wall temperature and bulk temperature respectively. The experimental Nusselt numbers, shown in Table B.6 of Appendix B, were corrected to $\Delta t_b = 0$ condition by James et al. using the extrapolation technique established by Eagle and Ferguson[14].

The steel-heated width of Bruzzi's[6] channel was fixed at 0.25" while the aspect ratios were 0.54, 1.12 and 3.01. The test fluid was Arcton-113 which gave a range of Prandtl number from 6.9 to 8.1 in this case. There was a moderate radial temperature difference with $\mu_b/\mu_w = 1.10$ to 1.25. Pressure drops in the channel were reported, but they were not accurate enough for the purpose of calculating of friction factors. The experimental data are tabulated in Table B.7 of Appendix B.

In the design of a flat-plate solar air heater with rectangular flow-passages, Tan and Charters[45] undertook an experimental investigation of asymmetrical heat transfer. The regulated electrical power input on the top heated wall of a rectangular channel was adjusted to simulate solar conditions, i.e an intensity of approximately 300 Btu/hr-ft^2. The Reynolds number range tested was from 9,500 to 22,000. All test runs were carried out under steady-state conditions. Table B.8 of Appendix B gives the results of their test runs.

CHAPTER 8

COMPUTATIONS AND DISCUSSION

8.1 Symmetrical Heat Transfer

8.1.1 Method

In Chapter 3, there were considered, of the various ones available, four of the more commonly used, or especially interesting, correlations for heat transfer for turbulent flow in circular tubes. These are:

1. Dittus-Boelter[13],
2. Sieder-Tate[42],
3. Petukhov-Popov[39],

and 4. Spalding-Jayatilleke[22,43].

From Chapter 4, there are two correlations of symmetrical heat transfer for turbulent flow between parallel plates. They are:

5. Barrow[2],

and 6. the present author's extension of the Spalding-Jayatilleke method. The published experimental data available for comparison with the above correlations have been discussed in Chapter 7, Section 7.2. They include the works of:

1. Levy et al.[30]

and 2. Novotny et al.[36]

The experimental data are tabulated in Tables B.1 and B.2 of Appendix B.

In order to be consistent with all the correlations, the basis of comparison is the predicted Stanton number from the correlations versus the experimental Stanton number. The percentage root mean square deviation, PD_{rms}, of Stanton number is defined as

$$PD_{rms} \equiv \sqrt{\frac{1}{N}\sum_{i=1}^{N}\left(\frac{St_{exp} - St_{pred}}{St_{pred}} \times 100\right)^2} \qquad (8.1)$$

where N = number of data

St_{exp} = experimental Stanton number

St_{pred} = predicted Stanton number from correlation.

The relationship among Stanton, Nusselt, Prandtl and Reynolds numbers is

$$St = \frac{Nu}{Pr\ Re} \qquad (8.2)$$

Levy et al.[30] in their paper report data already corrected to constant-property conditions by the Sieder-Tate method. In the present case, for certain comparison, their reported data were used to deduce as-measured conditions and these in turn were corrected to constant-property conditions using the methods of Deissler[9] and of Petukhov[38]. All these corrected experimental data were then compared with the predicted values from the correlations. No attempt was made to correct experimental data of Novotny et al.[36] to constant-property conditions because their experimental T_b and T_w had not been specified.

In applying the Dittus-Boelter, Sieder-Tate, and Barrow correlations, the experimental Prandtl and Reynolds numbers from Tables B.1 and B.2 of Appendix B were subsituted into equations (3.3), (3.5) and (4.2). The predicted Stanton numbers were then compared with the corresponding experimental data.

The friction factor, c_f, in the Petukhov-Popov equation (3.6) was obtained from the Blasius equation (2.2) by using the Reynolds numbers in Tables B.1 and B.2 of Appendix B. The Blasius equation is used instead of the Karman-Nikuradse because the former is much more convenient to apply and both equations give more or less identical results for Reynolds number between 4×10^3 and 10^5. With the calculated friction factors and the tabulated values of Prandtl number, the predicted Stanton numbers from equation (3.6) were obtained and compared.

The Spalding-Jayatilleke P-function, P, was calculated from equation (3.31) with Pr from Tables B.1 and B.2 of Appendix B. Pr_{turb} and κ were taken as 0.9 and 0.4 respectively. The friction factor, c_f, again was obtained from the Blasius equation (2.2) by using the Reynolds numbers in Tables B.1 and B.2 of Appendix B. By subsituting the above appropriate P, Pr_{turb}, κ , and c_f into equation (3.30), the predicted Stanton numbers were obtained and compared.

In the calculation of the present author's extension of Spalding-Jayatilleke P-function, P was taken as

$$P = 9.24 \left\{ \left(\frac{Pr}{Pr_{turb}}\right)^{3/4} - 1 \right\} \qquad (3.31)$$

where $Pr_{turb} = 0.9$

and Pr was obtained from Tables B.1 and B.2 of Appendix B. The friction factor, c_f, was calculated from the Blasius equation (2.2) by using (a) the Reynolds numbers tabulated in Tables B.1 and B.2 of Appendix B and (b) the "laminar Reynolds numbers", Re^*, as suggested by Jones[23] (see Chapter 2, section 2.3). The value of κ was taken as 0.4. By substituting the above appropriate P, Pr_{turb}, κ, and c_f into equation (4.17), the predicted Stanton numbers were obtained and compared.

8.1.2 Results and Discussion

The resulting percentage root mean square deviations, as defined in equation (8.1), on Stanton number by using the different correlations and experimental data are summarized in Table 8.1.

The upper half of the last column in Table 8.1 indicates that the use of circular-tube correlations, with the concept of hydraulic equivalent diameter, on the prediction of symmetrical heat transfer in rectangular channels and parallel plates would result in a 28 to 35 per cent error. Dittus-Boelter and Sieder-Tate correlations, the two most commonly used circular-tube equations, give percentage root mean square deviations of 27.8% and 30.6% respectively.

Table 8.1 Symmetrical Heat Transfer:
Percentage Root Mean Square Deviation on Stanton Number

Correlation	Equations Involved	Experimental Data (1) Levy et al. (Constant-Property#)	Experimental Data (2) Novotny et al. (As-measured)	Combined All Data
Circular-Tube				
1. Dittus-Boelter	(3.3)	33.9	10.9	27.8
2. Sieder-Tate	(3.5)	35.0	20.8	30.6
3. Petukhov-Popov	(2.2) (3.6)	35.4	9.2	28.8
4. Spalding-Jayatilleke*	(2.2) (3.30) (3.31)	43.1	4.7	34.5

Table 8.1 (cont'd)

Correlation	Equations Involved	Experimental Data (1) Levy et al. (Constant-Property#)	(2) Novotny et al. (As-measured)	Combined All Data
Parallel-Plate				
5. Barrow	(4.2)	28.3	4.5	22.9
6. Present author's extension of Spalding-Jayatilleke				
Case (a)*	(2.2), (2.8)@, (3.31), (4.17)	41.8	4.8	33.5
Case (b)*@		29.1	13.0	24.5

\# Corrected by the Sieder-Tate[42] method

* $Pr_{turb} = 0.9$

@ c_f corrected by the Jones[23] method

The Petukhov-Popov correlation produces a percentage root mean square deviation of 28.8%. The Spalding-Jayatilleke P-function correlation provides the largest difference between the predicted and experimental Stanton numbers with a percentage root mean square deviation of 34.5%.

It is interesting to examine the lower half of the last column in Table 8.1. Those three figures of percentage root mean square deviation are derived from parallel-plate correlations with the concept of hydraulic equivalent diameter. The Barrow correlation gives a percentage root mean square deviation of 22.9% which is an improvement compared with the use of any circular-tube correlations. Also, the Barrow correlation, equation (4.2), is as simple to apply as any circular-tube equation because the Nusselt number is simply expressed as an explicit function of Reynolds numbers. The corresponding results of the present author's extension of Spalding-Jayatilleke correlation, equation (4.17), for parallel plates as compared with the original Spalding-Jayatilleke circular-tube correlation, equation (3.30), show only a small improvement: $PD_{rms} = 33.5\%$ versus 34.5%. However, the friction factor for the above calculations was obtained from the Blasius equation with the concept of hydraulic equivalent diameter. As pointed out by Jones[23], the aspect ratio of the channel plays an impotant role in the friction characteristics of the fluid flow and the "laminar Reynolds number" should be used in the friction factor calculation. With the friction factor corrected by the Jones method, there is a marked improvement in the results of heat-transfer prediction by using the present author's extension of Spalding-Jayatilleke correlation: PD_{rms} = 24.5% versus 33.5%.

The P-function concept is attractive because of the physical significance of P, namely, P being essentially the extra thermal resistance in the viscous sublayer of the fluid flow. With the following data:

1. experimental Stanton number,
2. $Pr_{turb} = 0.9$,
3. $\kappa = 0.4$,

and 4. c_f from the Blasius equation,

the experimental P-values can then be obtained from equation (4.17). Figures 8.1 and 8.2 show the experimental P-value based on the constant-property (corrected by the Sieder-Tate method) experimental data of Levy et al.[30] and the as-measured data of Novotny et al.[36] respectively. Equation (3.31) is superimposed onto Figures 8.1 and 8.2 for comparison purposes because this equation has already been established for circular tubes. Figures 8.3 and 8.4 are similar to Figures 8.1 and 8.2 with the exception that c_f was obtained from the Blasius equation with correction by the Jones[23] method. Owing to the scarcity of experimental data, no attempt is made here to produce a new P-function equation equivalent to equation (3.31) for parallel plates only.

Figure 8.5 shows the changes of the predicted Stanton number with respect to the changes of the P-value, with

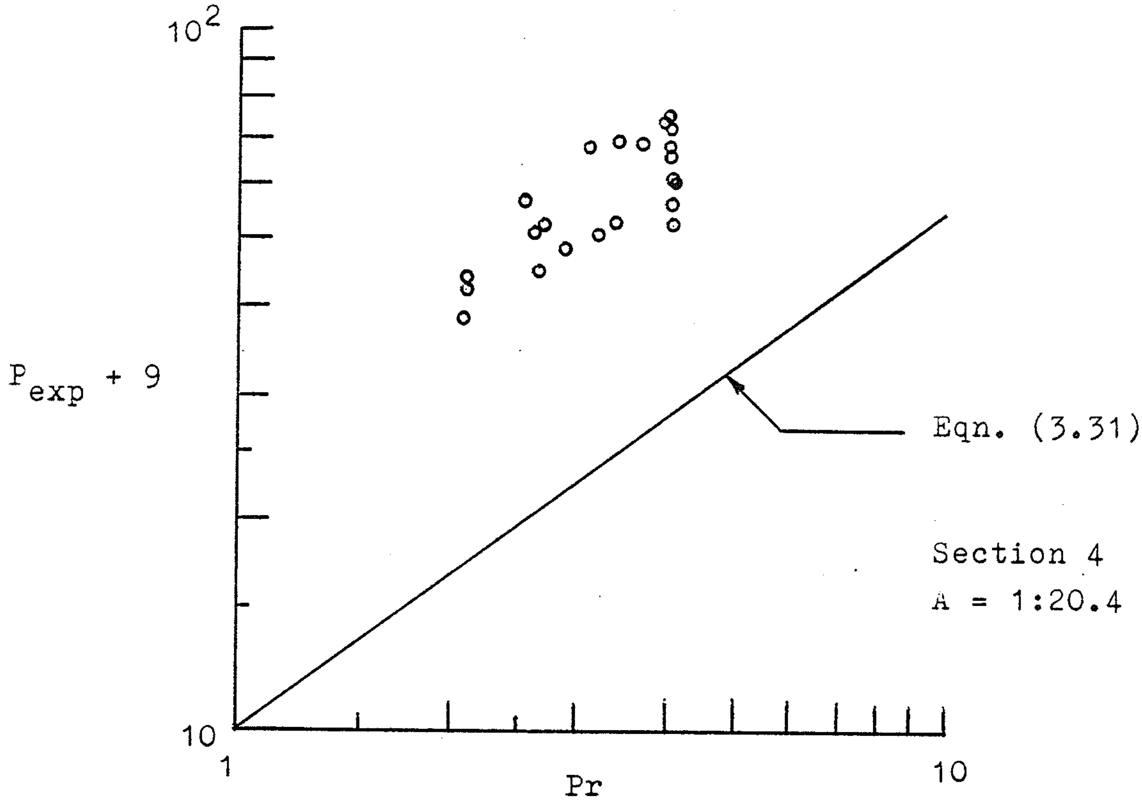

Fig. 8.1 Experimental P-Values: Symmetrical Heat-Transfer Constant-Property Data of Levy et al.

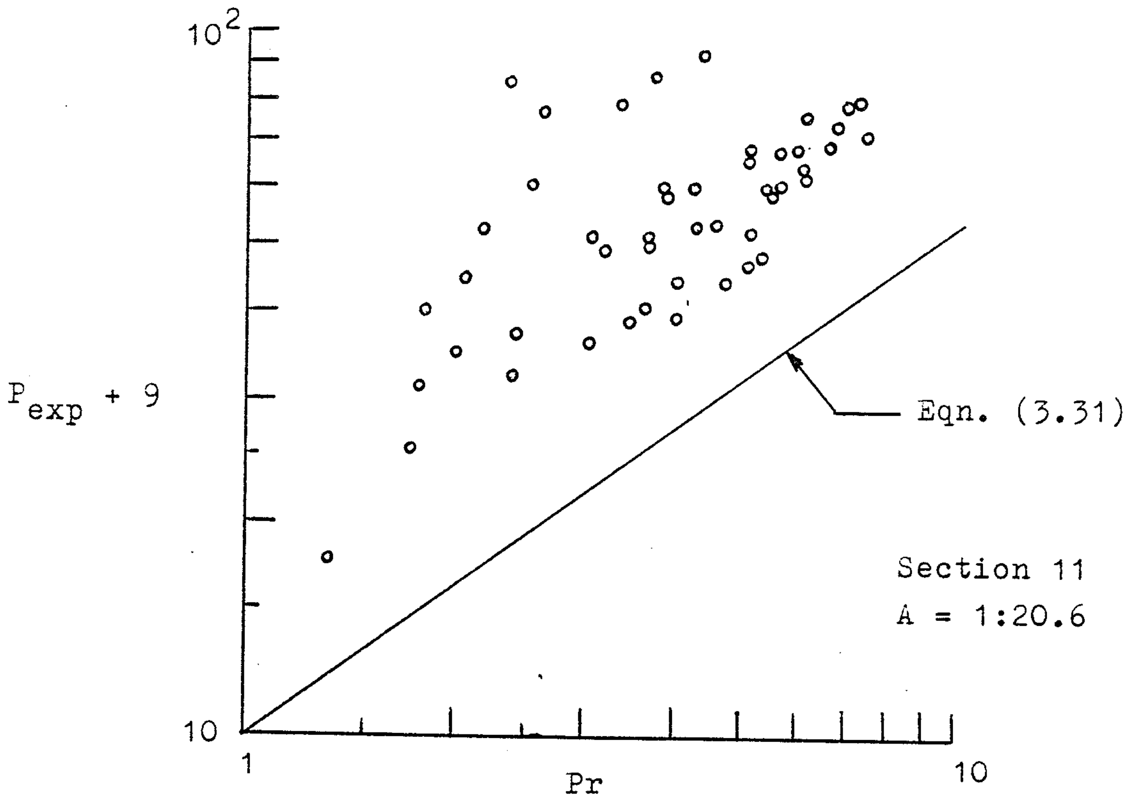

10^2
$P_{exp} + 9$
Eqn. (3.31)
Section 11
A = 1:20.6
10
1
Pr
10

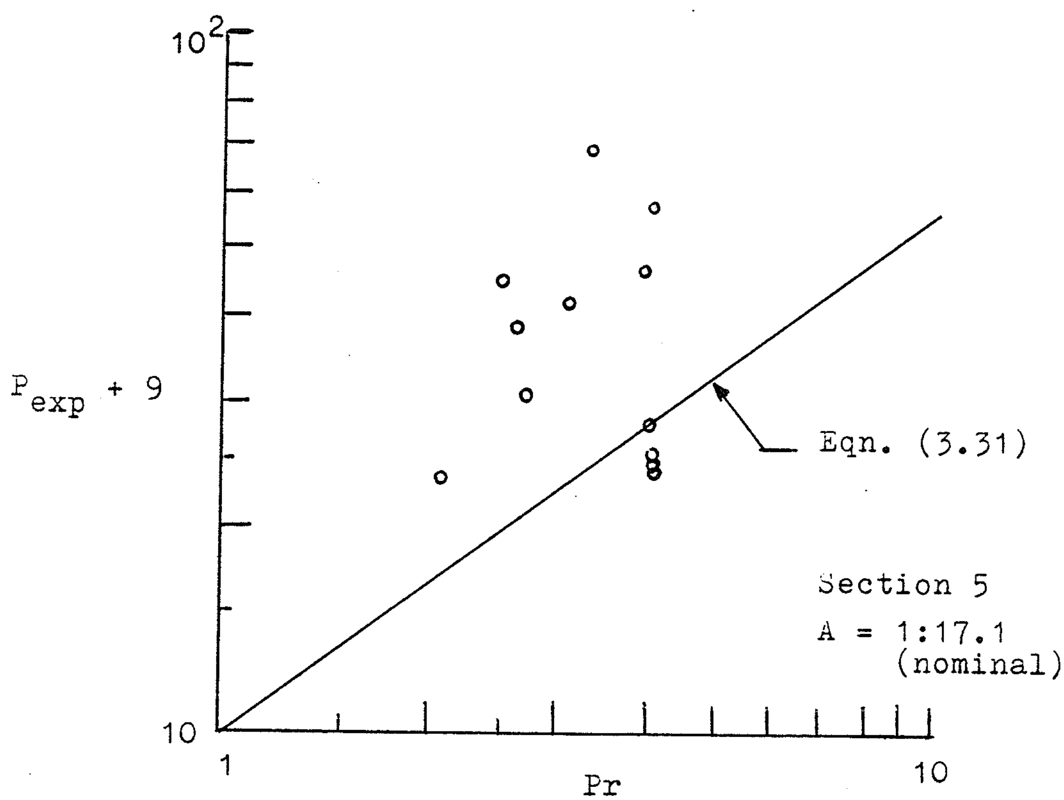

10^2
$P_{exp} + 9$
Eqn. (3.31)
Section 5
A = 1:17.1
(nominal)
10
1
Pr
10

Fig. 8.1 (cont'd)

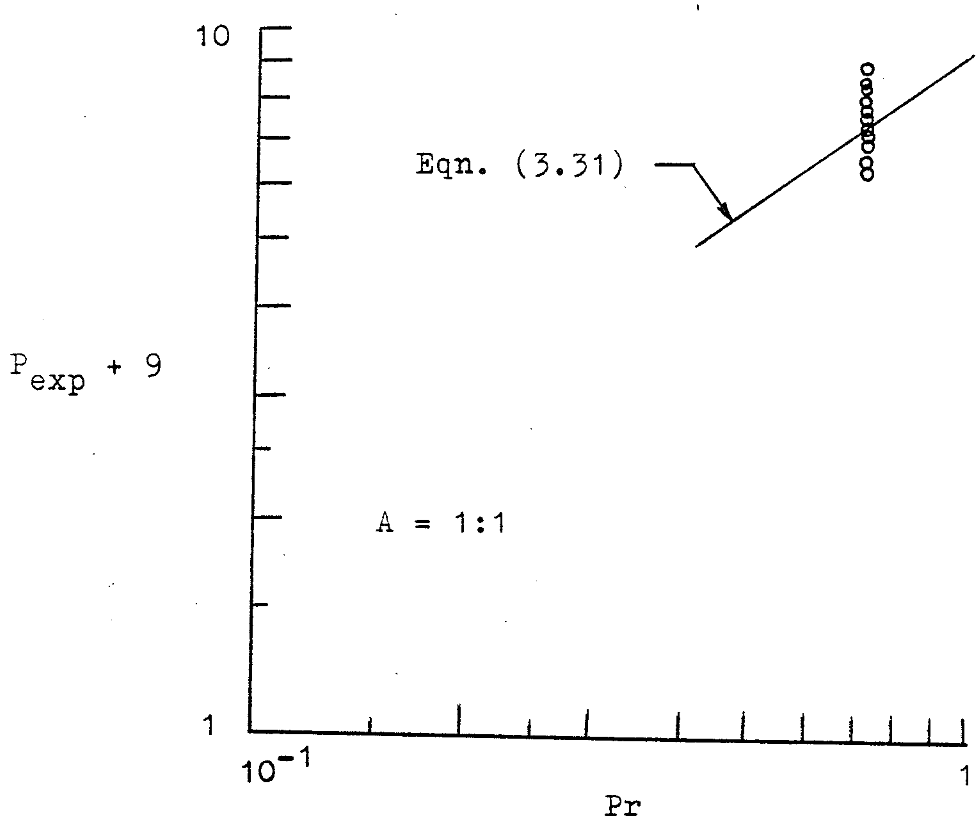

Fig. 8.2 Experimental P-Values: Symmetrical Heat-Transfer As-Measured Data of Novotny et al.

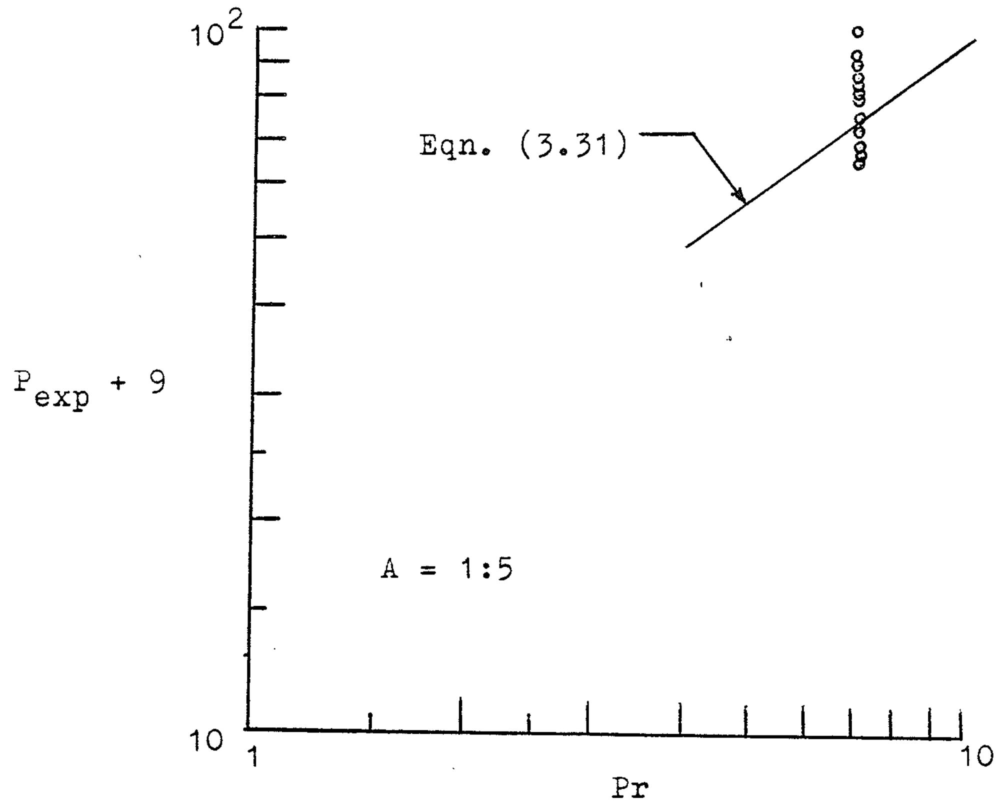

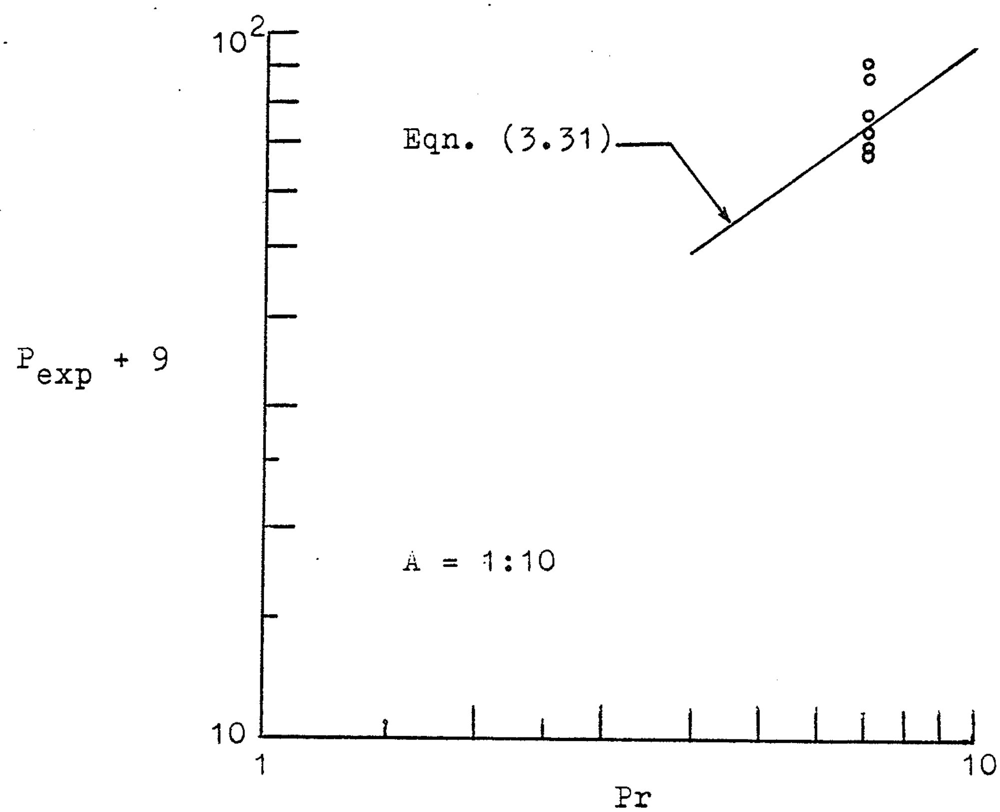

Fig. 8.2 (cont'd)

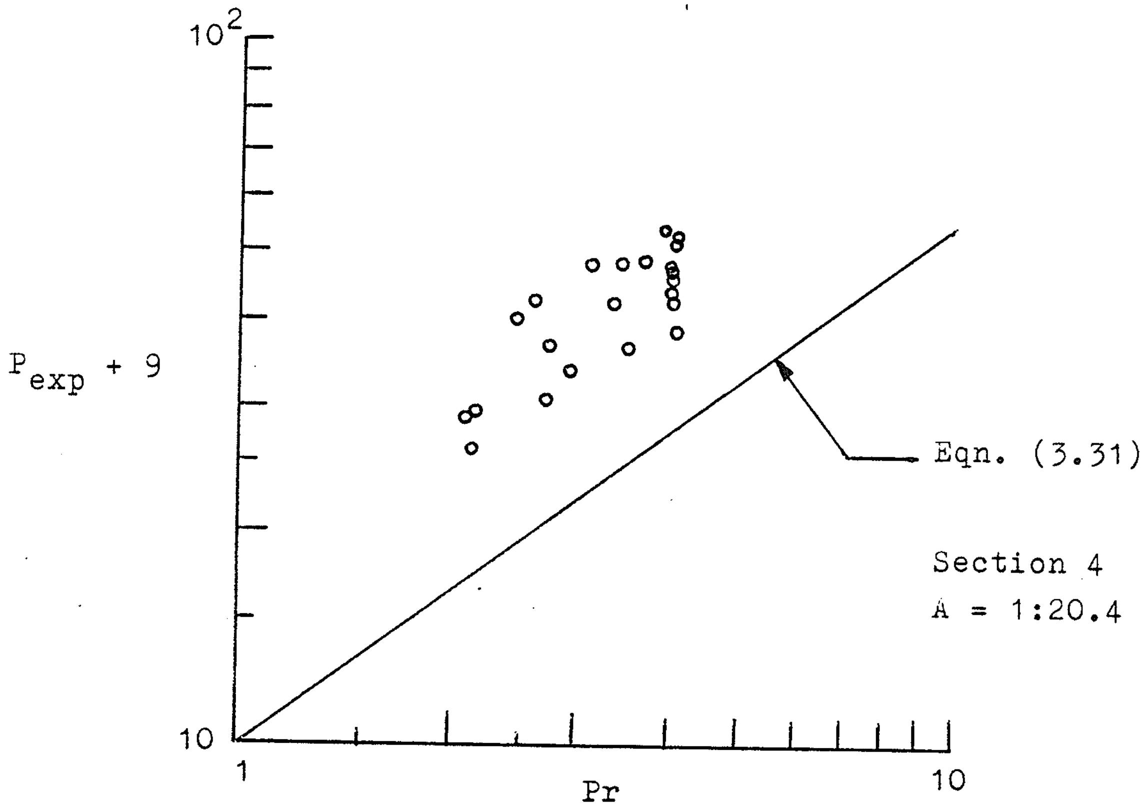

Fig. 8.3 Experimental P-Values:
Symmetrical Heat-Transfer Constant-Property Data of Levy et al. (c_f Corrected by Jones Method)

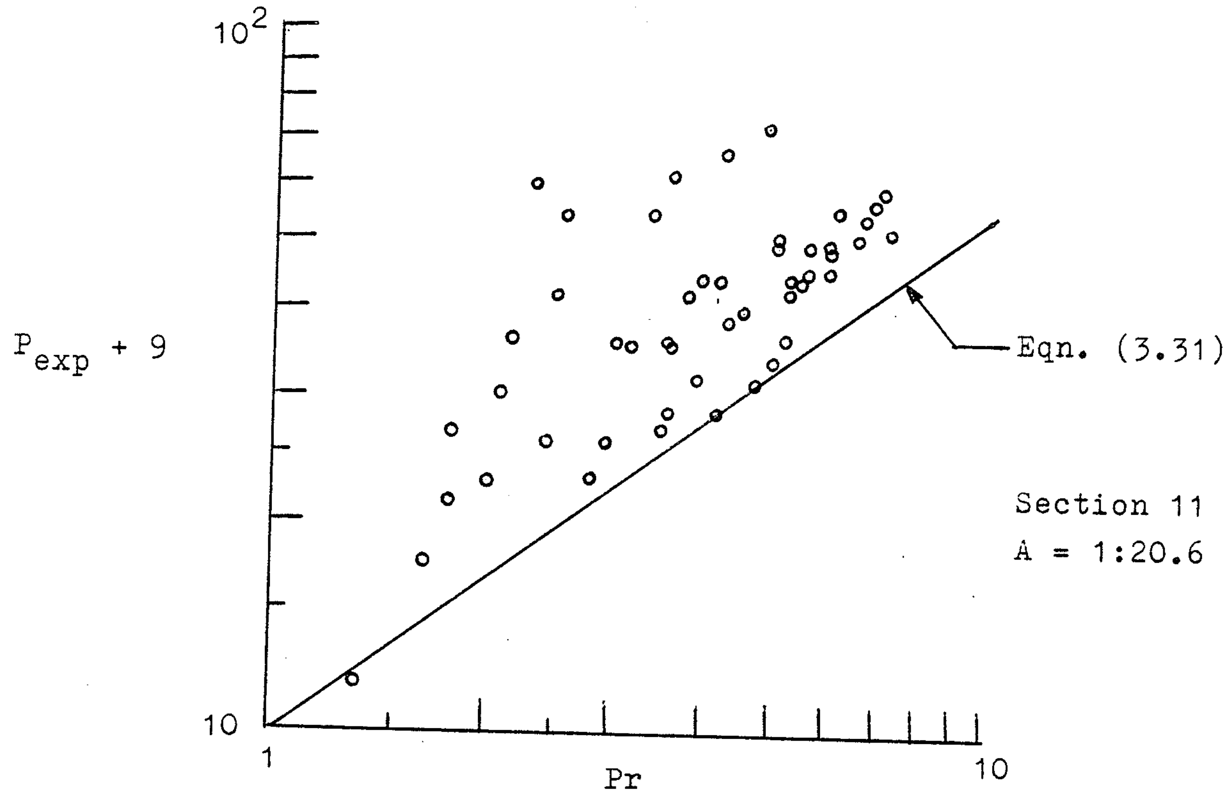
10^2
$P_{exp} + 9$
10
1
Pr
10
Eqn. (3.31)
Section 11
A = 1:20.6

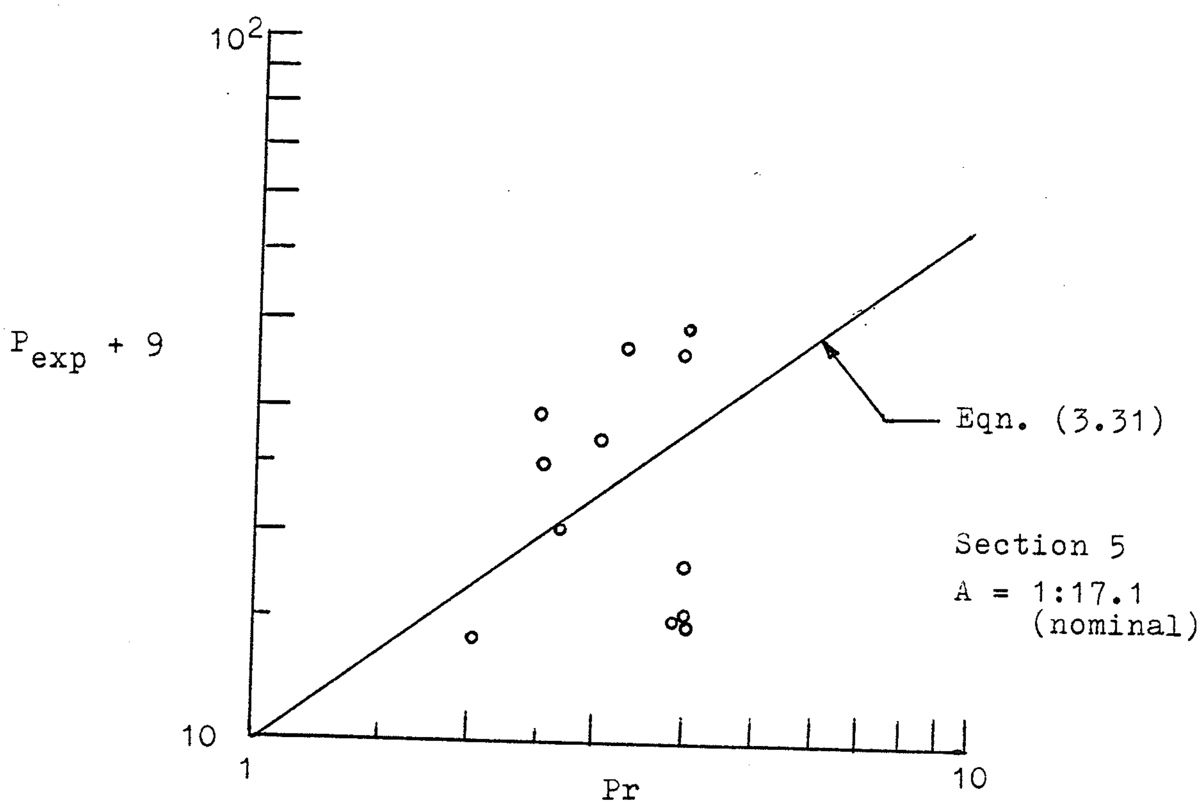
10^2
$P_{exp} + 9$
10
1
Pr
10
Eqn. (3.31)
Section 5
A = 1:17.1
(nominal)

Fig. 8.3 (cont'd)

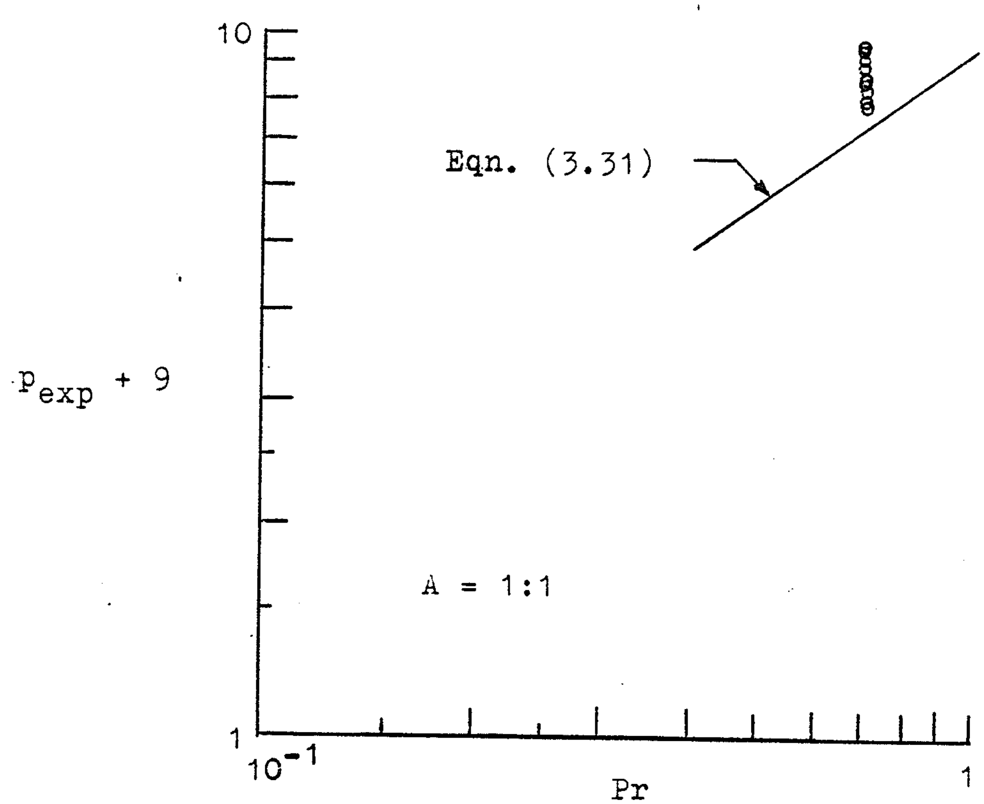

Fig. 8.4 Experimental P-Values: Symmetrical Heat-Transfer As-Measured Data of Novotny et al. (c_f Corrected by Jones Method)

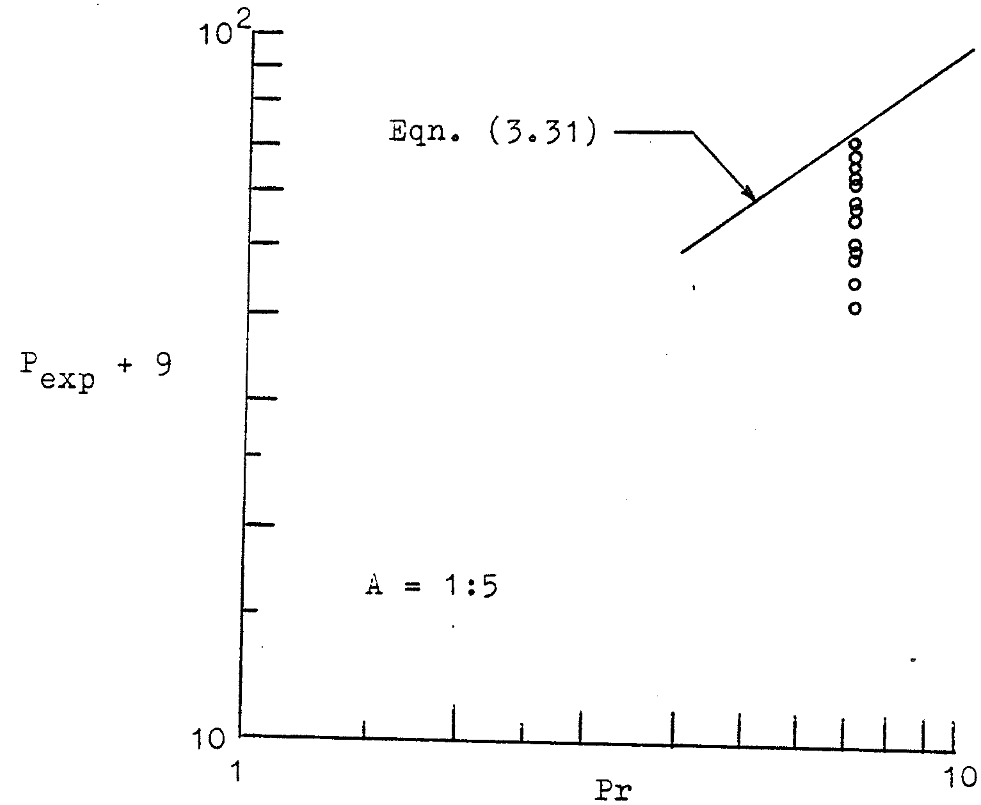

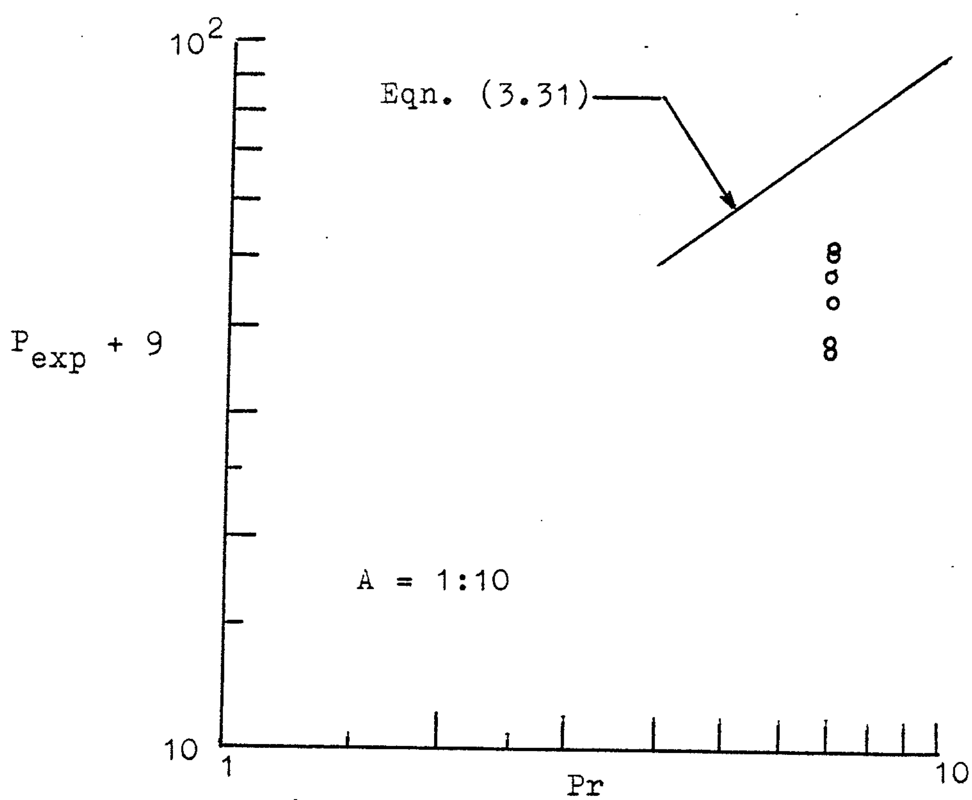

Fig. 8.4 (cont'd)

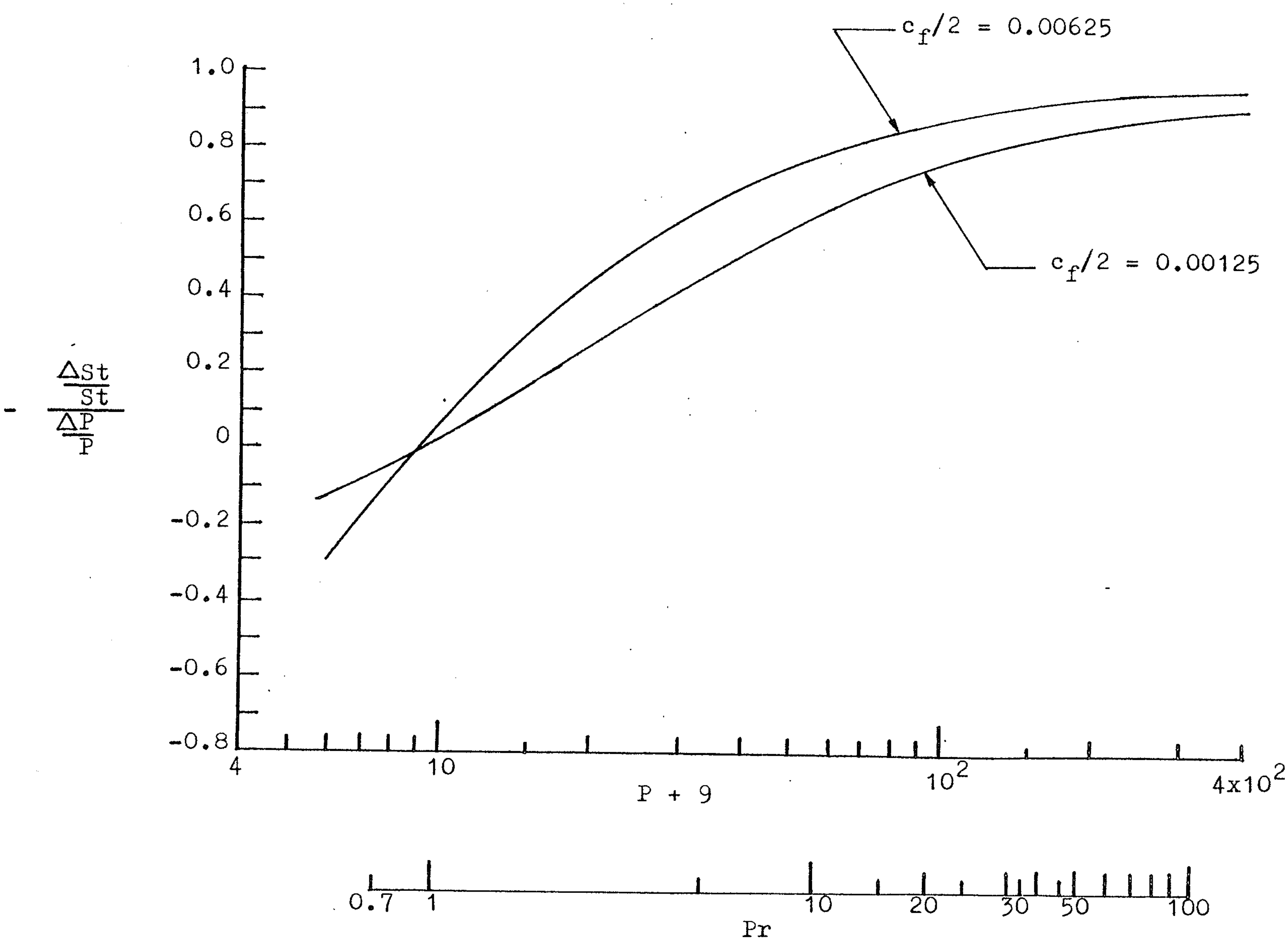

Fig. 8.5 Changes in St w.r.t. Changes in P

$c_f/2$ as an independent parameter. The relation between the two scales of the abscissa is via equation (3.31). For small Prandtl numbers, large errors in P cause only small errors in the predicted Stanton number. For example, with $Pr = 0.7$ and $c_f/2 = 0.00625$, Figure 8.5 gives $\frac{\Delta St}{St}/\frac{\Delta P}{P} = 0.12$, i.e a 50% error in P would yield an error of only 6% in the predicted Stanton number. In the case of large Prandtl numbers, the percentage changes of the predicted Stanton number with respect to the percentage changes in P approach an asymptotic value of 90% approximately. Thus, when the P-function equation (3.30) for circular tubes is applied to the parallel-plate case, the resulting errors in the predicted Stanton number would not be too large, especially in the cases of small Prandtl numbers.

All the correlations in Table 8.1, with the exception of Sieder-Tate, are intended for fluids under constant-property conditions. Table 8.2 shows the effect of different fluid-property corrections on the comparison between the experimental data of Levy et al.[30] and the correlations. Levy et al. in their paper report data already corrected to constant-property conditions by the Sieder-Tate method[42]. The as-measured data were deduced from their reported data using equation (6.2). These as-measured data, in turn, were corrected to constant-property conditions using equation (6.1) with Table 6.1 and equation (6.1) with $n = 0.11$ for the methods of Deissler[9] and of Petukhov[38] respectively. After the correction to constant-property

Table 8.2 Symmetrical Heat-Transfer Data of Levy et al.: Percentage Root Mean Square Deviation with Fluid Properties Correction

Correlation	As-Measured Data	Data Corrected to Constant-Fluid-Property Conditions by: Sieder-Tate Method	Deissler Method	Petukhov Method
Circular-Tube				
1. Dittus-Boelter	29.6	33.9 (4.3)#	36.6 (7.0)	31.9 (2.3)
2. Sieder-Tate	30.8	---	---	---
3. Petukhov-Popov	31.0	35.4 (4.4)	40.2 (9.7)	34.5 (3.5)
4. Spalding-Jayatilleke*	38.8	43.1 (4.3)	47.9 (9.1)	42.2 (3.4)

Table 8.2 (cont'd)

Correlation	As-Measured Data	Data Corrected to Constant-Fluid-Property Conditions by:		
		Sieder-Tate Method	Deissler Method	Petukhov Method
Parallel-Plate				
5. Barrow	26.0	28.3 (2.3)	32.9 (6.9)	27.6 (1.6)
6. Present author's extension of Spalding-Jayatilleke				
Case (a)*	38.6	41.8 (3.2)	48.0 (9.4)	42.3 (3.7)
Case (b)*@	25.6	29.1 (3.5)	34.3 (8.7)	28.3 (2.7)
		Av. Diff. = (3.7)	Av. Diff. = (8.5)	Av. Diff. = (2.9)

The difference in PD_{rms} as compared with Variable Fluid Properties is in brackets.

* $Pr_{turb} = 0.9$

@ c_f corrected by the Jones[23] method

conditions, there is an increase in the percentage root mean square deviation compared with the as-measured conditions. The Petukhov correction has the least effect and gives an average difference of 2.9 in the percentage root mean square deviation. The Sieder-Tate correction is similar to Petukhov with an average difference of 3.7. The Deissler correction gives the largest average difference of 8.5 which is more than twice those of the other two corrections. In general, the effect of the variable fluid properties on heat-transfer prediction is not significant for the fluid flows with small or moderate temperature differences.

8.2 Asymmetrical Heat Transfer

8.2.1 Method

The four correlations for symmetrical heat-transfer calculations of turbulent flow in circular tubes are also used here for correlating asymmetrical heat transfer in rectangular channels and parallel plates. These correlations are:

1. Dittus-Boelter[13],
2. Sieder-Tate[42],
3. Petukhov-Popov[39],

and 4. Spalding-Jayatilleke[22,43].

From Chapter 5, there are three correlations for asymmetrical heat-transfer calculations for turbulent flow in rectangular channels and/or parallel plates. They are the correlations of:

5. Barrow[2],

6. James, Martin and Martin[21],

and 7. the present author's extension of the Spalding-Jayatilleke method for the:

-- uniform-temperature-profile case,

-- two-portion-temperature-profile case.

The published experimental data available for comparison with the above correlations have been discussed in Chapter 7, Section 7.3. They include the works of:

1. Barrow[3],
2. Hines[18],
3. Sparrow et al.[44],
4. James et al.[21],
5. Bruzzi[6],

and 6. Tan and Charters[45].

The experimental data are tabulated in Tables B.3 to B.8 of Appendix B.

Again, the percentage root mean square deviation between the predicted Stanton number from the correlations and the experimental ones is used as the basis for comparison.

The experimental data of Bruzzi were corrected to constant-property conditions by means of:

i. Sieder-Tate method[42],

ii. Deissler method[9],

iii. Petukhov method[38],

and iv. James-Martin-Martin method[21].

The test fluid of Barrow, Sparrow et al. and Tan and Charters is air. As a result, their experimental data were corrected to constant-property conditions by means of equation (6.4) with m = 0.5, a figure recommended by both Kays[26] and Petukhov[38] (see Chapter 6). James et al. and Hines had corrected their experimental data to constant-property conditions by the Eagle and Ferguson method[14] and the Sieder-Tate method respectively.

In applying the circular-tube correlations, i.e Dittus-Boelter, Sieder-Tate, Petukhov-Popov, and Spalding-Jayatilleke, the procedures used for the symmetrical heat-transfer case was also followed here. Of course in this case, the experimental Prandtl, Reynolds, Nusselt and Stanton numbers were taken from Tables B.3 to B.8 of Appendix B.

The Barrow correlation for asymmetrical heat transfer was again applied in a similar manner as in the symmetrical heat-transfer case. However, the predicted Nusselt number in this case was from equation (5.1). The James-Martin-Martin correlation involved the substitution of the appropriate experimental Pr, Re, A and μ_R into equation (5.2). The predicted Nusselt numbers, and subsequently the Stanton numbers, were obtained and compared with the experimental ones. In the calculation of the present author's extension of Spalding-Jayatilleke P-function, the values of P and friction factor, c_f, were obtained in the same manner as in the symmetrical heat-transfer case. Again, κ was taken as 0.4. The values of Pr were obtained from Tables B.3 to B.8 of Appendix B. In the uniform-termperature-profile case, the appropriate P, Pr_{turb}, κ , and c_f were substituted into equation (5.11) while equation (5.17) was used in the two-portion-temperature-profile case. The predicted Stanton numbers which were obtained from these two equations, were then compared with the experimental Stanton numbers.

8.2.2 Results and Discussion

The resulting percentage root mean square deviations on Stanton number by using the various correlations and experimental data without any fluid-property correction (except those for Hines[18] and James et al.[21] which they corrected to constant-property conditions by the Sieder-Tate and the Eagle and Ferguson methods respectively) are summarized in Table 8.3.

Table 8.3 indicates that the use of circular-tube correlations for the prediction of asymmetrical heat transfer in rectangular channels and parallel plates would result in a 19 to 35 per cent error. This is because of the differences in heat-transfer conditions and cross-sectional geometry. Futhermore, this confirms similar findings of other works, such as James et al.[21], who did research in this area.

The pioneering work of Barrow[2,3] on asymmetrical heat transfer in parallel plates resulted in equation (5.1).

Table 8.3 Asymmetrical Heat Transfer: Percentage Root Mean Square Deviation on Stanton Number

Correlation	Equations Involved	Experimental Data# (1) Barrow△	(2) Hines	(3) Sparrow et al.△	(4) James et al.	(5) Bruzzi	(6) Tan & Charters△	Combined All Data (1) to (6)	Combined Parallel-Plate Data (1), (3) &(6)
Circular-Tube									
1. Dittus-Boelter	(3.3)	30.4	9.7	20.0	25.5	11.0	25.2	20.1	27.0
2. Sieder-Tate	(3.5)	37.6	8.0	29.5	43.0	13.4	34.3	30.4	35.0
3. Petukhov-Popov	(2.2)	24.0	17.3	3.6	32.3	10.3	16.5	22.8	19.3
4. Spalding-Jayatilleke Case (a)*	(2.2) (3.30) (3.31)	27.9	24.5	10.2	32.3	15.3	22.6	25.5	23.4

\# As-measured values, except those for Hines[18] and James et al.[21], which they corrected to constant-property conditions by the Sieder-Tate and the Eagle and Ferguson methods respectively.

△ Approaching parallel-plate conditions.

* $Pr_{turb} = 0.9$

@ c_f corrected by Jones method

Table 8.3 (cont'd)

Correlation	Equations Involved	(1) Barrow	(2) Hines	(3) Sparrow et al.	(4) James et al.	(5) Bruzzi	(6) Tan & Charters	Combined All Data (1) to (6)	Combined Parallel-Plate Data (1),(3)&(6)
		Experimental Data#							
Rectangular Channel & Parallel-Plate									
5. Barrow	(5.1)	29.3	76.6	46.4	281.3	65.2	14.8	171.2	33.4
6. James-Martin-Martin	(5.2)	21.8	18.0	19.0	5.7	9.2	9.8	13.4	19.2
7. Present author's extension of Spalding-Jayatilleke									
Uniform Temp.	(2.2)@ (2.8) (3.31) (5.11)								
Case (a)*		22.5	23.0	3.6	33.0	12.9	12.6	24.2	17.7
Case (b)*@		28.5	26.6	15.9	44.7	17.7	7.3	28.4	23.1
2-Portion Temp.	(2.2)@ (2.8) (3.31) (5.17)								
Case (a)*		25.0	23.8	5.9	32.6	14.1	17.8	24.8	20.2
Case (b)*@		24.2	27.4	10.0	44.0	18.8	12.9	28.5	19.5

With the exception of the experimental data from Tan and Charters[45] and Barrow's own, the percentage root mean square deviations between the predicted Stanton number from equation (5.1) and the other experimental data are extremely large. This is especially marked for data from Hines[18], James et al.[21] and Bruzzi[6]; all have much higher Prandtl numbers than 0.7.

The equation (5.2) of James et al.[21] gives the best correlation, with a percentage root mean square deviation of 13.4% between the predicted Stanton number and all the experimental data involved. When the James-Martin-Martin correlation is compared with their own experimental data, the percentage root mean square deviation is 5.7. Good agreement is also obtained when using the experimental data of Hines[18] and Bruzzi[6]. It is interesting to note that the Reynolds numbers, Prandtl numbers and aspect ratios are within the "with reasonable certainty" range of the recommendation of James et al..

The corresponding results of the present author's extension of the Spalding-Jayatilleke correlation, equations (5.11) and (5.17), for asymmetrical heat transfer in parallel plates as compared with the original Spalding-Jayatilleke correlation, equation (3.27), for circular tubes show little improvement, as indicated in Tables 8.3 (24.2% and 24.8% versus 25.5%).

It is interesting to note, from Tables 8.3 and 8.4, that the present author's extension of the Spalding-

Table 8.4 Asymmetrical Heat Transfer:
Percentage Root Mean Square Deviation on Stanton Number

Correlation	Combined All Data (As-Measured)	Experimental Data: Combined All Parallel-Plate Data, Constant-Property#	Experimental Data: Combined All Parallel-Plate Data, As-Measured
Present author's extension of Spalding-Jayatilleke			
Uniform Temp.			
Case (a)*	24.2	17.0	17.7
Case (b)*@	28.4	24.2	23.1
2-Portion Temp.			
Case (a)*	24.8	19.3	20.2
Case (b)*@	28.5	19.9	19.5

\# Data corrected to constant-property conditions using equation (6.4) with m=0.5

* $Pr_{turb} = 0.9$

@ c_f corrected by Jones[23] method

Jayatilleke correlation yields better results in the precentage root mean square deviation when only the experimental parallel-plate data are considered (24.2% to 17.7%, 28.4% to 23.1%, 24.8% to 20.2% and 28.5% to 19.5%). The parallel-plate data are data which are related to small aspect ratios; A less than, say, 0.5. These include the data of Barrow[3], Sparrow et al.[44] and Tan and Charters[45]. Furthermore, the uniform-temperature-profile correlation, equation (5.11), yields percentage root mean square deviations of 17.7% for as-measured data and 17.0% for corrected constant-property data (see Table 8.4) and is superior to all the other correlations for parallel-plate conditions. The application of Jones "laminar Reynolds number" correction[23] on friction factor is not as successful here as in the case of symmetrical heat transfer. In fact, it tends to make matters worse.

With the following data:

1. Parallel-plate experimental Stanton number under constant-property conditions*,
2. $Pr_{turb} = 0.9$,
3. $\kappa = 0.4$,

and 4. c_f from Blasius equation,

the experimental P-values of Barrow[3], Sparrow et al.[44] and Tan and Charters[45] can then be obtained from equations (5.11) and (5.17). The results, with equation (3.31), are

---

* Data corrected to constant-property conditions by using equation (6.4) with m = 0.5.

shown in Figures 8.6 and 8.7. Figures 8.8 and 8.9 are similar to Figures 8.6 and 8.7 with the exception that c_f was obtained from the Blasius equation with correction by the Jones[23] method. These figures, 8.6 to 8.9, provide similar information as in Table 8.3, Item 7, Experimental Data (1), (3) and (6). In Table 8.3, the parameter is the percentage root mean square deviation on Stanton number, while in Figures 8.6 to 8.9, it is the P-value. Figures 8.6, 8.8, 8.7 and 8.9 correspond to Table 8.3, Item 7, Uniform-Temperature Case (a) and (b) and Two-Portion-Temperature Case (a) and (b) respectively. The large deviation between the experiemtnal P-values and the line of equation (3.31), as shown in some of the figures in Figures 8.6 to 8.9, should not be mistaken as large error in the predicted Stanton number because the Prandtl number involved is small (Pr = 0.7).

The effects of fluid property correction* on the parallel-plate data are illustrated in Table 8.5. The average difference on the percentage root mean square deviation between the as-measured and constant-property data is only 1.5. Furthermore, by comparing Figures 8.6 with 8.10, the difference in the experimental P-values due to the changes in fluid properties is small. Bruzzi[6] provided accurate information on μ_b and μ_w of his experiments. Hence, the data of Bruzzi were corrected to constant-property conditions by the Sieder-Tate, Deissler, Petukhov

* Data corrected to constant-property conditions by using equation (6.4) with m = 0.5.

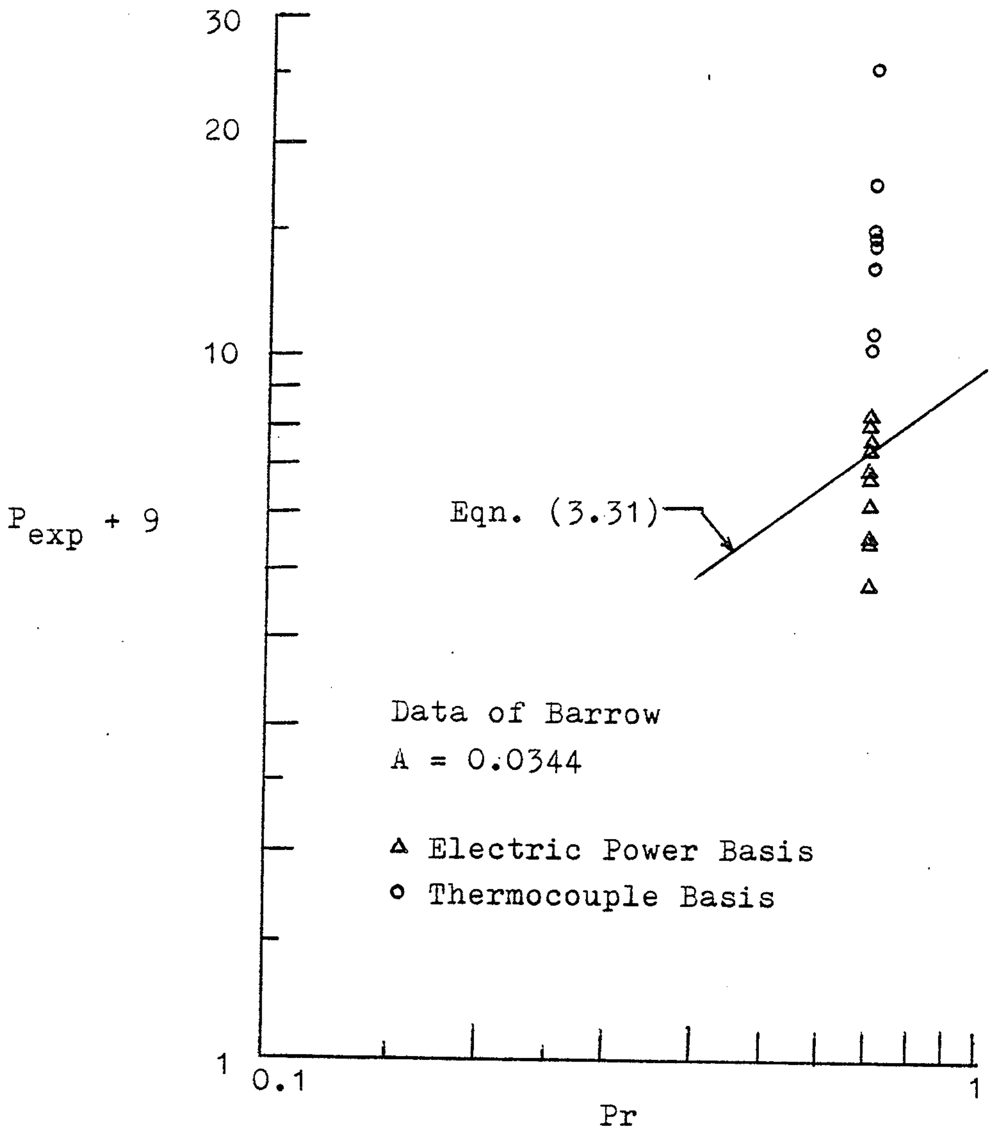

Fig. 8.6 Experimental P-Values:
Asymmetrical Heat-Transfer Constant-Property Data with Uniform Temperature Profile

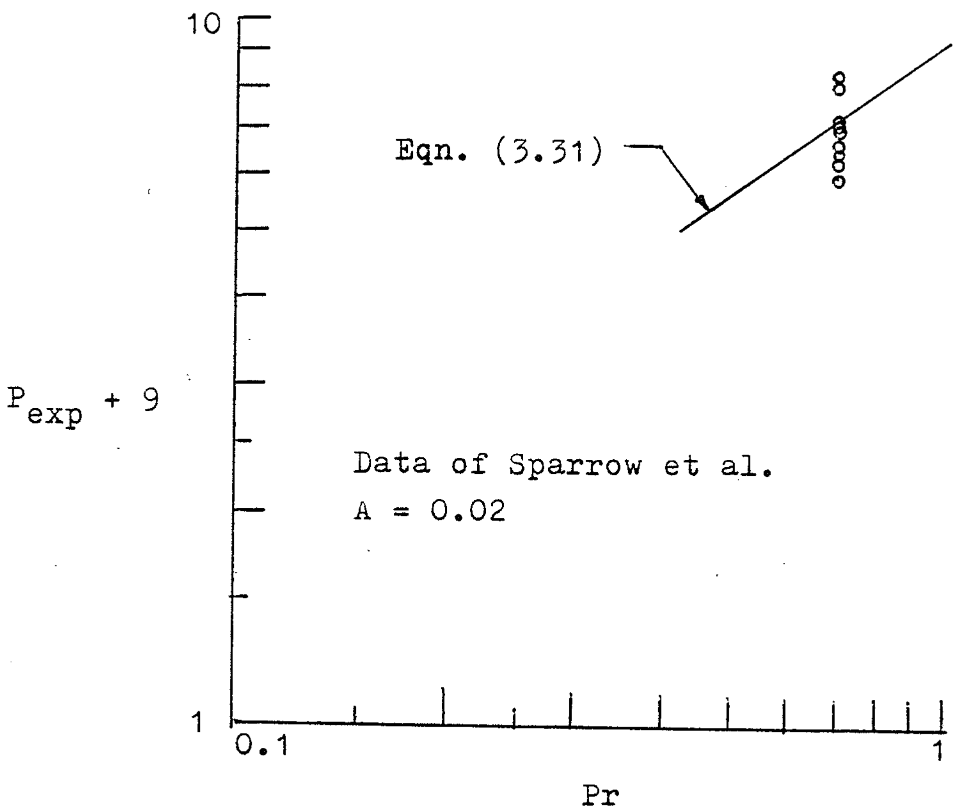

Fig. 8.6 (cont'd)

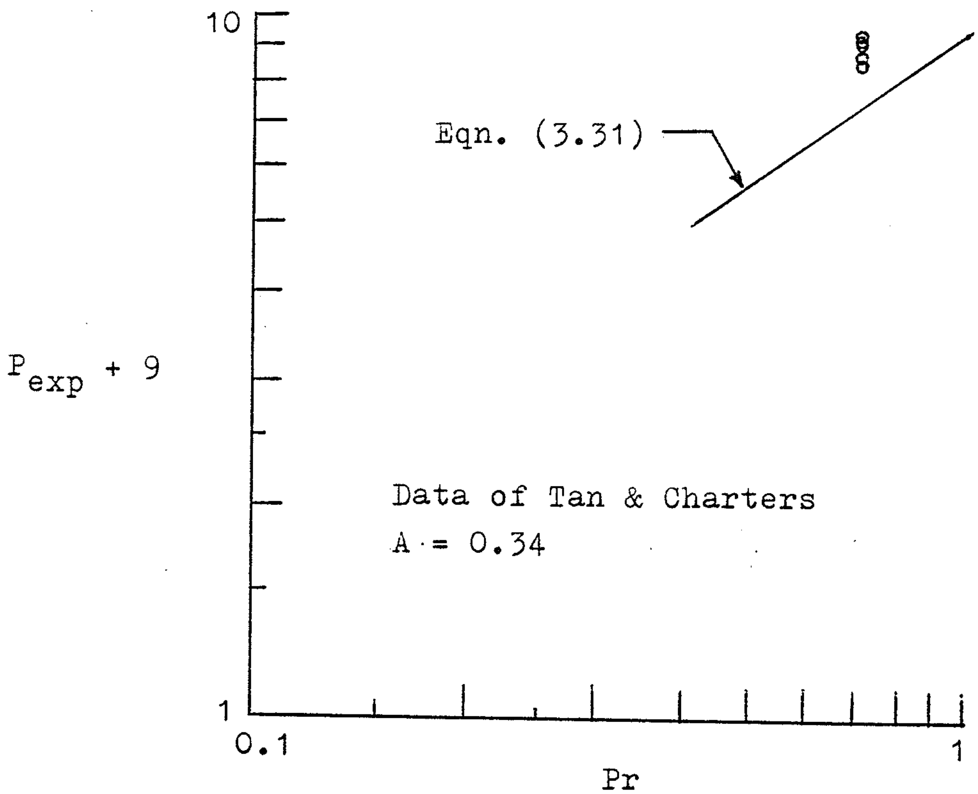

Fig. 8.6 (cont'd)

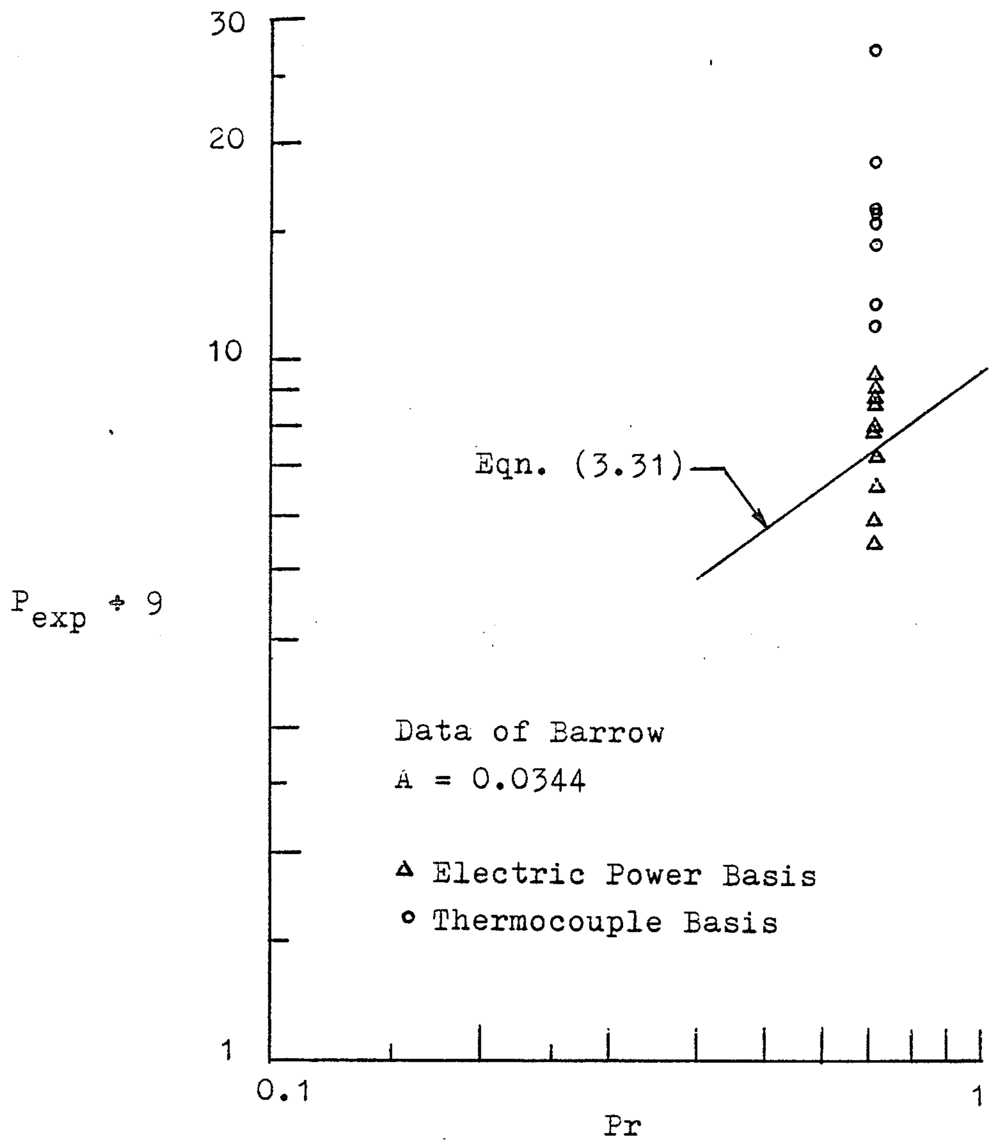

Fig. 8.7 Experimental P-Values: Asymmetrical Heat-Transfer Constant-Property Data with Two-portion Temperature Profile

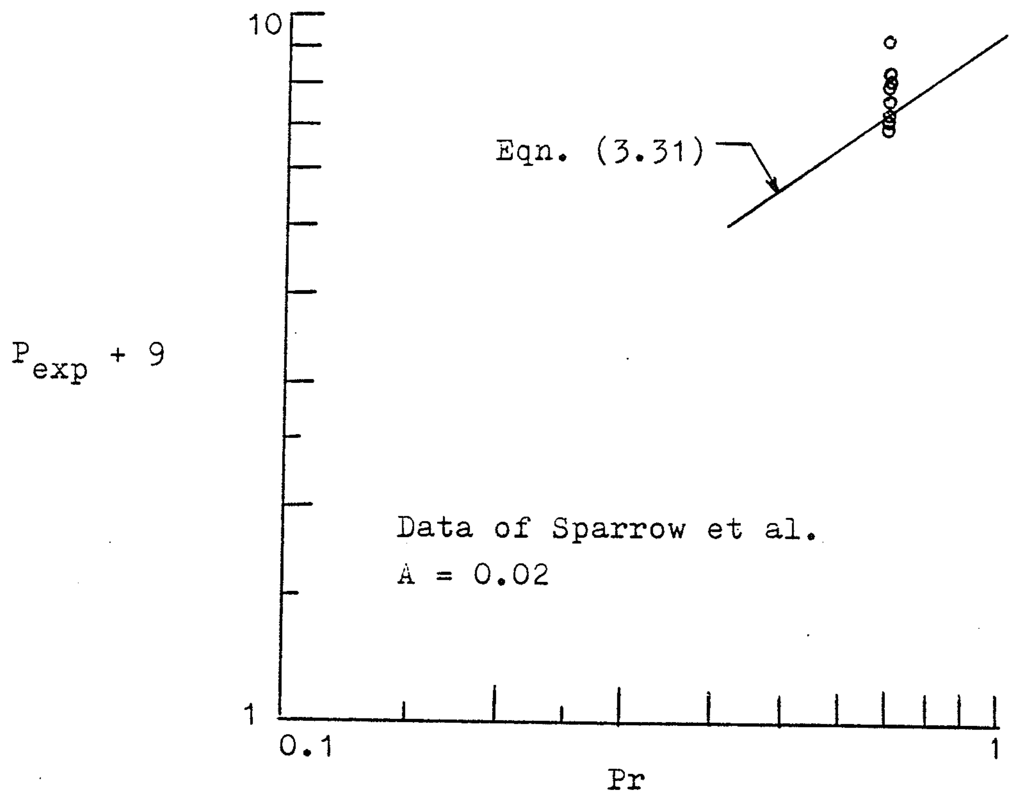

Fig. 8.7 (cont'd)

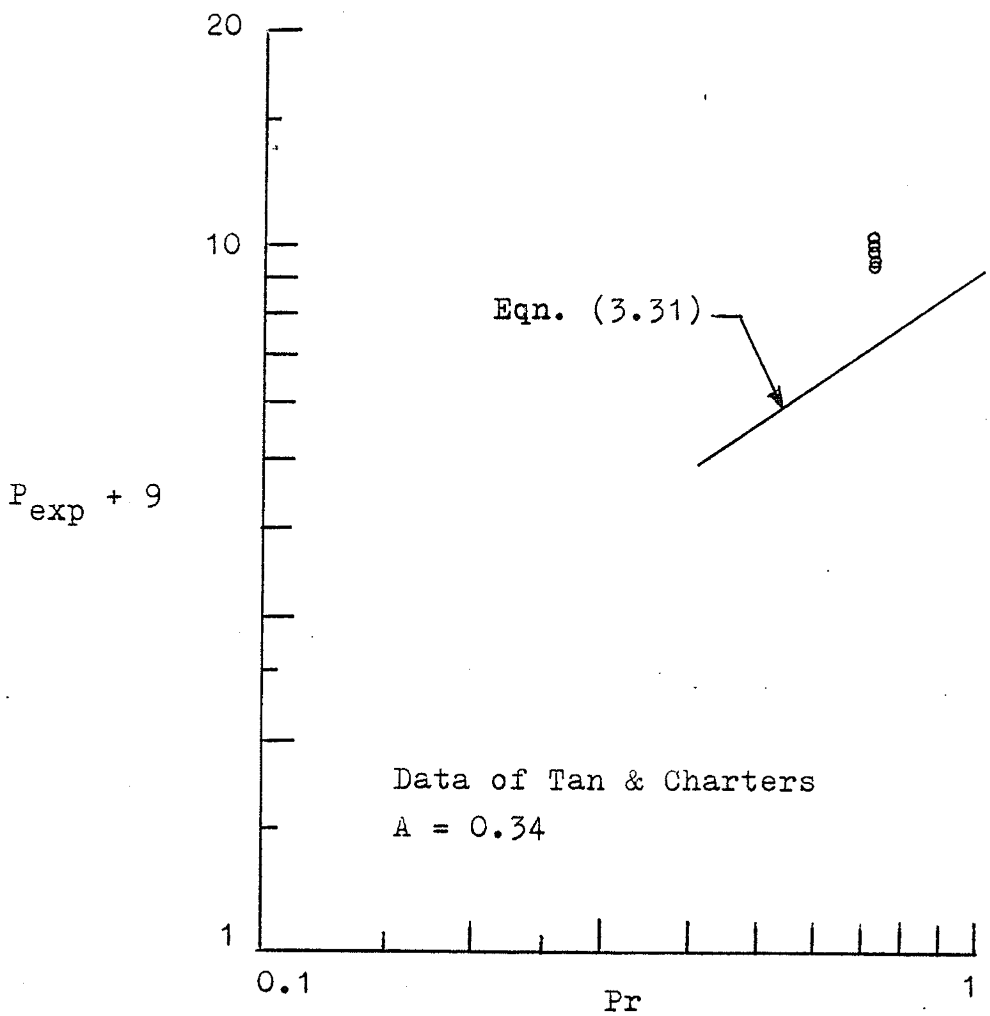

Fig. 8.7 (cont'd)

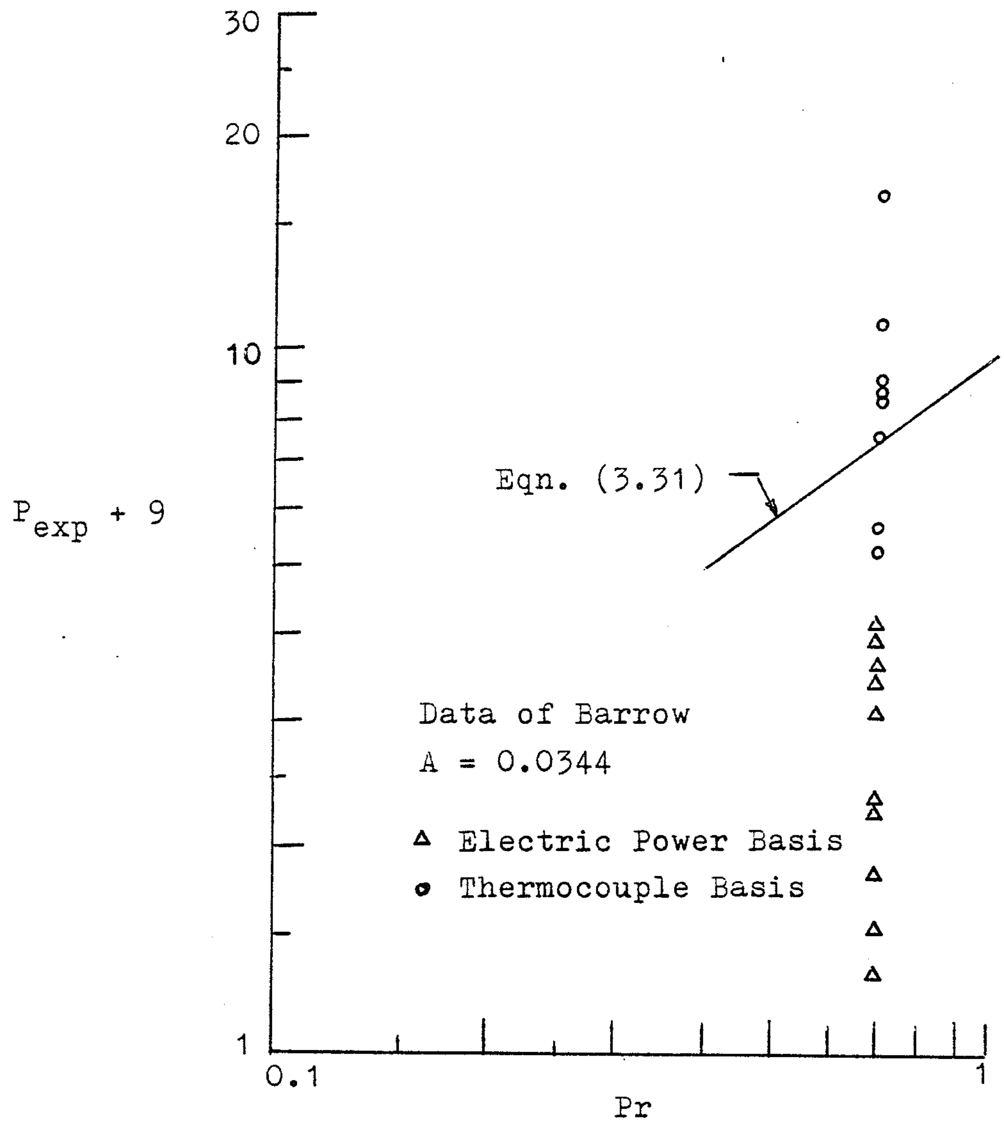

Fig. 8.8 Experimental P-Values:
Asymmetrical Heat-Transfer Constant-Property Data with Uniform Temperature Profile (c_f Corrected by Jones Method)

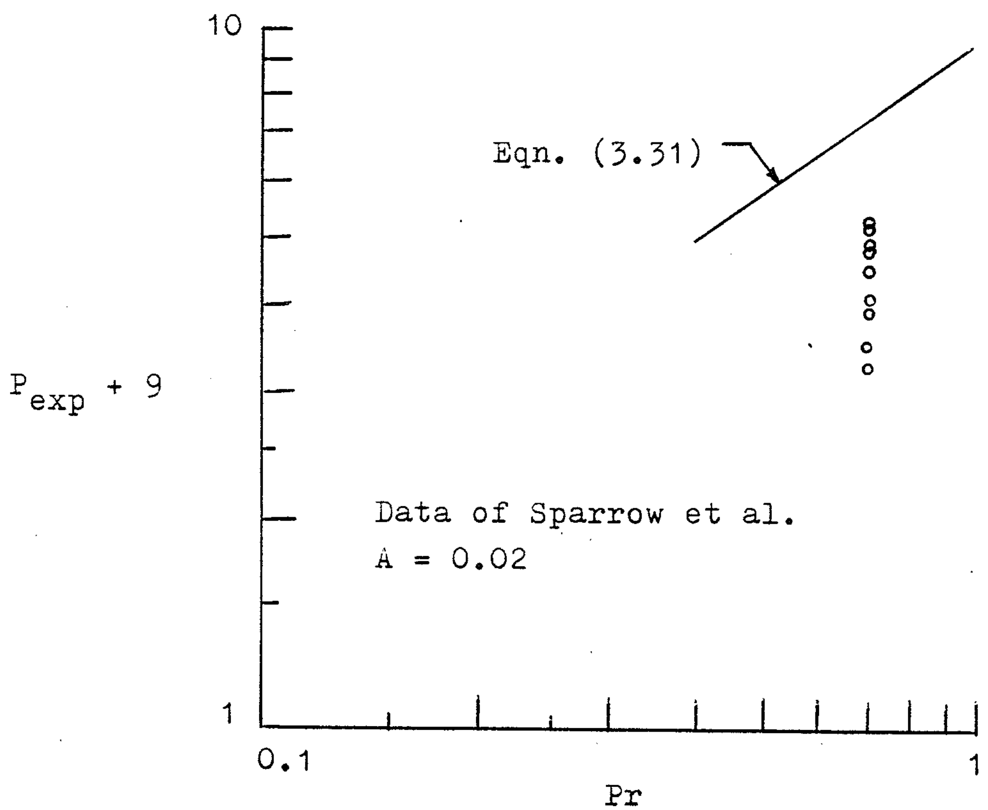

Fig. 8.8 (cont'd)

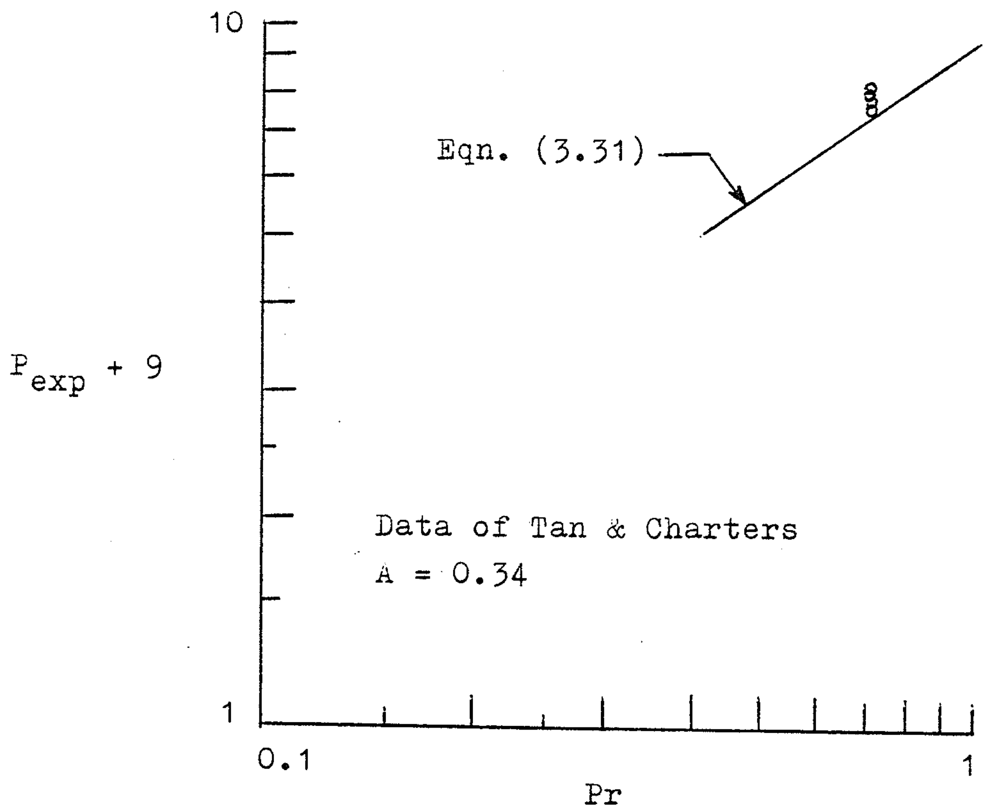

Fig. 8.8 (cont'd)

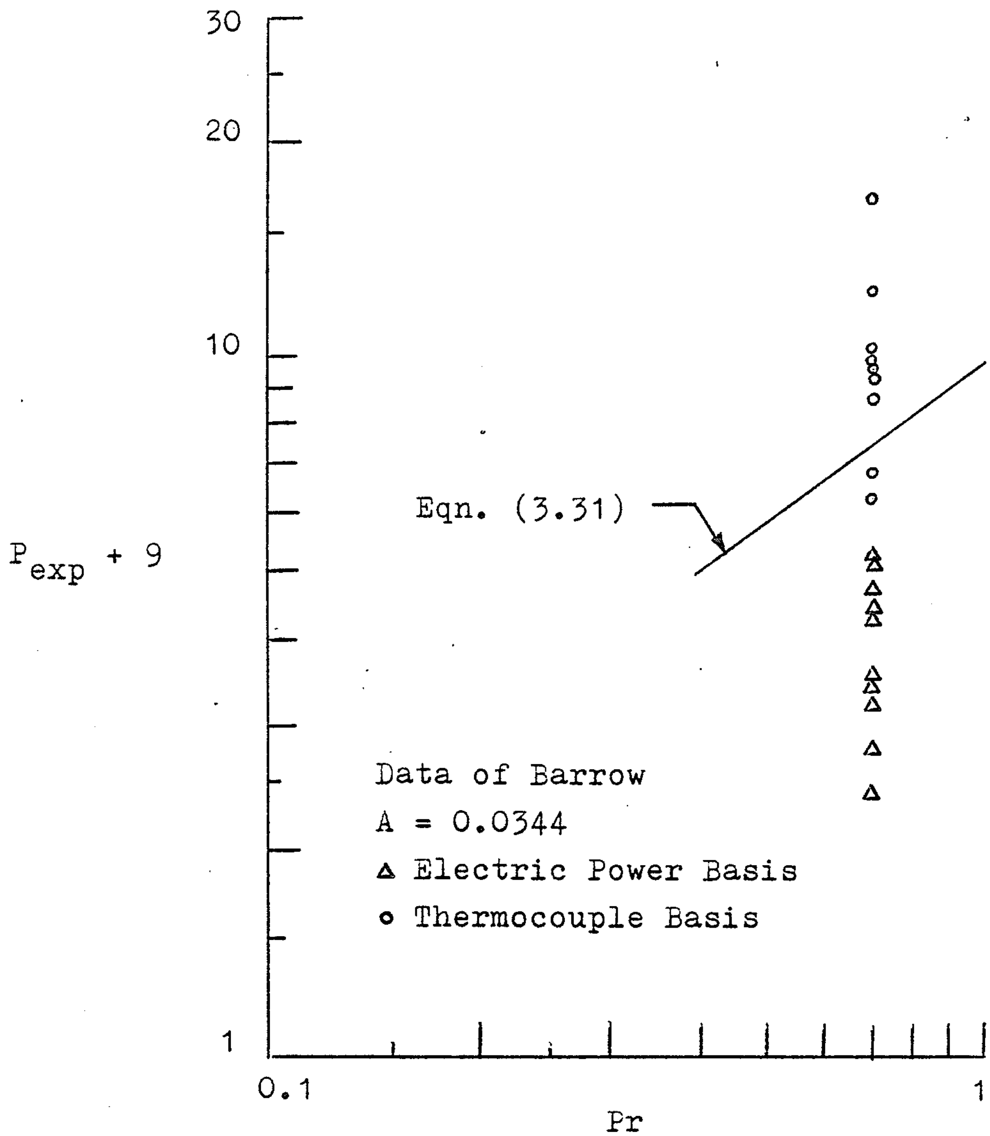

Fig. 8.9 Experimental P-Values: Asymmetrical Heat-Transfer Constant-Property Data with Two-Portion Temperature Profile (c_f Corrected by Jones Method)

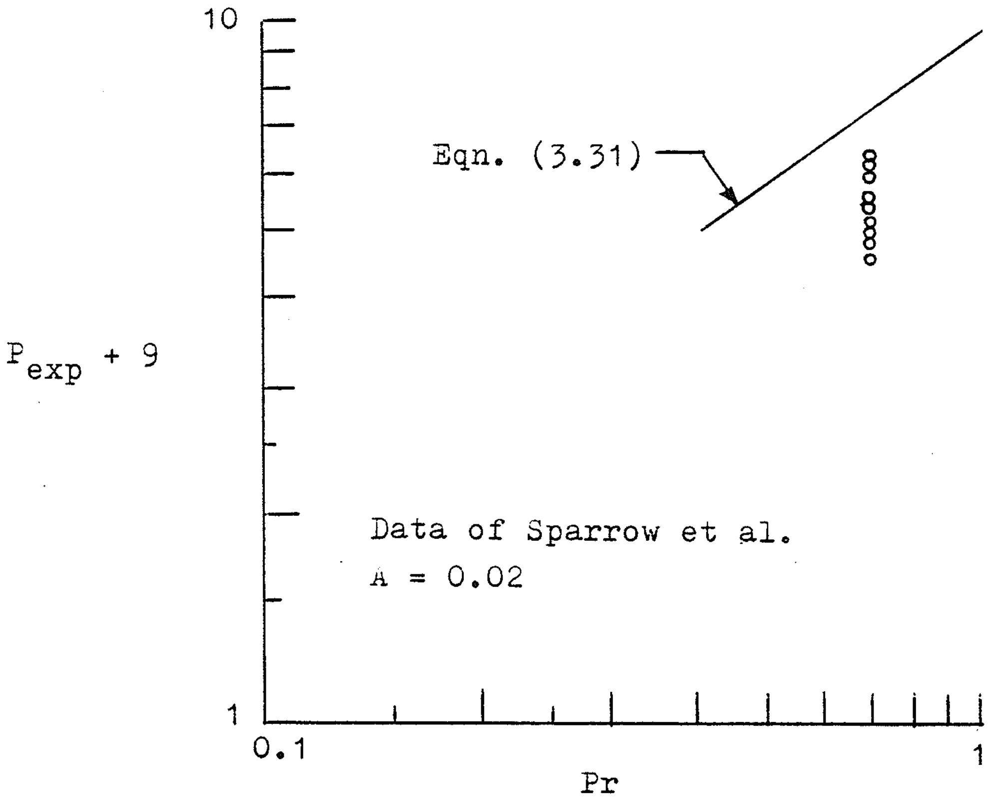

Fig. 8.9 (cont'd)

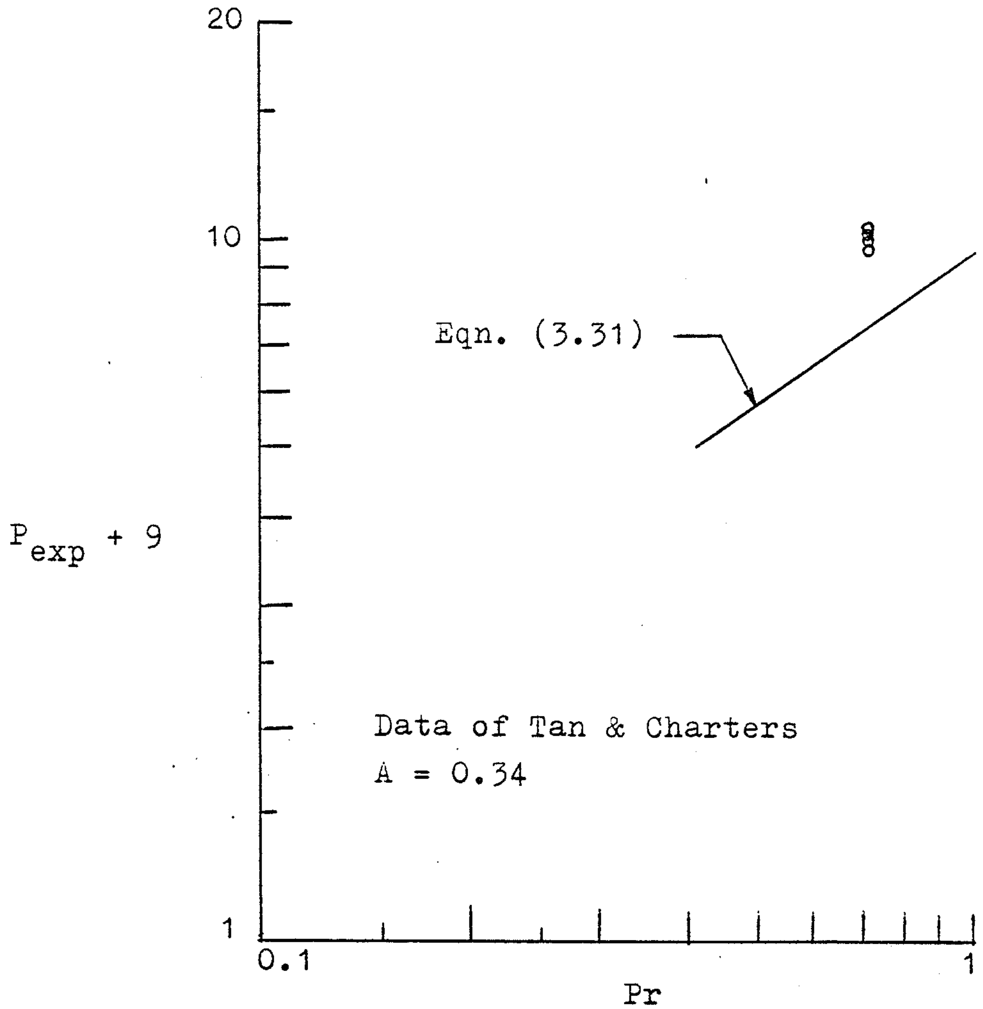

Fig. 8.9 (cont'd)

Table 8.5 Asymmetrical Heat-Transfer Parallel-Plate Data: Percentage Root Mean Square Deviation with Fluid Properties Correction

Correlation	Barrow		Sparrow et al.		Tan & Charters		Combined	
	As-Measured	Constant-Property$^{\Delta}$	As-Measured	Constant-Property$^{\Delta}$	As-Measured	Constant-Property$^{\Delta}$	As-Measured	Constant-Property$^{\Delta}$
Circular-Tube								
1. Dittus-Boelter	30.4	29.8 (-0.6)#	20.0	17.6 (-2.4)	25.2	21.3 (-3.9)	27.0	23.6 (-3.4)
2. Sieder-Tate	37.6	---	29.5	---	34.3	---	35.0	---
3. Petukhov-Popov	24.0	23.6 (-0.4)	3.6	4.5 (0.9)	16.5	12.1 (-4.4)	19.3	18.5 (-0.8)
4. Spalding-Jayatilleke								
Case (a)*	27.9	26.5 (-1.4)	10.2	7.6 (-2.6)	22.6	18.6 (-4.0)	23.4	21.6 (-1.8)

Table 8.5 (cont'd)

Correlation	Barrow		Sparrow et al.		Tan & Charters		Combined	
	As-Measured	Constant-Property $^{\Delta}$	As-Measured	Constant-Property $^{\Delta}$	As-Measured	Constant-Property $^{\Delta}$	As-Measured	Constant-Property $^{\Delta}$
<u>Rectangular Channel & Parallel-Plate</u>								
5. Barrow	29.3	30.2 (0.9)	46.4	50.9 (4.5)	14.8	20.7 (5.9)	33.4	36.0 (2.6)
6. James-Martin-Martin	21.8	---	19.0	---	9.8	---	19.2	---
7. Present author's extension of Spalding-Jayatilleke								
<u>Uniform Temp.</u>								
Case (a)*	22.5	22.2 (-0.3)	3.6	5.1 (1.5)	12.6	8.0 (-4.6)	17.7	17.1 (-0.6)
Case (b)*@	28.5	29.4 (0.9)	15.9	19.4 (3.5)	7.3	2.6 (-4.7)	23.1	24.2 (1.1)

Table 8.5 (cont'd)

Correlation	Barrow		Sparrow et al.		Tan & Charters		Combined	
	As-Measured	Constant-Property$^{\Delta}$	As-Measured	Constant-Property$^{\Delta}$	As-Measured	Constant-Property$^{\Delta}$	As-Measured	Constant-Property$^{\Delta}$
Rectangular Channel & Parallel-Plate								
7. Present author's extension (cont'd)								
2-Portion Temp								
Case (a)*	25.0	24.6 (-0.4)	5.9	4.0 (-1.9)	17.8	13.5 (-4.3)	20.2	19.3 (-0.9)
Case (b)*@	24.2	24.8 (0.6)	10.0	13.2 (3.2)	12.9	4.7 (-8.2)	19.5	19.9 (0.4)
							Av. Diff. =	|1.5|

Δ Data corrected to constant-property conditions using equation (6.4) with m=0.5

\# The difference in PD_{rms} as compared with as-measured values is in brackets

* $Pr_{turb} = 0.9$

@ c_f corrected by the Jones[23] method

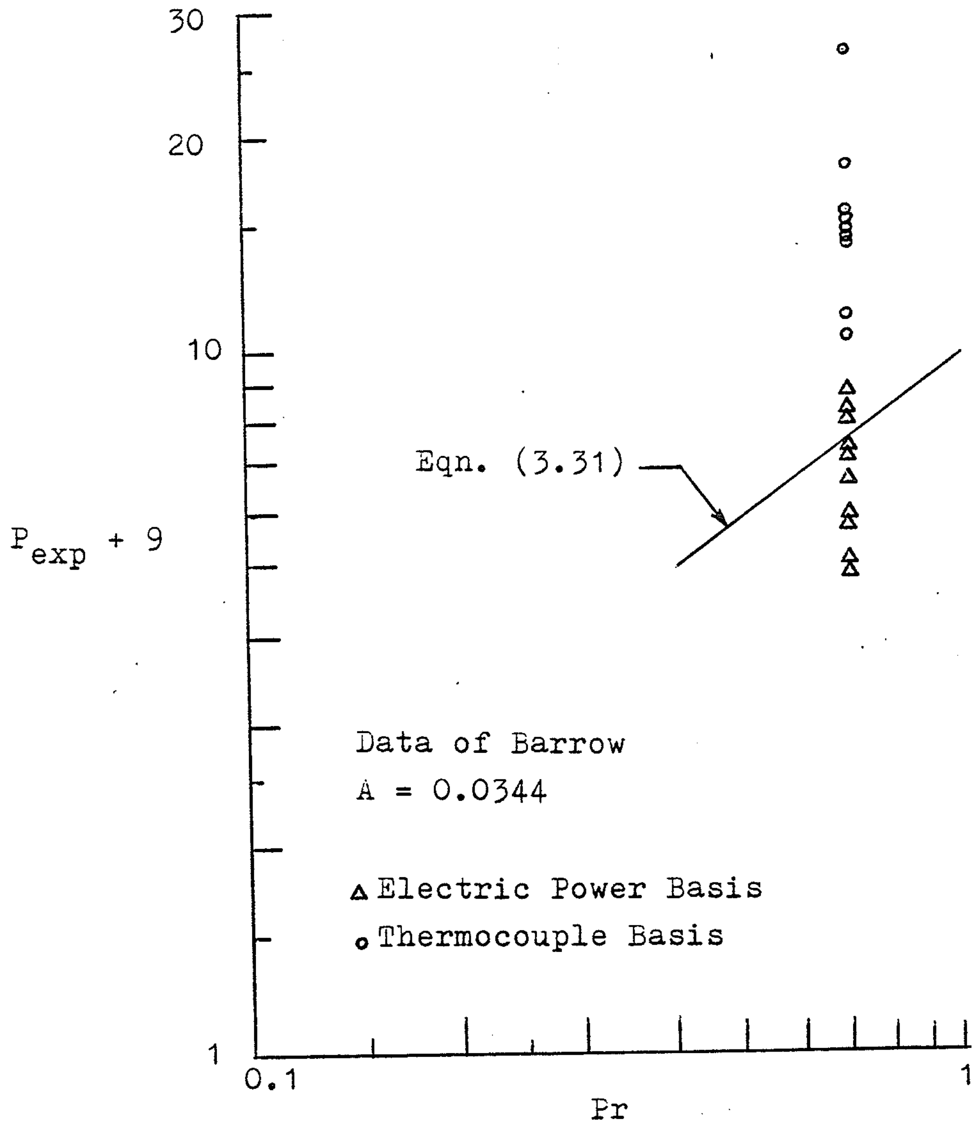

Fig. 8.10 Experimental P-Values:
Asymmetrical Heat-Transfer As-Measured
Data with Uniform Temperature Profile

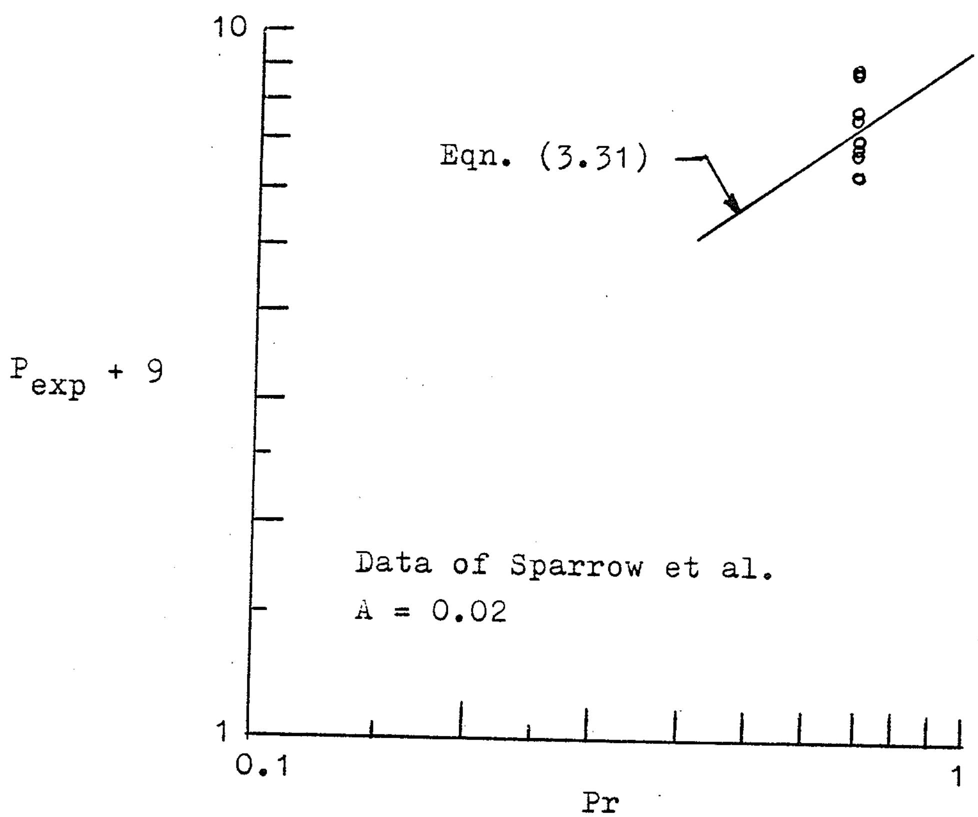

Fig. 8.10 (cont'd)

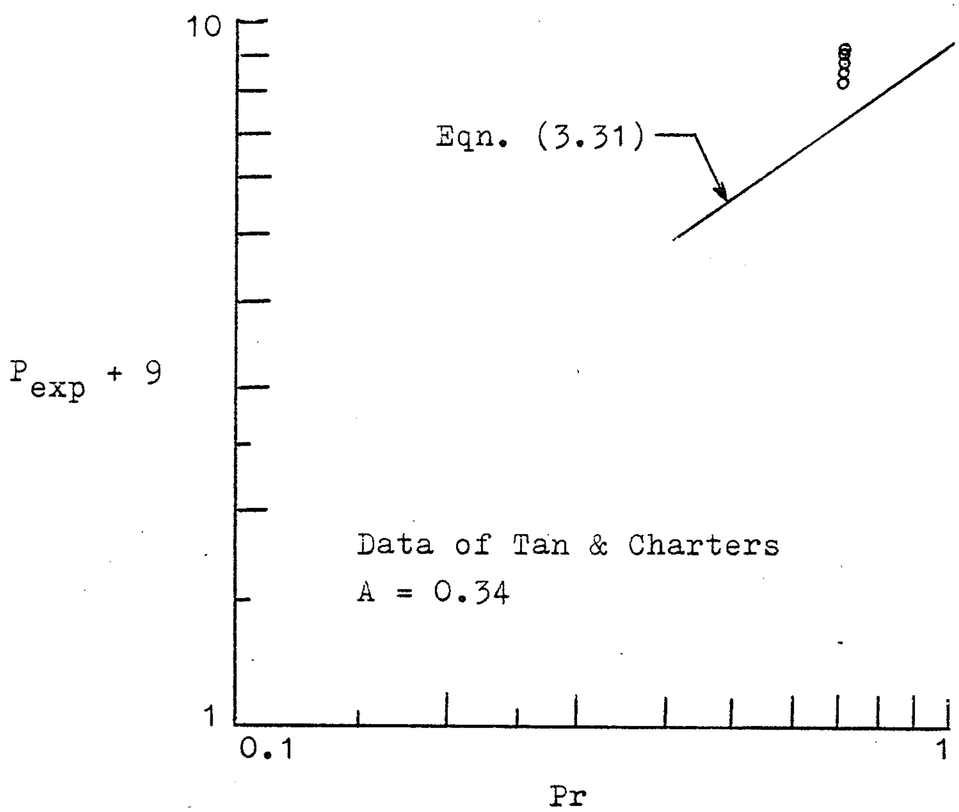

Fig. 8.10 (cont'd)

and James-Martin-Martin methods. The average difference on the percentage root mean square deviation between the as-measured and constant-property data as indicated in Table 8.6, is again small (0.5 to 4.5).

Table 8.6 Asymmetrical Heat-Transfer Data of Bruzzi: Percentage Root Mean Square Deviation with Fluid Properties Correction

Correlation	As-Measured Data	Correction to Constant Fluid Properties Using: Sieder-Tate Method	Deissler Method	Petukhov Method	James-Martin-Martin Method
Circular-Tube					
1. Dittus-Boelter	11.0	9.3 (-1.7)#	9.4 (-1.6)	9.6 (-1.4)	10.5 (-0.5)
2. Sieder-Tate	13.4	11.0 (-2.4)	9.6 (-3.8)	11.5 (-1.9)	12.8 (-0.6)
3. Petukhov-Popov	10.3	9.6 (-0.7)	11.9 (1.6)	9.5 (-0.8)	10.0 (-0.3)
4. Spalding-Jayatilleke*	15.3	17.4 (2.1)	20.8 (5.5)	17.0 (1.7)	15.6 (0.3)

Table 8.6 (cont'd)

Correlation	As-Measured Data	Correction to Constant Fluid Properties Using:			
		Sieder-Tate Method	Deissler Method	Petukhov Method	James-Martin-Martin Method
Rectangular Channel & Parallel-Plate					
5. Barrow	65.2	60.1 (-5.1)	53.6 (-11.6)	61.1 (-4.1)	64.2 (-1.0)
6. James-Martin-Martin	9.2	9.3 (0.1)	9.5 (0.3)	9.7 (0.5)	10.2 (1.0)
7. Present author's extension of Spalding-Jayatilleke					
Uniform Temp					
Case (a)*	12.9	14.8 (1.9)	18.2 (5.3)	14.5 (1.6)	13.1 (0.2)
Case (b)*@	17.7	19.5 (1.8)	22.4 (4.7)	19.1 (1.4)	18.0 (0.3)

Table 8.6 (cont'd)

Correlation	As-Measured Data	Correction to Constant Fluid Properties Using: Sieder-Tate Method	Deissler Method	Petukhov Method	James-Martin-Martin Method
Rectangular Channel & Parallel-Plate					
7. Present author's extension (cont'd)					
2-Portion Temp					
Case (a)*	14.1	16.2 (2.1)	19.5 (5.4)	15.8 (1.7)	14.4 (0.3)
Case (b)*@	18.8	20.7 (1.9)	23.6 (4.8)	20.3 (1.5)	19.1 (0.3)
		Av. Diff. = |2.0|	Av. Diff. = |4.5|	Av. Diff. = |1.7|	Av. Diff. = |0.5|

The difference in PD_{rms} as compared with as-measured values is in brackets

* $Pr_{turb} = 0.9$

@ c_f corrected by the Jones[23] method

CHAPTER 9

CONCLUSIONS AND RECOMMENDATIONS

9.1 Conclusions

The Spalding-Jaytilleke[22,43] method of heat-transfer prediction is attractive because it is a delicate blend of theory and empiricism. It is simple and directly-usable and there is some distinct physical significance to the various terms appearing in the correlation. The present author extended the Spalding-Jayatilleke method for parallel plates for conditions of symmetrical and asymmetrical heating. An assessment of the various existing correlations, including the extension of the Spalding-Jayatilleke method, was conducted. It was found that for symmetrical heat transfer, the present author's extension of the Spalding-Jayatilleke method is as good as the Barrow's[2] correlation for parallel-plate prediction and they both yield better results than all the existing circular-tube correlations. As for asymmetrical heat transfer, the Spalding-Jayatilleke extension is better than any existing correlation for parallel-plate prediction.

9.2 Recommendations

9.2.1 Symmetrical Heat Transfer

(1) In symmetrical heat-transfer predictions for

turbulent fluid flow in rectangular channels and/or parallel plates, recommended are Barrow's[2] correlation, equation (4.2) or the present author's extension of the Spalding-Jayatilleke P-function method, equation (4.17).

(2) In applying the present author's extension of the Spalding-Jayatilleke P-function method, use should be made of

A. friction factor, c_f, from Blasius's equation with Jones'[23] correction to rectangular or parallel-plate geometries, equations (2.2) and (2.8),

B. turbulent Prandtl number, Pr_{turb}, as 0.9,

C. value of P as recommended by Spalding and Jayatilleke, equation (3.31),

and D. κ as 0.4.

9.2.2 Asymmetrical Heat Transfer

(1) In asymmetrical heat-transfer predictions for turbulent fluid flow between parallel plates, the present author's extension of the Spalding-Jayatilleke P-function method, equations (5.11) or (5.17), is recommended.

(2) In applying the present author's extension of the Spalding-Jayatilleke P-function method, use should be made of

A. either the uniform temperature profile, equation (5.11), or the two-portion temperature profile, equation (5.17),

B. friction factor, c_f, from Blasius's equation (2.2),

C. turbulent Prandtl number, Pr_{turb}, as 0.9,

D. value of P as recommended by Spalding and Jayatilleke, equation (3.31),

and E. k as 0.4.

(3) In the case of rectangular channels (aspect ratio greater than, say, 0.5) the correlation of James, Martin and Martin[21] is recommended.

9.2.3 Further Work

(1) It would be extremely interesting to learn if the Spalding-Jayatilleke P-function for circular tubes, equation (3.31), is equally applicable to other geometries, i.e. the effect of the aspect ratio on the P-value. Although good predictions are possible using it with other geometries (and the appropriate equations), a thorough test awaits further data.

(2) Further experimental work on symmetrical and asymmetrical heating of liquids between parallel plates would be desirable.

REFERENCES

1. J. Allen and N. D. Grundbery, The Resistance to the Flow of Water Along Smooth Rectangular Passages, and the Effect of a Slight Convergence or Divergence of the Boundaries, Philosophical Magazine, 7, 490 (1937).

2. H. Barrow, Convection Heat Transfer Coefficients for Turbulent Flow Between Parallel Plates with Unequal Heat Fluxes, Int. J. Heat Mass Transfer, 1, 306 (1961).

3. H. Barrow, An Analytical and Experimental Study of Turbulent Gas Flow Between Two Smooth Parallel Walls with Unequal Heat Fluxes, Int. J. Heat Mass Transfer, 5, 469 (1962).

4. E. Brundrett and W. D. Baines, The Production and Diffusion of Vorticity in Duct Flow, J. Fluid Mechanics, 19, No. 3, 375 (1964).

5. E. Brundrett and P. R. Burroughs, The Temperature Inner-Law and Heat Transfer for Turbulent Air Flow in a Vertical Square Duct, Int. J. Heat Mass Transfer, 10, 1133 (1967).

6. S. Bruzzi, Forced Convection Boiling Heat Transfer in a Rectangular Duct Heated on One Side, PhD. Thesis, Mech. Engg. Dept., Imperial College, London, U.K. (Oct. 1969).

7. R. J. Cornish, Flow in a Pipe of Rectangular Cross-Section, Proc. Royal Society of London, 120, Series A, 691 (1928).

8. S. C. Davies and C. M. White, An Experimental Study of Flow of Water in Pipes of Rectangular Section, Proc. Royal Society of London, 119, Series A, 92 (1928).

9. R. G. Deissler, Analysis of Turbulent Heat Transfer, Mass Transfer and Friction in Smooth Tubes at High Prandtl and Schmidt Numbers, NACA, TN 3145 (May 1954).

10. R. G. Deissler, Analysis of Turbulent Heat Transfer, Mass Transfer and Friction in Smooth Tubes at High Prandtl and Schmidt Numbers, NACA, Report 1210 (1955).

11. R. G. Deissler and M. F. Taylor, Analysis of Axial Turbulent Flow and Heat Transfer Through Banks of Rods or Tubes, Heat Transfer Conf. Sponsored by AEC, New York (November 1956).

12. R. G. Deissler and M. F. Taylor, Analysis of Turbulent Flow and Heat Transfer in Non-Circular Passages, NACA, TN4384 (1958).

13. F. W. Dittus and L. M. K. Boelter, Heat Transfer in Automobile Radiators of the Tubular Type, University of California, Pub. in Engg., 2, 44 (1930).

14. A. E. Eagle and R. M. Ferguson, On the Coefficient of Heat Transfer from the Internal Surface of Tube Walls, Proc. Royal Society, 127, Series A, 540 (1930).

15. E. R. G. Eckert and T. F. Irvine, Jr., Incompressible Friction Factor, Transition and Hydrodynamic Entrance-Length Studies of Ducts with Triangular and Rectangular Cross-Section, Fifth Mid-Western Conference on Fluid Mechanics (1957).

16. E. R. G. Eckert and T. F. Irvine, Jr., Pressure Drop and Heat Transfer in a Duct with Triangular Cross-Section, J. Heat Transfer, Trans. ASME, Series C, 82, 125 (1960).

17. J. P. Hartnett, J. C. Y. Koh and S. T. McComas, A Comparison of Predicted and Measured Friction Factors for Turbulent Flow Through Rectangular Ducts, J. Heat Transfer, Trans. ASME, Series C, 84, 82 (1962).

18. W. S. Hines, Heat Transfer to RP-Kerosene in Turbulent Flow under Asymmetric Heating Conditions, Chem. Engg Progress, Symp. Series, 59, 41, 193 (1963).

19. L. C. Hoagland, Fully Developed Turbulent Flow in Straight Rectangular Ducts, PhD. Thesis, M.I.T., Cambridge, U.S.A. (1960).

20. P. S. Huebscher, Friction in Round, Square, and Rectangular Ducts, Heating, Piping and Air Conditioning, 19, 127 (1947).

21. D. D. James, B. W. Martin and D. G. Martin, Forced Convection Heat Transfer in Asymmetrically Heated Ducts of Rectangular Cross-Section, 3rd. Int. Heat Transfer Conference, Chicago (August 1966).

22. C. L. V. Jayatilleke, The Influence of Prandtl Number and Surface Roughness on the Resistance of the Laminar Sub-layer to Momentum and Heat Transfer, Progress in Heat and Mass Transfer, 1, 193 (1969).

23. O. C. Jones, An Improvement in the Calculation of Turbulent Friction in Rectangular Ducts, ASME Paper, 75-WA/FE-12 (1975).

24. J. M. Kay, An Introduction to Fluid Mechanics and Heat Transfer, p.69, Cambridge University Press, Cambridge (1963).

25. W. M. Kay, Convective Heat and Mass Transfer, p.68, McGraw-Hill, New York (1966).

26. Ibid., p.264.

27. J. G. Knudsen and D. L. Katz, Fluid Dynamics and Heat Transfer, p.451, McGraw-Hill, New York (1958).

28. F. C. Lea and A. G. Tadros, Flow of Water Through a Circular Tube with a Central Core and Through Rectangular Tubes, Philosophical Magazine, 7, 1235 (1931).

29. H. J. Leutheusser, Turbulent Flow in Rectangular Ducts, J. Hydraulic Division, Proc. ASCE, 89, HY3 (1963).

30. S. Levy, R. A. Fuller and R. O. Niemi, Heat Transfer to Water in Thin Rectangular Channels, J. Heat Transfer, Trans. ASME, 81, 129 (1959).

31. B. S. Massey, Mechanics of Fluids, p.190, Van Nostrand Reinhold, London (1975).

32. G. W. Maurer and B. W. LeTourneau, Friction Factor for Fully Developed Turbulent Flow in Ducts With and Without Heat Transfer, J. Basic Engg, Trans. ASME, 86, 627 (1964).

33. W. H. McAdams, Heat Transmission, p.157, McGraw-Hill, New York (1954).

34. T. Mizushina, Analogy between Fluid Friction and Heat Transfer in Annuli, Proc. of General Discussion on Heat Transfer, Inst. Mech. Engg./ASME, (September 1951).

35. J. Nikuradse, Investigation of Turbulent Flow in Tubes of Non-circular Cross-Section, Ingenieur Archiv., 1, 306 (1939).

36. J. L. Novotny, S. T. McComas, E. M. Sparrow and E. R. G. Eckert, Heat Transfer for Turbulent Flow in Rectangular Ducts with Two Heated and Two Unheated Walls, AIChE Journal, 10, No.4, 466 (1964).

37. V. C. Patel and M. R. Head, Some Observations on Skin Friction and Velocity Profiles in Fully Developed Pipe and Channel Flows, J. Fluid Mechanics, 38, part 1, 181 (1969).

38. B. S. Petukhov, Heat Transfer and Friction in Turbulent Pipe Flow with Variable Physical Properties, Advances in Heat Transfer, 6, 502 (1970).

39. B. S. Petukhov and V. N. Popov, Theoretical Calculation of Heat Exchange and Frictional Resistance in Turbulent Flow in Tubes of an Incompressible Fluid with Variable Physical Properties, Trans. in High Temperature, 1, No.1, 69 (1963).

40. H. Reichardt, The Principles of Turbulent Heat Transfer, Trans. by P. A. Schoeck in Recent Advances in Heat and Mass Transfer, p.223, McGraw-Hill, New York (1961).

41. L. Schiller, Zeitschrift Angewandte Mathematik und Mechanik, p.2 (1923).

42. E. N. Sieder and G. E. Tate, Heat Transfer and Pressure drop of Liquids in Tubes, Ind. and Engg. Chem., 28, 1429 (1936).

43. D. B. Spalding and C. L. V. Jayatilleke, A Survey of Theoretical and Experimental Information on the Resistance of the Laminar Sub-layer to Heat and Mass Transfer, Mechanical Engg. Dept., Imperial College, London, U.K. (October 1963).

44. E. M. Sparrow, J. R. Lloyd and C. W. Hixon, Experiments on Turbulent Heat Transfer in an Asymmetrically Heated Rectangular Duct, J. Heat Transfer, Trans. ASME, 9, 170 (1966).

45. H. M. Tan and W. W. S. Charters, An Experimental Investigation of Forced-Convective Heat Transfer for Fully-Developed Turbulent Flow in a Rectangular Duct with Asymmetric Heating, Solar Energy, 13, 121 (1970).

46. L. Washington and W. M. Marks, Heat Transfer and Pressure Drop in Rectangular Air Passages, Ind. Engg. Chemistry, 29, No.3, 337 (1937).

47. G. A. Whan and R. R. Rothfus, Characteristics of Transition Flow Between Parallel Plates, AIChE Journal, 204 (June 1959).

APPENDIX A

DERIVATION OF EQUATIONS

This appendix **consists** of four sections. Sections A.1, A.3 and A.4 show the derivation of equations (3.23), (3.27) and (3.28) respectively. Section A.2 demonstrates that Pr_{turb} = constant in the turbulent core of pipe flow.

A.1 Derivation of Equation (3.23)

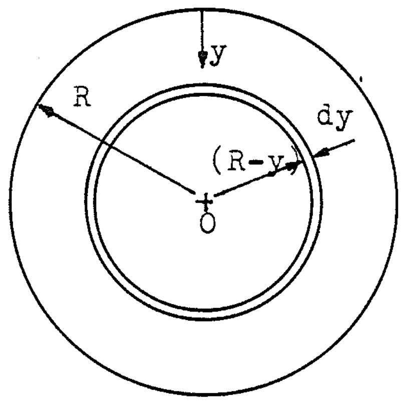

The bulk velocity, $\bar{u}$, of pipe flow is defined through

$$(\text{Area})\rho\bar{u} \equiv \rho \int_{\text{Area}} u\,d(\text{Area})$$

or, $$\pi R^2 \rho \bar{u} = 2\pi\rho \int_0^R u(R - y)dy$$

Then, $$\bar{u}^+ = 2\int_0^{y_R^+} \frac{1}{y_R^+} u^+ \left(1 - \frac{y^+}{y_R^+}\right)dy^+$$

$$= 2\left\{\int_0^{y_R^+} \frac{u^+}{y_R^+}dy^+ - \int_0^{y_R^+} \frac{y^+}{y_R^{+2}}u^+dy^+\right\}$$

$$= 2\ (A - B) \qquad (A.1)$$

$$A = \int_0^{y_R^+} \frac{u^+}{y_R^+} dy^+$$

$$= \frac{1}{y_R^+} \int_0^{y_R^+} \left(\frac{1}{\kappa} \ln y^+ + c\right) dy^+$$

$$= \frac{1}{y_R^+} \left[\frac{1}{\kappa}(y^+ \ln y^+ - y^+) + c y^+ \right]_0^{y_R^+}$$

$$= \frac{1}{\kappa} \ln y_R^+ - \frac{1}{\kappa} + c$$

$$= u_R^+ - \frac{1}{\kappa} \tag{A.2}$$

$$B = \int_0^{y_R^+} \frac{y^+}{y_R^{+2}} u^+ \, dy^+$$

$$= \frac{1}{y_R^{+2}} \int_0^{y_R^+} y^+ \left(\frac{1}{\kappa} \ln y^+ + c\right) dy^+$$

$$= \frac{1}{y_R^{+2}} \left[\frac{1}{\kappa}\left(\frac{y^{+2}}{2} \ln y^+ - \frac{y^{+2}}{4}\right) + \frac{c y^{+2}}{2} \right]_0^{y_R^+}$$

$$= \frac{1}{2} u_R^+ - \frac{1}{4\kappa} \tag{A.3}$$

Substitute (A.2) and (A.3) into (A.1),

$$\bar{u}^+ = u_R^+ - \frac{3}{2\kappa} \tag{3.23}$$

A.2 Derivation of Pr_{turb} = Constant in the Turbulent Core

From equation (3.22),

$$\frac{dy^+}{du^+} = K_1 \, y^+ \tag{A.4}$$

where K_1 is a constant.

Since $\phi^+ \sim y^+$ is logarithmic over the turbulent core,

$$\phi^+ = \frac{1}{K_2} \ln y^+ + K_3 \tag{A.5}$$

where K_2 and K_3 are constants.

From (A.5),

$$\frac{dy^+}{d\phi^+} = K_2 \, y^+ \tag{A.6}$$

From equations (3.17) and (3.18),

$$Pr_{tot} = \frac{dy^+}{du^+} \Bigg/ \frac{dy^+}{d\phi^+} \tag{A.7}$$

Substitute (A.4) and (A.6) into (A.7),

$$Pr_{tot} = \frac{K_1}{K_2} = \text{constant} \tag{A.8}$$

This Pr_{tot} in the turbulent core corresponds to Pr_{turb},

i.e $\quad Pr_{turb}$ = constant

A.3 Derivation of Equation (3.27)

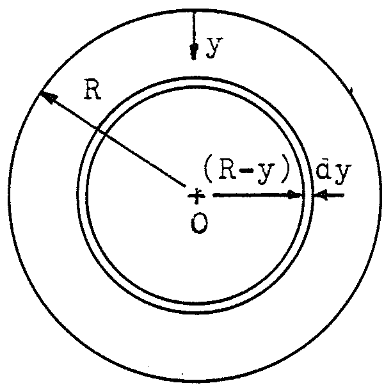

Through the definition of $\overline{u\phi}$,

$$\pi R^2 \rho \overline{u\phi} \equiv 2\pi\rho \int_0^R u\phi\ (R - y)dy$$

then, $$\overline{u^+\phi^+} = 2\int_0^{y_R^+} \frac{1}{y_R^+} u^+\phi^+ \left(1 - \frac{y^+}{y_R^+}\right)dy^+ \qquad (A.9)$$

Now, $$u^+ = \frac{1}{\kappa}\ln y^+ + c \qquad (3.22)$$

and $$\phi^+ = \int_0^{u^+} Pr_{tot}du^+ \qquad (3.20)$$

$$\simeq Pr_{turb}\int_0^{u^+} du^+$$

$$= Pr_{turb}\ u^+ \qquad (A.10)$$

or, $$\phi^+ = Pr_{turb}\left(\frac{1}{\kappa}\ln y^+ + c\right) \qquad (A.11)$$

Substitute equations (3.22) and (A.10) into (A.9),

$$\bar{u}^+\bar{\phi}^+ = 2\, Pr_{turb}\int_0^{y_R^+} \frac{1}{y_R^+}\left(\frac{1}{\kappa^2}\ln^2 y^+ + \frac{2c}{\kappa}\ln y^+ + c^2\right) \times \left(1 - \frac{y^+}{y_R^+}\right)dy^+$$

$$= 2\, Pr_{turb}\left\{\int_0^{y_R^+} \frac{1}{y_R^+}\left(\frac{1}{\kappa^2}\ln^2 y^+ + \frac{2c}{\kappa}\ln y^+ + c^2\right)dy^+ - \int_0^{y_R^+} \frac{y^+}{y_R^{+2}}\left(\frac{1}{\kappa^2}\ln^2 y^+ + \frac{2c}{\kappa}\ln y^+ + c^2\right)dy^+\right\}$$

$$= 2\, Pr_{turb}\,(A - B) \qquad (A.12)$$

By integration,

$$A = \frac{1}{\kappa^2}(\ln^2 y_R^+ - 2\ln y_R^+ + 2) + \frac{2c}{\kappa}(\ln y_R^+ - 1) + c^2 \qquad (A.13)$$

and $$B = \frac{1}{\kappa^2}\left(\frac{1}{2}\ln^2 y_R^+ - \frac{1}{2}\ln y_R^+ + \frac{1}{4}\right) + \frac{2c}{\kappa}\left(\frac{1}{2}\ln y_R^+ - \frac{1}{4}\right) + \frac{c^2}{2} \qquad (A.14)$$

Substitute (A.13) and (A.14) into (A.12),

$$\bar{u}^+\bar{\phi}^+ = Pr_{turb}\left\{\frac{1}{\kappa^2}(\ln^2 y_R^+ - 3\ln y_R^+ + \frac{7}{2}) + \frac{c}{\kappa}(2\ln y_R^+ - 3) + c^2\right\} \qquad (A.15)$$

Also, from (A.10)

$$\phi_R^+ = Pr_{turb}\ u_R^+ \qquad (A.16)$$

or

$$\phi_R^+ = Pr_{turb}\ (\frac{1}{\kappa}\ln y_R^+ + c) \qquad (A.17)$$

$$\bar{u}^+ = u_R^+ - \frac{3}{2\kappa} \qquad (3.23)$$

or

$$\bar{u}^+ = (\frac{1}{\kappa}\ln y_R^+ + c) - \frac{3}{2\kappa} \qquad (A.18)$$

From (A.17) and (A.18),

$$\bar{u}^+\phi_R^+ = (\frac{1}{\kappa}\ln y_R^+ + c - \frac{3}{2\kappa}) \times Pr_{turb}\ (\frac{1}{\kappa}\ln y_R^+ + c) \qquad (A.19)$$

Compare (A.15) and (A.19),

$$\bar{u}^+\bar{\phi}^+ = \bar{u}^+\phi_R^+ - Pr_{turb}\ (\frac{3}{2\kappa^2}\ln y_R^+ + \frac{3c}{2\kappa} - \frac{7}{2\kappa^2})$$

Dividing by $\bar{u}^+$,

$$\bar{\phi}^+ = \phi_R^+ - Pr_{turb}\ (\frac{3}{2\kappa} - \frac{5}{4\kappa^2\bar{u}^+}) \qquad (3.27)$$

A.4 Derivation of equation (3.28)

From equations (3.20) and (3.27),

$$\bar{\phi}^{+} = \int_{0}^{u_R^{+}} (Pr_{tot} - Pr_{turb})du^{+} - Pr_{turb}\left(\frac{3}{2\kappa} - \frac{5}{4\kappa^{2}\bar{u}^{+}}\right)$$

$$+ \int_{0}^{u_R^{+}} Pr_{turb}\ du^{+} \qquad \text{(A.20)}$$

From equations (3.21) and (3.26),

$$\phi^{+} = \frac{\sqrt{\frac{c_f}{2}}}{St} \qquad \text{(A.21)}$$

From equations (3.23) and (3.21)

$$\int_{0}^{u_R^{+}} Pr_{turb}\ du^{+} = Pr_{turb}\left(\bar{u}^{+} + \frac{3}{2\kappa}\right)$$

$$= Pr_{turb}\left(\frac{1}{\sqrt{\frac{c_f}{2}}} + \frac{3}{2\kappa}\right) \qquad \text{(A.22)}$$

Substitute (A.21) and (A.22) into (A.20),

$$\frac{\sqrt{\frac{c_f}{2}}}{St} = \int_0^{u_R^+} (Pr_{tot} - Pr_{turb})du^+ - Pr_{turb}\left(\frac{3}{2\kappa} - \frac{5}{4\kappa^2 \bar{u}^+}\right)$$

$$+ Pr_{turb}\left(\frac{1}{\sqrt{\frac{c_f}{2}}} + \frac{3}{2\kappa}\right)$$

or,

$$\frac{\sqrt{\frac{c_f}{2}}}{St} = \int_0^{u_R^+} (Pr_{tot} - Pr_{turb})du^+$$

$$+ \frac{Pr_{turb}}{\sqrt{\frac{c_f}{2}}}\left(1 + \frac{5}{4\kappa^2} \cdot \frac{c_f}{2}\right) \tag{3.28}$$

APPENDIX B

EXPERIMENTAL DATA

Table B.1 to B.8 are collected experimental data.

Summary:

Table	Ref.	Investigator(s)	Total Number of Data
B.1	(30)	Levy et al.	86
B.2	(36)	Novotny et al.	49
B.3	(3)	Barrow	22
B.4	(18)	Hines	48
B.5	(44)	Sparrow et al.	12
B.6	(21)	James et al.	73
B.7	(6)	Bruzzi	52
B.8	(45)	Tan and Charters	7

Table B.1. Experimental data of Levy et al.[30]

Notes:

1. The data are obtained from Table 1 and Figure 6 of Reference 30.
2. All the data are based on bulk conditions for fluid properties.
3. The characteristic length of the Reynolds numbers, Re, is the hydraulic equivalent diameter.
4. The Nusselt numbers, Nu, have been corrected to the constant-property conditions by Levy et al. using the Sieder-Tate method.

Table B.1 (cont'd)

(A) Section No. 4 (0.118" x 2.405")

Run No.	Pr	$Rex10^{-4}$	$Nux10^{-2}$ (Constant-Property)	$\frac{\mu_b}{\mu_w}$
8	4.09 3.45	10.40 12.40	3.04 3.33	1.44 1.37
9	2.71	15.20	3.07	1.58
10	4.09 3.38	10.40 12.50	2.56 2.63	1.50 1.45
11	4.09 2.67	10.40 15.10	3.28 3.47	2.01 1.62
12	4.06 3.31	9.30 11.20	2.55 2.61	1.49 1.44
13	4.09 2.60	9.40 14.10	2.40 2.48	2.15 1.79
14	3.95 3.10	8.90 11.00	2.13 2.19	1.59 1.52
15	4.06 2.43	8.50 12.60	2.31 2.22	2.03 1.74
16	4.06 2.88	4.10 5.40	1.36 1.49	1.57 1.50
17	4.06 3.67	10.40 11.70	2.55 2.70	1.28 1.25
18	4.02 2.10	12.00 19.50	3.10 3.46	2.58 1.70
19	4.02 2.12	12.00 19.60	3.02 3.47	2.57 1.71
20	4.06 2.16	12.00 19.00	3.11 3.75	2.36 1.71

Table B.1 (cont'd)

(B) Section No. 11 (0.114" x 2.349")

Run No.	Pr	$Re \times 10^{-4}$	$Nu \times 10^{-2}$ (Constant-Property)	$\frac{\mu_b}{\mu_w}$
100	3.88 1.78	7.70 12.60	2.28 2.55	2.76 1.75
101	3.58 1.98	7.10 13.50	2.22 2.83	2.26 1.69
103	3.59 1.80	11.00 20.00	2.07 3.22	2.61 1.81
108	2.15	19.10	2.97	1.79
109	2.31	18.60	2.12	2.02
110	4.27 2.55	11.30 19.20	2.35 2.60	2.76 2.17
111	4.89 3.34	10.30 15.00	2.29 2.70	2.46 2.11
113	2.48	19.40	3.11	2.15
114	5.98 5.01	1.06 1.24	0.60 0.77	1.29 1.17
115	5.98 4.02	0.90 1.33	0.55 0.76	1.64 1.41
116	5.59 2.95	0.84 1.73	0.49 0.75	2.21 1.56
117	6.63 4.70	2.94 3.97	1.41 2.01	1.70 1.39
118	5.07 2.99	5.32 8.79	2.41 2.33	2.29 1.83
119	5.01 2.41	3.64 7.25	1.39 1.94	2.70 1.86
120	5.51 3.17	3.48 5.96	1.47 1.74	2.36 1.81

Table B.1 (cont'd)

Run No.	Pr	$Rex10^{-4}$	$Nux10^{-2}$ (Constant-Property)	$\frac{\mu_b}{\mu_w}$
121	6.08 3.91	3.20 4.88	1.37 1.97	2.11 1.68
122	3.88 2.05	9.52 16.83	2.75 2.92	2.49 1.78
123	6.54 3.56	2.29 4.09	1.20 1.68	2.38 1.77
124	7.13 4.95	2.16 2.94	1.08 1.14	1.66 1.47
125	6.82 4.24	2.21 3.35	1.08 1.21	2.06 1.65
126	7.30 5.81	1.88 2.27	1.11 1.08	1.43 1.35
127	5.28 3.59	0.93 1.37	0.51 0.58	1.65 1.38
128	5.37 3.42	0.79 1.24	0.46 0.63	1.79 1.40
129	5.28 2.38	0.77 1.63	0.45 0.63	2.43 1.57
130	4.50 1.70	0.73 1.79	0.39 0.59	2.63 1.54
131	4.27 1.33	0.71 2.14	0.37 0.68	3.17 1.47

Table B.1 (cont'd)

(C) Section No. 5 (Variable, 0.14" x 2.40" nominal)

Run No.	Pr	Rex10^{-4}	Nux10^{-2} (Constant-Property)	$\frac{\mu_b}{\mu_w}$
24	3.91	10.50	3.70	2.29
	2.48	15.70	3.38	1.80
25	4.06	10.10	3.11	1.78
	3.27	12.50	2.60	2.17
27	3.99	9.60	5.55	1.61
	2.71	13.10	4.11	1.49
28	3.99	10.50	6.03	1.79
	2.53	15.70	3.82	1.57
29	4.02	8.30	4.93	1.48
	3.02	10.70	3.18	1.34
34	3.95	10.70	5.45	2.40
	2.03	19.30	5.07	1.44

Table B.2 Experimental data of Novotny et al.[36]

Notes:

1. The data are obtained from Figure 6 of Reference 36.

2. All the data are based on bulk conditions for fluid properties.

3. The characteristic length of the Reynolds numbers, Re, is the hydraulic equivalent diameter.

4. The Nusselt numbers, Nu, are as-measured values (i.e no constant-property correction).

Table B.2 (cont'd)

(A) Duct with Aspect Ratio 1:1 (0.98" x 0.98")

Pr	$Rex10^{-4}$	Nu (As-Measured)
0.7	1.05	34
"	1.15	39
"	1.45	43
"	1.70	50
"	2.05	58
"	2.40	67
"	2.50	70
"	2.80	72
"	3.20	80
"	3.90	88
"	4.50	100
"	4.90	105
"	5.30	115
"	5.70	115
"	6.10	125
"	7.10	140
"	8.70	160
"	8.80	165
"	10.00	175
"	14.00	220

Table B.2 (cont'd)

(B) Duct **with** Aspect Ratio 1:5 (0.604" x 3.0")

Pr	Rex10^{-4}	Nu (As-Measured)
0.7	1.40	38
"	1.70	49
"	1.95	51
"	2.05	52
"	2.22	54
"	2.25	59
"	2.25	63
"	2.30	61
"	2.45	64
"	2.80	67
"	2.70	72
"	3.00	70
"	3.20	80
"	3.25	77
"	3.40	80
"	3.80	86
"	5.00	115
"	6.00	120
"	7.00	135
"	7.80	145
"	10.50	200
"	11.00	190
"	14.00	210

Table B.2 (cont'd)

(C) Duct with Aspect Ratio 1:10 (0.40" x 4.0")

Pr	Rex10^{-4}	Nu (As-Measured)
0.7	1.40	42
"	2.20	60
"	2.60	70
"	3.20	82
"	4.20	90
"	7.00	130

Table B.3 Experimental data of Barrow[3]

Notes:

1. The data are obtained from Figure 11 of Reference 3.

2. All the data are based on bulk conditions for fluid properties.

3. The characteristic length of the Reynolds numbers, Re, is the hydraulic equivalent diameter.

4. The as-measured Nusselt numbers, Nu, were corrected to the constant-property conditions by the present author using equation (6.4) with $T_b = 531^{\circ}R$, $T_w = 542.5^{\circ}R$ and $m = 0.5$.

Table B.3 (cont'd)

(A) Electrical Basis

A	Pr	$Re \times 10^{-4}$	Nu (As-Measured)	Corrected Nu (Constant-Property)
0.0344	0.7	1.05	31	31.31
		1.10	30	30.30
		1.25	35	35.35
		1.30	39	39.39
		1.55	38	38.38
		1.55	47	47.47
		1.80	44	44.44
		2.05	49	49.49
		2.05	58	58.58
		2.10	50	50.50
		2.50	64	64.64
		2.60	63	63.63

Table B.3 (cont'd)

(B) Thermocouple Basis

A	Pr	Rex10^{-4}	Nu (As-Measured)	Corrected Nu (Constant-Property)
0.0344	0.7	1.05	21	21.21
		1.30	22	22.22
		1.70	30	30.30
		1.80	32	32.32
		2.10	36	36.36
		2.10	38	38.38
		2.10	44	44.44
		2.15	37	37.37
		2.50	29	29.29
		2.60	50	50.50

Table B.4 Experimental data of Hines[18]

Notes:

1. The data are obtained from Figure 10 of Reference 18.

2. All the data are based on bulk conditions for fluid properties.

3. The characteristic length of the Reynolds numbers, Re, is the hydraulic equivalent diameter.

4. The Nusselt numbers, Nu, have been corrected to the constant-property conditions by Hines using the Sieder-Tate method.

Table B.4 (cont'd)

A	Re x 10^{-4}	Pr = 18 Nu x 10^{-2} (Constant-Property)	Pr = 22 Nu x 10^{-2} (Constant-Property)
1.75	2.70	2.32	2.50
	2.90	2.26	2.43
	2.90	2.43	2.62
	2.90	2.21	2.37
	3.00	2.49	2.68
	5.00	4.53	4.89
	5.30	4.81	5.17
	5.70	4.39	4.72
	5.70	4.95	5.32
	6.00	4.67	5.02
	6.20	4.95	5.32
	8.00	6.23	6.69
	8.60	6.79	7.30
	9.50	7.08	7.61
	11.50	8.21	8.82
	12.00	8.78	9.43
	13.00	9.06	9.74
	14.00	9.20	9.89
	15.00	10.90	11.71
	15.50	10.33	11.11
	16.00	11.04	11.87
	17.00	11.32	12.17
	18.00	11.89	12.78
	19.00	12.74	13.69

Table B.5 Experimental data of Sparrow et al.[44]

Notes:

1. The data are obtained from Figure 1 of Reference 44.

2. All the data are based on bulk conditions for fluid properties.

3. The characteristic length of the Reynolds numbers, Re, is the hydraulic equivalent diameter.

4. The as-measured Nusselt numbers, Nu, were corrected to the constant-property conditions by the present author using equation (6.4) with $T_b = 554^{\circ}R$, $T_w = 592.5^{\circ}R$ and $m = 0.5$.

Table B.5 (cont'd)

A	Pr	Re x 10^{-4}	Nu (As-Measured)	Corrected Nu (Constant-Property)
0.020	0.7	1.8	45	46.39
		3.3	70	72.16
		4.5	93	95.88
		4.8	98	101.03
		5.5	108	111.34
		6.4	120	123.71
		6.5	125	128.87
		9.0	150	154.64
		9.8	170	175.26
		12.0	195	201.03
		13.0	190	195.88
		14.0	200	206.19

Table B.6 Experimental data of James et al.[21]

Notes:

1. The data are obtained from Figure 4 of Reference 21.

2. All the data are based on bulk conditions for fluid properties.

3. The characteristic length of the Reynolds numbers, Re, is the hydraulic equivalent diameter.

4. The Nusselt numbers, Nu, have been corrected to the constant-property conditions by James et al. using the extrapolation technique of the Eagle and Ferguson method[14].

Table B.6 (cont'd)

(A) Pr = 6.5

A	Re x 10^{-4}	Nu (Constant-Property)
0.5	1.00	80
"	4.40	230
1.0	0.50	50
"	1.00	88
"	2.40	170
"	7.10	385
2.0	0.40	45
"	0.52	60
"	7.00	430
2.5	0.40	48
"	2.20	180
"	4.00	285
3.0	2.00	180
"	3.00	250
"	6.00	410
"	9.80	570
4.0	1.05	110
"	2.10	200
"	5.90	400
"	8.20	520

Table B.6 (cont'd)

(B) Pr = 32.5

A	Re x 10^{-4}	Nu (Constant-Property)
0.5	0.36	60
"	0.51	84
"	1.00	145
"	1.60	190
1.0	0.32	62
"	0.515	100
"	0.97	175
2.0	0.31	68
"	0.51	110
"	1.80	300
2.5	0.505	110
"	1.20	240
"	1.60	280
"	2.00	330
"	2.20	380
3.0	0.505	110
"	0.73	160
"	1.00	190
"	1.60	280
4.0	0.30	80
"	0.73	150
"	0.83	180
"	1.40	270

Table B.6 (cont'd)

(C) Pr = 100

A	Re x 10^{-4}	Nu (Constant-Property)
0.5	0.30	80
"	0.30	82
"	0.405	100
"	0.40	100
"	0.52	140
"	0.68	200
1.0	0.395	120
"	0.81	250
"	0.36	100
"	0.505	170
"	0.79	220
"	1.00	280
"	1.00	300
2.0	0.29	105
"	0.40	150
"	0.50	190
2.5	0.30	110
"	0.38	140
"	0.42	160
"	0.59	220
"	0.80	310
"	1.00	340
3.0	0.29	130
"	0.39	155
"	0.52	195
"	0.62	205
"	0.70	270
"	0.90	320
4.0	0.60	250
"	0.70	280

Table B.7 Experimental data of Bruzzi[6]

Notes:

1. The data are obtained from Table 6 of Reference 6.

2. All the data are based on bulk conditions for fluid properties.

3. The characteristic length of the Reynolds numbers, Re, is the hydraulic equivalent diameter.

4. The Nusselt numbers, Nu, are as-measured values (i.e no constant-property correction).

Table B.7 (cont'd)

(A) A =0.54

Run No.	Pr	Re x 10^{-4}	Nu (As-Measured)	$\frac{\mu_b}{\mu_w}$
055	8.06	1.439	132.22	1.18
062	7.01	1.792	132.03	1.16
074	8.04	2.734	213.66	1.22
080	7.01	3.388	208.52	1.10
156	8.09	2.579	195.50	1.43
157	8.08	2.228	172.46	1.44
158	8.08	2.009	159.08	1.42
159	8.07	1.695	141.30	1.43
160	8.07	1.388	118.17	1.48
161	8.03	0.991	94.94	1.47
162	8.02	0.561	60.02	1.47
163	8.05	0.743	74.35	1.50
197	8.10	2.570	178.40	1.46
198	8.09	2.220	161.10	1.46

Table B.7 (cont'd)

(B) A = 1.12

Run No.	Pr	Re x 10^{-4}	Nu (As-Measured)	$\frac{\mu_b}{\mu_w}$
1	8.46	4.409	328.99	1.26
15	7.01	2.550	192.16	1.17
16	8.08	2.034	179.80	1.20
22	8.08	2.048	181.36	1.42
23	8.01	3.996	298.63	1.38
35	6.65	2.688	185.72	1.09
117	8.33	6.244	369.29	1.20
118	8.33	5.442	335.46	1.22
119	8.33	4.340	295.60	1.20
120	8.33	4.337	289.02	1.10
121	8.05	0.855	81.63	1.27
128	8.31	6.260	365.70	1.21
129	8.20	6.013	400.86	1.20
130	8.20	5.508	387.97	1.19
131	8.21	4.638	334.71	1.20
132	8.21	3.466	263.22	1.23
133	8.20	2.529	206.34	1.27
134	8.20	1.791	151.56	1.26
135	7.00	2.553	174.60	1.17
140	7.00	2.554	175.92	1.20
152	6.81	2.684	175.47	1.17
199	8.22	4.736	195.87	1.25
200	8.21	5.624	321.36	1.21
201	8.20	2.583	170.72	1.32
202	7.02	1.093	80.26	1.18
212	6.93	1.113	95.49	1.18
221	8.02	0.877	101.78	1.46

Table B.7 (cont'd)

(C) A = 3.01

Run No.	Pr	Re x 10^{-4}	Nu (As-Measured)	$\frac{\mu_b}{\mu_w}$
87	8.10	3.07	266.08	1.19
88	8.10	3.06	265.21	1.14
89	7.01	1.56	134.51	1.11
90	7.02	1.56	131.41	1.08
96	8.08	1.27	130.32	1.15
113	7.25	3.58	293.29	1.25
114	7.25	3.58	262.15	1.15
115	7.25	3.58	251.76	1.10
153	8.15	3.23	255.35	1.27
154	8.15	3.24	256.14	1.52
155	8.15	1.40	143.77	1.50

Table B.8 Experimental data of Tan and Charters[45]

Notes:

1. The data are obtained from Figure 3 of Reference 45.

2. All the data are based on bulk conditions for fluid properties.

3. The characteristic length of the Reynolds numbers, Re, is the hydraulic equivalent diameter.

4. The as-measured Nusselt numbers, Nu, were corrected to the constant-property conditions by the present author using equation (6.4) with $T_b = 585^{\circ}R$, $T_w = 655^{\circ}R$ and $m = 0.5$.

Table B.8 (cont'd)

A	Pr	Re x 10^{-4}	Nu (As-Measured)	Corrected Nu (Constant-Property)
0.34	0.7	0.95	24	25.26
		1.15	28	29.47
		1.27	30	31.58
		1.44	34	35.79
		1.74	39	41.05
		1.98	43	45.26
		2.12	45	47.37